

If you have discovered material in AURA which is unlawful e.g. breaches copyright, (either yours or that of a third party) or any other law, including but not limited to those relating to patent, trademark, confidentiality, data protection, obscenity, defamation, libel, then please read our [Takedown Policy](#) and [contact the service](#) immediately.

GAS-METAL REACTIONS AND POROSITY IN
THE INERT GAS ARC WELDING OF COPPER

by

J. LITTLETON, B.Sc.,

V12 562

A thesis submitted for the degree of
Doctor of Philosophy of
The University of Aston in Birmingham

JANUARY, 1974

THESIS
621.7918
LIT

SYNOPSIS

A study has been made of the effects of welding and material variables on the occurrence of porosity in the tungsten inert gas arc welding of copper. The experiments were based on a statistical design and variables included, welding current, welding speed, arc atmosphere composition, inert gas flow rate, weld preparation, and base material. The extent of weld metal porosity was assessed by density measurement and its morphology by X-ray radiography and metallography. In conjunction with this the copper-steam reaction has been investigated under conditions of controlled atmosphere arc melting.

The welding experiments have shown that the extent of steam porosity is increased by increased water vapour content of the arc atmosphere, increased oxygen content of the base material and decreased welding speed. The arc melting experiments have shown that the steam reaction occurs in the body of the weld pool and proceeds to an apparent equilibrium state appropriate to its temperature, the hydrogen and oxygen being supplied by the dissociation of water vapour in the arc atmosphere.

It has been shown conclusively that nitrogen porosity can occur in the tungsten inert gas arc welding of copper and that this porosity can be eliminated by using filler wires containing small amounts of aluminium and titanium.

Since it has been shown to be much more difficult to produce sound butt welds than melt runs it has been concluded that the porosity associated with joint fit up is due to nitrogen entrained into the arc atmosphere. Clearly atmospheric entrainment would

also, to a much lesser extent, involve water vapour. From a practical welding point of view it has thus been postulated that use of a filler wire containing small amounts of aluminium and/or titanium would eliminate both forms of porosity since these elements are both strongly deoxidising and denitrifying.

GAS-METAL REACTIONS AND POROSITY IN THE
INERT GAS ARC WELDING OF COPPER

<u>CONTENTS</u>	<u>PAGE</u>
1. <u>INTRODUCTION</u>	1
2. <u>LITERATURE REVIEW</u>	4
2.1. T.I.G. TECHNIQUE FOR COPPER WELDING	4
2.2. PHYSICS OF THE WELDING ARC	5
2.3. TEMPERATURE CONDITIONS IN THE WELD POOL	8
2.4. GAS-METAL REACTIONS AND POROSITY IN GENERAL	9
2.4.1. GENERAL CONSIDERATIONS	9
2.4.2. ABSORPTION	10
2.4.3. REACTION	11
2.4.4. REJECTION	12
2.5. GAS-METAL REACTIONS IN ARC WELDING	14
2.5.1. GAS-ABSORPTION IN THE WELD POOL	15
2.5.2. GAS-METAL REACTIONS IN THE WELD POOL	18
2.5.3. GAS REJECTION AND POROSITY IN ARC WELDING	19
2.6. GAS-METAL REACTIONS AND POROSITY IN COPPER CASTING	20
2.7. GAS-METAL REACTIONS AND POROSITY IN THE WELDING OF COPPER AND ITS ALLOYS	23
3. <u>INVESTIGATIONAL WORK</u>	27
3.1. QUANTITATIVE STUDY OF THE FACTORS AFFECTING WELD METAL POROSITY IN THE INERT GAS ARC WELDING OF COPPER	28
3.1.1. EXPERIMENTAL TECHNIQUE AND RESULTS	30
3.1.2. THE EFFECT OF BASE MATERIAL	33
3.1.3. THE INTERACTION OF WELDING SPEED AND WATER VAPOUR IN THE ARGON SHIELDING GAS	33
3.1.4. THE INTERACTION OF WATER VAPOUR IN THE ARGON SHIELDING GAS AND BASE MATERIAL	34

3.1.5.	THE INTERACTION OF BASE MATERIAL AND WELDING SPEED	35
3.1.6.	THE EFFECT OF WELDING SPEED ON THE COPPER-STEAM REACTION	36
3.1.7.	THE INTERACTION OF WELDING SPEED AND WELD PREPARATION	36
3.2.	THE OCCURRENCE OF NITROGEN POROSITY IN THE T.I.G. ARC WELDING OF COPPER	37
3.2.1.	POROSITY IN NITROGEN SHIELDED T.I.G. WELDING OF COPPER	38
3.2.2.	EFFECT OF SMALL NITROGEN ADDITIONS AND WELDING SPEED ON THE DENSITY OF T.I.G. WELDED COPPER	39
3.2.3.	EFFECT OF FILLER WIRE COMPOSITION AND SMALL NITROGEN ADDITIONS ON THE DENSITY OF T.I.G. WELDED COPPER	41
3.2.4.	CONTROLLED ATMOSPHERE ARC WELDING OF O.P.H.C. COPPER IN AN ARGON, NITROGEN ATMOSPHERE	42
3.3.	THE STEAM REACTION IN COPPER UNDER ARC WELDING CONDITIONS	43
3.3.1.	EXPERIMENTAL TECHNIQUE	43
3.3.2.	CLEANLINESS OF THE WELDING BOX ATMOSPHERE	47
3.3.3.	ARC MELTING UNDER ARGON, WATER VAPOUR MIXTURES	48
3.3.4.	EFFECT OF INCREASING THE ARC MELTING CURRENT	49
3.3.5.	REPRODUCIBILITY OF EXPERIMENTAL TECHNIQUE	49
3.3.6.	ARC MELTING COPPER TITANIUM ALLOYS UNDER AN ARGON, WATER VAPOUR ATMOSPHERE	49
3.3.7.	ARC MELTING COPPER ALUMINIUM ALLOYS UNDER AN ARGON, WATER VAPOUR ATMOSPHERE	50
3.3.8.	GENERAL BUTTON MELTING CHARACTERISTICS	51
3.3.9.	CALCULATION OF "WATERVAPOUR" EQUILIBRIUM CONCENTRATIONS UNDER ARC MELTING CONDITIONS	52
3.3.10.	BUTTON TEMPERATURE MEASUREMENT	52
3.3.11.	W.P.T. COPPER ARC MELTED TO AN ARGON, HYDROGEN AT C. ATMOSPHERE	53

3.3.12.	POROSITY IN ARC WELDED BUTT JOINTS	54
3.3.13.	O.F.H.C. COPPER ARC WELDED IN ARGON, HYDROGEN AND ARGON, OXYGEN AIR OSMOSPHERES.	54
4.	<u>DISCUSSION</u>	
4.1.	THE OCCURRENCE OF STEAM POROSITY IN T.T.G. WELDED COPPER	56
4.2.	THE COPPER-STEAM REACTION UNDER ARC WELDING AND ARC WELDING CONDITIONS	59
4.3.	THE OCCURRENCE OF NITROGEN POROSITY IN ARC WELDED COPPER	67
4.4.	PRACTICAL SIGNIFICANCE FOR WELDING OF COPPER	72
5.	<u>CONCLUSIONS</u>	75
6.	<u>RECOMMENDATIONS FOR FURTHER WORK</u>	76
7.	<u>ACKNOWLEDGEMENTS</u>	77
8.	<u>APPENDIX</u>	78
8.1.	COMPARISON OF MEASURED FINAL O.F.H.C. COPPER HYDROGEN CONTENTS WITH THE EQUILIBRIUM HYDROGEN SOLUBILITY AT 2000°C	78
8.2.	FREE ENERGY OF FORMATION OF CUPROUS OXIDE FOR AN ARGON, 77 V.P.M. OXYGEN AIR OSMOSPHERE AT 2027°C	79
8.3.	PARTIAL PRESSURE OF HYDROGEN IN EQUILIBRIUM WITH THE COPPER-STEAM REACTION FOR AN ARGON, 230 V.P.M. WATER VAPOUR MIXTURE AT A TEMPERATURE OF 2027°C	80
9.	<u>REFERENCES</u>	82
	<u>TABLES</u> 1 - 28	
	<u>FIGURES</u> 1 - 35	

1 INTRODUCTION

Copper is used extensively in the electrical and chemical engineering industries on account of its high electrical and thermal conductivity and good corrosion resistance. The commercially available grades of copper fall into two groups depending on the presence or absence of oxygen. Electrolytic tough pitch copper (E.T.P.) containing 0.02 to 0.05 weight per cent (Wt.%) oxygen is the most widely used in the oxygen bearing group and phosphorus deoxidised (P.D.) and oxygen free high conductivity (O.F.H.C.) coppers are the most widely used in the oxygen free group.

Most of the available fusion welding techniques can be applied to the welding of copper and these are briefly discussed below. Although gas welding is still used to an appreciable extent, Inglis and Michie ⁽¹⁾ point out that most people concerned in copper welding prefer inert gas shielded arc methods. A much more recent technique, capable of yielding very high rates of heat input has been electron beam welding. Several disadvantages however, exist with this technique. It is expensive and inconvenient since welding must be carried out under vacuum. The technique is also restricted to autogenous welding and as pointed out by Inglis and Michie ⁽¹⁾ and Johnson ⁽²⁾ it is subject to porosity due mainly to cold shutting at the weld root. Carbon arc welding ^(3 - 8), bare electrode welding, coated electrode welding ^(9, 10) and plasma arc welding have all been used for the welding of copper. However, the inert gas arc welding techniques are the most widely used. The two techniques in use are the tungsten inert gas (T.I.G.) and metal inert gas (M.I.G.). The advantage of the inert gas shielded arc processes lies in the

fact that a high intensity heat source coupled with a protective inert gas shield is available. The high intensity heat source minimises the need for pre-heat and makes greater welding speeds possible and the inert gas shield avoids the complications of fluxes or consumable electrode coatings.

In spite of the improvements in copper welding brought about by the inert gas shielded arc processes, fundamental material problems still exist. One of the main advantages of copper over other metals is its high thermal conductivity. Typical thermal conductivities are listed in table 1 taken from Smithells (11). It can be seen that the thermal conductivity of copper is 1.6 times that of aluminium and 5.5 times that of iron. The high thermal conductivity of copper means that high heat inputs are necessary to make welding possible and except for thin material, pre-heating is essential. With argon arc welding it is generally accepted that pre-heating is necessary at thicknesses greater than 6 millimetres.(mm)

Although high thermal conductivity is less of a problem when alloying additions are made to copper, certain of these additions can promote another problem, hot cracking. Copper and copper alloys are rendered brittle and sensitive to hot cracking if excessive amounts of low melting point impurities, notably bismuth and lead are present. However, the only copper alloy which is notably sensitive to this defect is aluminium bronze.

A third and serious material problem is the incidence of porosity in the casting and welding of copper and some of its alloys. Although the widespread use of the inert gas arc processes has eliminated some of the difficulties encountered, the incidence of

porosity in welds made in copper and cupro-nickel alloys remains a major problem. (1) (12) This according to Taylor and Burn (12) can result in a marked decrease in joint strength. In contrast the aluminium bronzes and silicon bronzes, where the alloying elements are strong deoxidisers, are largely free from this trouble. As a consequence special filler alloys containing small amounts of powerful deoxidisers such as silicon, manganese, titanium, aluminium and boron have been developed for welding copper and cupro-nickel alloys. Although use of these fillers has greatly reduced weld porosity it has not eliminated the defect so that the resulting radiographic standards of weld deposits remain inferior to those achieved in the welding of steel. Failure to avoid this porosity would suggest that the basic causes are not well understood and this is the view of several investigators. (1) (13) Since the level of deoxidation of the weld pool has proved to be an important factor, the general assumption has been that the steam reaction is largely responsible for porosity as in the casting of copper and its alloys. (14) (15)

The present investigation involves a study of gas-metal reactions and porosity in the inert gas arc welding of copper. The basic aims have been to identify, the mechanism and gas responsible for porosity formation, the factors affecting it and possible ways of its elimination. Two approaches have been adopted to tackle the problem. The first approach has been a quantitative study of the factors affecting weld metal porosity under arc welding conditions. A second complementary approach has been a study of the steam reaction in copper under arc melting conditions.

2 LITERATURE REVIEW

In the following literature review the T.I.G. welding process will firstly be considered with respect to copper welding. This will be followed by a review of the physics of the welding arc, temperature conditions existing in the welding pool and gas metal reactions in general. Finally gas metal reactions and porosity will be considered for the casting and welding of copper.

2.1. T.I.G. TECHNIQUE FOR COPPER WELDING

With the T.I.G. process direct current electrode negative is preferred for copper and its alloys except those containing more than 0.5 Wt.% aluminium, for which alternating current must be used. With the exception of zinc deoxidised copper all the materials require special filler alloys in order to improve weld metal soundness. Appropriate filler wires for use by the T.I.G. or M.I.G. processes are listed in table 2, taken from the Institute of Welding Publication, "Inert Gas Arc Welding". (16)

In the inert gas arc processes argon is the customary shielding gas, but for the welding of copper, nitrogen and helium are possible substitutes. Both helium and nitrogen give higher anode heat inputs per ampere of welding current and thus greater thicknesses can be welded without pre-heat. Although helium is more expensive than argon in the United Kingdom, a recent review on shielding gases (17) points out that it offers considerable economic advantages especially with thicknesses over 3 mm. Using argon shielding in conjunction with a current of 300 amperes and

a welding speed of 3.3 mm per second, (mm/sec) a preheat of 400°C would be necessary to achieve an equivalent penetration possible in helium without preheat. Generally helium reduces pre-heat, makes greater welding speeds possible and simplifies joint design. The use of argon-nitrogen mixtures (18) (19) combines the advantages of both gases. Inglis and Michie (1) however, point out that the advantages of argon-nitrogen mixtures appear to be relatively marginal and only provide a minor alleviation of the heat input difficulty.

2.2. PHYSICS OF THE WELDING ARC

The physics of the welding arc has been well described by several investigators. (20-23) A brief summary of the important factors are given in the following section.

The electric arc used in welding is a high current, low voltage discharge, operating generally in the range 10 to 2,000 amperes and at 10 - 50 volts.

The space between the electrodes of an electric arc can be divided into three regions, which are represented schematically in fig. 1. The cathode fall region is located directly in front of the cathode. This is an extremely thin layer (approximately 10⁻⁵ mm) characterised by a positive space charge. This space charge causes a very steep local voltage rise and consequently a very strong electric field. The anode fall region, located immediately in front of the anode has similar properties. In this region a negative space charge leads to a very steep voltage drop and hence a very strong electric field.

The arc column region lies between the anode and cathode fall regions and occupies the majority of the space between the electrodes. An important aspect of the arc column is its electrical neutrality, each volume unit of the column contains equal numbers of positive and negative charge carriers. A consequence of the electrical neutrality or the absence of a space charge is the presence of a constant electric field in the arc column. The arc column also approximates to thermal equilibrium as a result of almost complete energy exchange between the different gas particles present.

The arc temperature determines many properties of the arc column, amongst others the degree of ionization. The degree of ionization α is defined as the fraction of atoms (or molecules) present in the arc column in the ionized state. The relation between temperature and degree of ionization is given by the Saha equation, which in a simplified form can be written as:-

$$\frac{\alpha^2}{1-\alpha^2} = 3.0 \times 10^{-7} \cdot \frac{T}{P}^{5/2} \exp. \left(\frac{-E_i}{KT} \right)$$

where P represents the gas pressure, E_i the ionization energy and K the Boltzmann constant. Table 3 from Den Ouden ⁽²²⁾ shows the ionization energies of some metals and gases. It is interesting to note in table 3 that metals have relatively low ionization energies compared to gases. As a result of this, in the welding arc the majority of ions contributing to the total current are metal ions.

It is also important to consider the dissociation of molecular gases in the arc. Most molecular gases dissociate in the temperature

range $2,000^{\circ}\text{C} - 10,000^{\circ}\text{C}$. This is within the temperature range of welding arcs as shown in table 4 from Lancaster. ⁽¹³⁾ The dissociation energies of some important molecular gases are given in table 5 from Den Ounden. ⁽²²⁾ Fig. 2 from Ludwig ⁽²⁴⁾ shows that in the case of carbon dioxide, hydrogen and nitrogen, molecular dissociation is complete for all three gases at $10,000^{\circ}\text{C}$.

Another important aspect of the welding arc is the thermal conductivity of gases present in the arc. Fig. 3 from Ludwig ⁽²⁴⁾ shows calculated values of the thermal conductivity of hydrogen, nitrogen, helium and argon for a wide temperature range. The thermal conductivity represents the total contribution due to molecules, atoms, ions and electrons. It can be seen that the thermal conductivity of all four gases increases with temperature. The contributions of the molecular dissociation - diffusion - association mechanism in the atomic gases, hydrogen and nitrogen are readily observed. The higher thermal conductivity of helium and nitrogen compared with argon is also illustrated.

Fig. 4 after Olsen ⁽²⁵⁾ shows the form and temperature distribution in the column of an argon shielded tungsten-copper arc. The region in which the constricted column meets an electrode is called the arc root. The column temperature is highest where it is most constricted, in this instance near the tungsten electrode. The spread of the arc has one important consequence, it results in the formation of a plasma jet which according to Haeceler ⁽²⁶⁾ and Wilkinson and Hilner ⁽²⁷⁾ flows at velocities of the order of 10^5 mm. per second along the axis towards the plate electrode.

The importance of plasma jets is pointed out by Wilkinson, Salter and Milner. (20) They are responsible for metal transfer and for the transport of gas through the arc to the weld metal surface and thus play an important part in mass and heat transfer and gas-metal reactions in general.

2.3. TEMPERATURE CONDITIONS IN THE WELD POOL

The temperature of the weld pool in arc welding has been investigated experimentally for a number of processes and metals using direct (28-34) and indirect methods. (34-38) The most detailed work is by Milner et. al. (33) (34) which involved thermocouple measurements in stationary arc melted pools in tin, lead, aluminium and copper. They showed that 75 - 80 per cent of the weld pool was within 300 - 400°C of the melting point but that there were small regions immediately under the arc at much higher temperatures. Indirect estimates of pool temperatures have been made by several investigators for slag-metal and gas-metal reaction data on the assumption that equilibrium is obtained between whole or part of the weld pool and either slag (28, 30, 35 - 37) or the arc atmosphere. (34) The overall picture to be derived from the available data would appear to be as follows:

- 1) Majority of the weld pool is within 300 - 400°C of the metal melting point.
- 2) A small high temperature zone exists immediately under the arc corresponding to the reaction temperature in gas-metal reactions. The values suggested by Howden and Milner (34) are: -

Iron 2100°C, Copper 1700°C and Aluminium 1900°C. Pollard and Milner (39) have recently suggested 2300°C for CO₂ welding of steel.

- 3) Steep temperature gradients occur in the liquid pool.
- 4) Vigorous stirring takes place in the pool as a result of Lorentz forces. (40)

Very little published information is available about cooling rates in the weld pool although indications can be obtained from full thermal cycles. Belton et. al. (30) reported 600°C/sec at 2300 - 1600°C and 60 - 100°C/sec at 1700 - 1500°C in the submerged arc welding of steel. It is certain that the rates of cooling are normally too rapid for equilibrium to be attained at the freezing point prior to solidification of the weld metal.

2.4. GAS-METAL REACTIONS AND POROSITY IN GENERAL

This section will be divided into two parts. Firstly general considerations such as absorption, reaction, rejection and porosity formation will be reviewed. In the second part a review of gas metal reactions in arc welding will be considered.

2.4.1. GENERAL CONSIDERATIONS

In any fusion welding process gas-metal reactions will occur between the welding atmosphere and the molten weld pool. In arc welding, in particular, these reactions are extremely important since both gas and metal temperatures are high compared with other melting processes.

Gas-metal interaction may take one of two forms, physical (endothermic) solution, or exothermic reaction to form a stable

chemical compound. Exothermic reactions may be further divided into three sub groups, those in which the reaction product is highly soluble in the melt, those in which there is a moderate degree of solubility, and those producing an insoluble compound. The first type of reaction does not prevent the formation of a weld pool, but generally causes embrittlement of the completed joint. The second and third types commonly result in the formation of a slag or a surface scale which may physically interfere with welding.

Endothermic solution does not inhibit fusion, but can result in porosity, either due to supersaturation of the weld pool with a particular gas or by reaction between two gases. It may also in certain cases result in embrittlement of the heat affected zone. The mechanism of endothermic solution is of particular importance in welding, especially of a metal such as copper which is susceptible to porosity formation, and will be further discussed under the sections: -

2.4.2. ABSORPTION

2.4.3. REACTION

2.4.4. REJECTION

2.4.2. ABSORPTION

The solution of diatomic gases in a liquid metal is described by Sievert's law:-

$$S = \sqrt{K.P.} \quad \text{-----} \quad (1)$$

where: -

$$S = \text{Solubility}$$

P = Partial pressure of gas

K = Constant.

The form of the law indicates that the gas dissolves in the dissociated condition, the solution reaction being: -



The corresponding equilibrium constant is

$$K = \frac{[G]^2}{P_{G_2}} \quad \text{_____} \quad (3)$$

where $[G]$ = concentration of gas in the metal
= S.

Hence: -

$$[G] = [S] = \sqrt{K P_{G_2}} \quad \text{_____} \quad (4)$$

and K in equation (1) is identical with the equilibrium constant:-

$$\text{Now, } K = e^{-\Delta G_s / RT} \quad \text{_____} \quad (5)$$

Where ΔG_s = free energy change of reaction (2)

R = universal gas constant

T = absolute temperature.

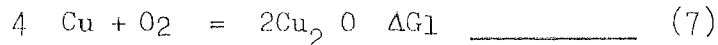
For endothermic solution ΔG_s is positive, therefore K and the solubility increase with temperature. As the temperature of the metal approaches the boiling point, however, its vapour pressure P_m becomes appreciable and for a total pressure of one atmosphere, the solubility becomes: -

$$S = \left[K P_{G_2} (1 - P_m) \right]^{1/2} \quad \text{_____} \quad (6).$$

2.4.3. REACTION

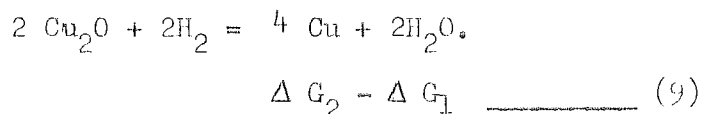
The probability of reactions between gas and metal and between

two gases may be assessed by the use of free energy, temperature diagrams. For example consider the copper-steam reaction:



Where ΔG_1 and ΔG_2 are the free energy changes for the two reactions.

Reversing (7) and adding: -



At the melting point of copper (1083°C)

$$\Delta G_1 = -163,000 \text{ Joule/mole oxygen.}$$

$$\Delta G_2 = -338,000 \text{ Joule/mole oxygen.}$$

$$\Delta G_2 - \Delta G_1 = -175,000 \text{ Joule/mole oxygen.}$$

Reaction (9) therefore proceeds to the right, under equilibrium conditions. Thus copper oxide is reduced by hydrogen at 1083°C with the formation of steam.

2.4.4. REJECTION

In almost all cases, the solubility of dissolved gases undergoes a large drop when metals freeze. For this reason gaseous solutes segregate during freezing. Segregation signifies, therefore, localised increases in the gas concentration of a liquid. Gas bubbles may form in the liquid in those regions where the concentration of a gas rises above the equilibrium concentration (saturation value). Homogeneous nucleation of bubbles, however, requires a high degree of supersaturation ⁽⁴¹⁾ since a surface with its inherent surface energy is formed. As a result, gas

bubbles usually form heterogeneously and, in most cases the nucleation centres lie on the liquid - solid interface. Nucleation at the interface is also furthered by the build up in concentration of the gaseous solutes at both the general interface and in between the dendrite arms as a result of segregation effects.

Gas bubble formation is a nucleation and growth phenomenon. In particular, as mentioned above, the formation of the interface makes bubble nucleation difficult. However, once a bubble has formed and grown to a size greater than its critical radius, its growth becomes progressively easier. This fact is easily shown in the following manner. A gas bubble in a liquid is analogous to a soap bubble, except that it consists of a single liquid-gas interface separating a gas phase from a liquid phase. By analogy with the soap bubble, we may write

$$P_g - P_l = \frac{2\sigma}{r}$$

where σ is the surface energy, P_g is the internal pressure in the gas bubble, P_l is the pressure in the liquid and r is the radius of curvature of the bubble. As the bubble grows in size, its radius of curvature increases. As a result, the pressure differential between the gas in the bubble and the pressure in the liquid falls. This implies (by Sievert's law) that the bubble, as it grows in size, is able to be in equilibrium with a decreasing concentration of gas atoms in the surrounding liquid. Continued growth of gas bubbles is also furthered by the solute concentration gradient which develops in the surrounding liquid as the gas bubble absorbs more and more gas atoms. The concentration falls toward the bubble,

causing a diffusion of gas atoms from the surrounding liquid toward the bubble.

In terms of welding, gas which has been dissolved in the high temperature part of the weld pool is transferred to cooler regions where it forms a supersaturated solution and is normally evolved. Under normal circumstances nuclei are abundant in the weld pool, and therefore bubbles are likely to appear when the concentration of gas is about equal to the solubility at one atmosphere. Bubble formation in molten metal is discussed in some detail by Howden and Milner. ⁽³⁴⁾ Their results are summarised in table 6 for buttons of iron, nickel, copper and aluminium arc melted in argon, hydrogen mixtures. It can be seen that aluminium is very sensitive to small amounts of hydrogen in the arc atmosphere, 0.04 volume per cent (per cent) hydrogen giving rise to spontaneous bubble formation in the liquid pool. For copper this level was increased to 6.8 per cent hydrogen and to 50 and 60 per cent respectively for iron and nickel.

2.5. GAS-METAL REACTIONS IN ARC WELDING

Hydrogen, nitrogen and oxygen are the gases commonly found in metal systems and all three are frequently involved in reactions in the weld pool because they are either present in the original shielding gas or are entrained into it during the welding process. In arc welding in particular, they create bigger problems than in other metallurgical processes because, as Pollard and Milner ⁽³⁹⁾ point out, there are a number of factors which cause the gas-metal reactions to occur with greater

intensity. The arc atmosphere is at a high temperature (20,000°C) and plasma jets in the arc (velocity $10^5 - 10^6$ mm/sec.) transport the reactive constituents rapidly to the molten metal surface. In addition the molten metal is highly superheated particularly over a small area under the arc and electromagnetic forces within the molten metal, transport the constituents to and from the reacting surface. As a consequence, weld metal often contains contents equivalent to saturation in the liquid state at the melting point.

A series of significant studies on the gas-metal reactions occurring in arc welding have been by Hilner and his associates (34, 39, 42, 43) and these have yielded not only a great deal of data but also give an insight into the basic mechanisms operating. The following review is based largely on their work.

2.5.1. GAS ABSORPTION IN THE WELD POOL

As already pointed out in section 2.4.2. the solution of a diatomic gas like hydrogen in a metal is described by Sievert's law so that its equilibrium concentration at any particular temperature is proportional to the square root of the partial pressure. It is also strongly temperature dependent and shows an increase with temperature rise until it approaches the metal boiling point. At this juncture the increasing metal vapour pressure produces first a reversal and ultimately a reduction to zero. Hydrogen solubility curves up to the boiling point for a number of metals are plotted in figure 5, for a hydrogen

partial pressure of 0.01 atmosphere. When Howden and Milner (34) arc melted buttons of iron, nickel, copper and aluminium in an argon, hydrogen atmosphere, they found that although the hydrogen content of the molten metal was proportional to the square root of the hydrogen partial pressure, it corresponded approximately to the maximum possible solubility, i.e. the peak values in fig. 5. Since the temperature of the majority of the weld pool was well below these peak values they proposed that absorption was occurring in the high temperature zone immediately under the arc. Subsequently it was being transported rapidly into the cooler parts of the pool as shown schematically in figure 6. Owing to the relatively slow rate of desorption in the pool, the overall hydrogen content approached that of the high temperature region. This meant that in their experiments the hydrogen content of the pool exceeded the melting point solubility by factors of 1.4 for iron, 1.3 for nickel, 3.7 for copper and 54 for aluminium.

Care must be exercised in applying these results to welding conditions in a detailed quantitative manner. However, it is reasonable to conclude that in welding also the liquid metal gas content will be dominated by the gas absorption occurring in the high temperature zone under the arc. As a result the weld pool will be rapidly supersaturated with respect to the partial pressure of the gas in the arc atmosphere. Evidence of this can be found not only in the absorption of hydrogen but also in the absorption of nitrogen in the arc welding of Iron, (44, 45, 46, 47) nickel (48) and Copper. (49) A typical nitrogen absorption curve for metal gas arc welding of mild steel, after Flake and Jordan, (44) is shown in figure 7. It can be seen that the observed nitrogen

absorption is well in excess of the equilibrium value at the expected weld pool temperature. This work is confirmed by Uda and Wada (47) who showed that the solubility of nitrogen in arc melted iron and iron alloys was about 20 times higher than that of non-arc-melted iron and iron alloys. This confirms that nitrogen atoms produced in the arc result in much greater nitrogen absorption than would be possible with molecular nitrogen.

The absorption of oxygen has also been studied in detail by Salter and Milner (42) for the titanium - oxygen - argon system. They came to the conclusion that the rate controlling process was the diffusion of oxygen across a stagnant boundary layer of gas adjacent to the molten metal. They explained their results using a modification of Ficks' law of diffusion:-

$$q = - \frac{D}{R T} \frac{dP}{dx} \quad (10)$$

where: - D = diffusion coefficient of oxygen through argon.

dP/dx = partial pressure gradient across
the boundary layer.

R & T = universal gas constant and
absolute temperature.

q = rate of diffusion of oxygen across
the boundary layer.

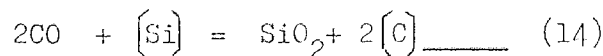
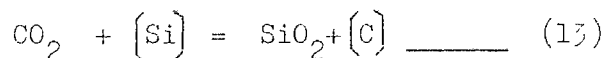
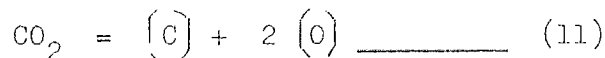
This model was in accord with the experimental determinations of time and oxygen partial pressure, which both resulted in a linear increase of oxygen absorption. They found that the shielding gas velocity however, had little effect on the rate of reaction. This

was explained by the fact that the plasma jet had a velocity of the order of 10^5 mm/sec. compared to a shrouding gas velocity only of the order of 10^3 mm/sec.

In practical terms the described work means that the level of contamination of the shielding gas by hydrogen, nitrogen or oxygen in their various forms must be maintained at very low levels in order to avoid excessive absorption by the weld metal.

2.5.2. GAS-METAL REACTIONS IN THE WELD POOL

In a detailed study of CO_2 welding of steel, Pollard and Milner (39) have shown that even when complex gas metal reactions occur in the weld pool their progress is determined largely by events at the high temperature zone at the arc roots. They found that the surface layers of both the pool and electrode tip rapidly attained a thermodynamic equilibrium corresponding to a temperature of about $2,300^\circ C$. The reactants were then transported rapidly throughout the weld pool and droplets so as to produce an overall equilibrium in a few seconds. The particular reactions that they studied included not only the carbon-oxygen interactions but also those involving deoxidants.



Since the effective reaction temperature is higher than the actual weld pool temperature the pool is supersaturated with respect to both carbon and oxygen, and so will react to form carbon monoxide in an attempt to establish local equilibrium. This effect is

normally eradicated in steel making practice by additions of deoxidants such as silicon but in welding the high temperature inevitably makes them much less effective. Their findings highlight the fact that carbon monoxide formation is a major problem in the welding of steels and necessitates higher deoxidant levels in the weld metal in order to avoid its effects.

While this work relates to the particular reactions in the CO₂ welding of steel it is evident that a similar situation exists in other systems where gas-metal reactions involve chemical combination.

2.5.3. GAS RETENTION AND POROSITY IN ARC WELDING

With their arc melted buttons Howden and Milner⁽³⁴⁾ found that between 50 - 75% of the hydrogen present in the weld pool was retained in the solidified buttons. In their experiments it resulted in the buttons containing twice the solid solubility at the melting point for iron and nickel, eight times the solubility for Copper and 450 times the solubility for aluminium. Again these results apply strictly to hydrogen-metal systems under arc melting conditions but they do indicate the likely situation in welding because both melting and solidification conditions are comparable.

The formation of porosity in weld metal is a complex issue as Salter and Milner⁽⁵⁰⁾ show and its characteristics vary widely with individual gas-metal systems. In their experiments hydrogen was added in increasing amounts to the argon stream until porosity could just be detected by radiography. The values at which this occurred for a welding speed of 3 mm/sec. are

shown in table 7. The levels needed were less than 0.3% for aluminium and magnesium, 0.7-1.0% for copper and 25 - 30% for nickel. They also investigated the effect of welding speed (varying the current to give a constant bead width) on the hydrogen threshold level. No discernible variation was detected with magnesium, aluminium or nickel in the range 1.0 - 9.0 mm/sec, however with copper the hydrogen threshold varied from less than 0.3% at 0.5 mm/sec, to 5 - 5.3% at 9.0 mm/sec. The morphology of the porosity also varied considerably. It was spherical in the case of aluminium, "herring-bone" in both copper and magnesium, and centre line in nickel. In all cases the level of porosity at any particular partial pressure of hydrogen was reduced by increasing the welding speed.

In the case of nitrogen porosity in the CO₂ welding of steel, O'Brien and Jordan (45) obtained a threshold value 1-8% but other workers have suggested levels as low as 0.5%. (51) Again the level of porosity at any particular partial pressure of gas is reduced by increasing the welding speed.

In the following sections gas-metal reactions will be looked at specifically for the casting and welding of copper and its alloys.

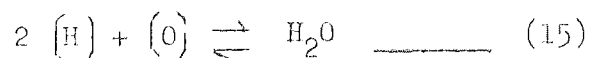
2.6. GAS-METAL REACTIONS AND POROSITY IN COPPER CASTING

Reviews of this topic have been made by several authors. (14) (52-54) The principal gases found in copper and its alloys are hydrogen, oxygen, steam, sulphur dioxide and carbon monoxide. Nitrogen has been shown to be insoluble in copper below 1400°C. (55) There seems to be general agreement that the most important porosity

producing gases are hydrogen and steam.

Hydrogen dissolves in copper according to the Sieverts relationship mentioned in section 2.4.2. Table 8 from Smithells (11) summarises the solubility of hydrogen in copper for a wide range of temperatures. Since determinations can be subject to variation, confirmatory data from four sources (56-59) is given. The solution is typically endothermic with the solubility falling with decreasing temperature and showing a sharp decrease at the freezing point, i.e. 6 to 2 ml per 100 grammes at E.T.P. This sudden fall of hydrogen solubility on solidification, produces a build up of the hydrogen level at the solid liquid interface and can lead to localised supersaturation of the melt. When this occurs bubbles nucleate at the interface and become entrapped as pores in the solidifying metal. Allen (54) has reported that hydrogen porosity occurs in cast copper in the form of elongated pores extending to the ingot centre, and can be eliminated by flush degassing of the melt.

Recognition that porosity can also be formed in copper alloys by compound gas formation was largely due to Allen. (54) He concluded that the uniformly distributed pores present in commercial copper which are not removed by flush degassing were due to steam produced during solidification by reaction of hydrogen and oxygen dissolved in the melt. The governing reaction was as follows: -



and the equilibrium controlled by the expression: -

$$K = \frac{\text{ [H] }^2 \text{ [O] }}{p\text{H}_2\text{O}} \quad \text{_____} \quad (16)$$

where it is assumed that the activity of oxygen can be taken as weight per cent. The equilibrium value of $[H]^2 [O]$ falls rapidly with temperature particularly in the region of the melting point. Consequently on solidification a build up of the oxygen and hydrogen content occurs at the solid liquid interface. Eventually the corresponding internal pressure of water vapour exceeds that for nucleation of bubbles and these form in the region of the interface and give rise to porosity in the cast ingot. This type of reaction gas porosity can be avoided by maintaining the $[H]^2 [O]$ product at a low level and one way of doing this is by use of powerful deoxidants such as silicon, aluminium and titanium which reduce the value of $[O]$.

From these considerations it is evident that porosity can form in copper alloys either as a result of high internal pressure of hydrogen alone or a high value of the $[H]^2 [O]$ product, giving rise to steam porosity. Important factors for both forms of porosity are the hydrogen and oxygen contents of the melt prior solidification. The level of these will be determined by the reaction of the copper melt with the hydrogen and water vapour in the atmosphere in contact with it. Under reducing conditions the oxygen content will be low and hydrogen porosity will be most likely but under oxidising conditions the oxygen content will be high and steam porosity will be favoured. Allen and Hewitt (15) studied the equilibrium of steam and copper in considerable detail. They showed that the melt hydrogen content was controlled by the expression:

$$H_m = A \sqrt{\frac{pH_2O}{[O]}} \quad (17)$$

where:-

W_m was in mg. hydrogen/100g.

p_{H_2O} in atmosphere (1 atmosphere = 760 mm mercury)
and (O) in weight per cent.

Values of A for various temperatures are given in Fig 8. They also examined the relationship of hydrogen and oxygen contents of a copper melt in equilibrium for constant water vapour pressure and varying temperature. The effect of increasing the temperature with an atmosphere of a given steam content was to increase the hydrogen content of a melt. A rise of $100^{\circ}C$ increased the hydrogen content of the copper by about 50 per cent. They also found no connection between the oxygen content of the melt and the amount of porosity in copper buttons which supports the opinion that, provided the copper contains enough oxygen to react with the hydrogen present, the porosity of the casting depends on the quantity of hydrogen in the metal.

Formation of other reaction gases in copper alloys such as sulphur dioxide and carbon monoxide have been reported by Floe and Chipman ⁽⁶⁰⁾ and Pearson, Baker and Child ⁽⁶¹⁾ respectively. In copper nickel zinc alloys carbon monoxide porosity resulting from the joint presence of carbon and oxygen in the melt seems to be of considerable importance.

2.7. GAS-METAL REACTIONS AND POROSITY IN THE WELDING OF COPPER AND ITS ALLOYS

Published literature ⁽¹⁾ ⁽¹²⁾ ⁽¹³⁾ leaves no doubt that in the absence of deoxidants such as aluminium, titanium,

silicon, manganese and boron severeweld metal porosity is unavoidable in the inert gas arc welding of copper. Furthermore the radiographs and micrographs indicate that the porosity invariably takes the form of randomly distributed spherical pores. Understandably the general assumption has been that since oxygen is an important factor the steam reaction is largely responsible for the porosity as in the melting and casting of copper. Some support for this view might be gained from Bartles' (62) study of weld heat affected zone porosity in the inert gas arc welding of tough pitch copper where the porosity was present as spherical pores associated with cuprous oxide inclusions and dependent on the oxide content of the metal. In a later paper by Taylor and Burn, (12) Bartle gave a contribution of some work at B.W.I.A. (now Welding Institute) which showed a correlation between oxide particle size in the parent metal, and the occurrence of severe edge of weld porosity in the weld metal of welds made in tough pitch copper, this porosity having a deleterious effect on strength.

Lancaster (13) has reported that analysis of the gas in the pores of copper welds reveals that it is largely hydrogen, a view also held by Taylor and Moore. (63) The simultaneous presence of both oxygen and hydrogen in the weld pool has yet to be explained.

The most significant contribution to the study of gas-metal reactions and porosity in the inert gas arc welding of copper was

by Milner and his associates. (33) (42) (50) This work has already been described in section 2.5.3. where it was shown that in the case of copper as little as 0.70 - 1.0 per cent hydrogen in the arc atmosphere was sufficient to cause porosity. This is a level of hydrogen which could occur under practical conditions due to contamination of the arc shroud with water vapour or hydrocarbons. This might not only suggest the formation of hydrogen porosity in practical circumstances but also explain how in the presence of oxygen the steam reaction can occur in the weld pool. Salter and Milner (50) also found in the case of copper, in particular, an interaction effect of hydrogen contamination and welding speed. The results are summarised in fig.9 where the porosity level is assessed by density determinations. It can be seen clearly that hydrogen porosity is less likely at higher welding speeds.

Radiographs of these welds revealed the typical "herringbone" porosity already described. This would suggest that hydrogen alone is not responsible for porosity in copper welding since that found in practice usually takes the form of rounded pores.

Another point of significance from Salter and Milner's (50) results is that sound melt runs were achieved, in the inert gas arc welding of copper, with relative ease.

It has been considered that nitrogen can be used as a shielding gas for welding copper without special precautions because it is insoluble in copper below 1400°C (55) and the possibility of substituting nitrogen for argon has been investigated. (18) (19) (64) (65) However, copper nickel castings produced by Ahmed and

Kahn (66) were found to be prone to nitrogen porosity when melted in an indirect arc furnace. As pointed out by Ames and Khan (66) if nitrogen is present in the dissociated or monatomic form nitrogen porosity is a possibility. Also the work of Kobayashi (49) showed that in the metal inert gas arc welding of copper, porosity was produced when O.F.W.C. filler wire was used in argon, nitrogen mixtures. This porosity was subsequently reduced and totally removed by the addition of titanium to the welding wire. Evidence of this is shown in fig. 10(a). Fig. 10(b) also shows an increase in weld metal nitrogen content with increasing titanium and with increasing nitrogen in the argon shielding gas.

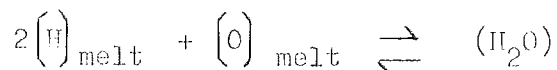
It could be argued that titanium acts only as a deoxidiser to counteract steam porosity present from the nitrogen. It is felt however that the work of Kobayashi (49) strongly indicates that nitrogen porosity is likely to occur and warrants further investigation. In this respect it is worth considering some work on nickel. Fease, Brien and Legrand (48) showed that as little as 0.20 percent nitrogen added to the helium shielding gas was sufficient to cause porosity in commercially pure nickel melt runs. Milner, (67) also working with nickel, showed that butt welds exposed at the root to the atmosphere were porous whereas tightly clamped backed welds were much less porous.

3. INVESTIGATIONAL WORK

There is clearly a need to investigate the nature and origin of weld metal porosity in copper. The indications from the literature are that it arises from the occurrence of the copper - steam reaction in the weld pool. Although additions of deoxidising elements markedly reduce porosity they do not eliminate it. This suggests that the effect is neither well understood nor under control. In spite of the fact that nitrogen is virtually insoluble in copper and has been used as a shielding addition, evidence is available which suggests that this gas could be a possible source of porosity in the arc welding of copper. Little work has been carried out on the effect of welding variables on porosity formation. Since investigators who have simulated welding by the use of melt or bead on plate runs have had little trouble producing sound weld metal there would appear to be some effect due to welding set up.

Two approaches were used to elucidate the mechanism of porosity formation in the present work. The first involved a quantitative assessment of the effect of welding parameters, and arc atmosphere and plate composition with a view to determining the significant factors affecting porosity. In the first instance this was carried out using melt runs and butt welds in the tungsten inert gas arc process. To maximise the information to be gained from these experiments the statistical technique of factorial design was used involving two extremes of each of the variables to be considered. Subsequently specific experiments were carried out to provide details of information with factors which emerged as significant.

The second approach involved a study of the copper-steam reaction in the weld pool under the conditions of arc welding using buttons of copper melted in a box using a tungsten electrode and variable arc atmosphere. The reaction investigated was that of Allen and Hewitt (15):-



It is anticipated that this will elucidate the mechanism of the steam reaction in the weld pool and indicate what part it plays in porosity formation in the arc welding of copper.

3.1. QUANTITATIVE STUDY OF THE FACTORS AFFECTING WELD METAL POROSITY IN THE INERT GAS ARC WELDING OF COPPER

The first stage in the investigation was an examination of the porosity occurring in practice, and a quantitative assessment of the influence of the main welding and material variables. A review of the problem and previous published work relating to it, suggested that the following variables warranted study:-

- i) Deoxidised state of the parent metal.
- ii) Composition of the shielding gas.
- iii) Efficiency of shielding gas coverage.
- iv) Weld preparation.
- v) Welding current.
- vi) Welding speed.
- vii) Welding voltage.

In view of the large number of variables and their probable interaction, it was decided to conduct a series of experiments based

on a statistical design. This permitted both concurrent variation of the selected variables and the obtaining of the maximum information from the experiments carried out. The technique adopted was factorial design which is adequately explained in Davies. ⁽⁶⁸⁾ The test results were examined by analysis of variance using the ICL 1905 computer statistics package. It was decided to select six of the variables and keep voltage constant, its main effect probably being to alter shielding gas efficiency which is already covered. Two levels of each of the six variables were chosen. This represents 2^6 (64) experiments. The number of experiments was reduced by using a standard half replicate. The statistical design for the 32 experiments is shown in table 9. Initially two levels of plate composition were selected, electrolytic tough pitch (E.T.P.) and deoxidised high phosphorus (D.H.P.) in order to give two levels of oxygen and include the normally used deoxidised state. At a later stage oxygen free high conductivity copper (O.F.H.C.) was also included using a quarter replicate analysis, the design of which is shown in experiments 1 - 16 of table 9. Addition of water vapour to the shielding gas was chosen as a variable since this would provide both a source of hydrogen and oxygen as well as representing a practical variable. Shielding gas efficiency was varied by adjustment of the inert gas flow rate. Inclusion of melt runs and butt welds as weld preparations was done not only to assess its importance but also to assist in the establishing of conditions for laboratory work representative of welding practice.

3.1.1. EXPERIMENTAL TECHNIQUE AND RESULTS

In principle the experiments involved making full penetration weld runs in 3mm thick copper plate using the T.I.G. autogenous welding process at two levels of each of the six selected variables. (On the basis of previous work with Cu-Cr sheet ⁽⁶⁹⁾ a specimen plate size of 300 mm x 300 mm was taken as representing an acceptable approximation to semi-infinite plate conditions. (Two 150 mm x 300 mm plates for butt welds.) Welding was carried out using the direct current process by traversing the welding torch along the centre line of the plates, these being clamped rigidly in a jig with a thin copper backing strip. In the case of the butt welds, closed square butts were used and the edges of the plates were cleaned by scratch brushing. In order to prevent weld cracking the butt welds were tacked at each end prior to welding. Plate surfaces were also cleaned by scratch brushing prior to welding.

Preliminary experiments were conducted to establish suitable combinations of current, voltage, welding speed and shielding gas flow rate. High purity argon (99.999%) was used as the shielding gas and water vapour introduced by bubbling through water at room temperature. A level of 0.0005 g/litre was chosen as the upper limit, and this was obtained by mixing streams of "wet" and "dry" argon in suitable proportions. In each case the water vapour level was checked by means of the weight change of three calcium chloride tubes in series. Details of the levels of the variables in the series of experiments are given in table 10. The order of experi-

mentation for the half replicate was carried out in a random manner. This is necessary because, with experiments done sequentially, there may be a trend in some parameter throughout the sequence of trials - the ambient temperature may be rising, an instrument may be deteriorating or an operator's skill may be increasing. These are all things trivial in themselves but should be guarded against in proper experimentation. In order to minimise these effects it is a useful safeguard to randomise the experiment. In all the experiments the porosity of the weld metal was assessed by X-ray radiography and careful density determination and the oxygen content was determined by vacuum fusion analysis.

Details of the experimental results for the half replicate experiment are given in table 11. An analysis of variance was carried out on the density results to determine which of the single factors and which first order interactions significantly affected the weld metal density. A summary of the calculated significance levels is given in table 12 where it can be seen that four of the single factors and six of the first order interactions achieved the 1 per cent significance level. An estimate of the magnitude and sign of the effect of all six single factors on weld metal density is shown in table 13. These figures were calculated as the difference in means of going from a low to a high level of each of the six variables.

In general porosity is increased (density decreased) by increasing water vapour content of the shielding argon, and by changing from D.H.P. to E.T.P. copper. Porosity is reduced (density

increased) by changing weld preparation from butt welds to melt runs and by increasing the welding speed. Over the range examined neither current nor argon flow rate have significant effects on porosity. Of the significant interactions the most important effects would be those associated with the significant single factors, namely: water vapour - welding speed, oxygen content - water vapour, weld preparation - welding speed and oxygen content - welding speed. These interactions are examined further in the next sections. Examination of the weld radiographs showed that the porosity was invariably in the form of scattered spherical pores and metallographic studies of weld metal sections showed that some of these pores were associated with oxide inclusions. This feature is illustrated clearly in fig. 11. which shows weld metal porosity in some cases associated with the Cu/Cu₂O eutectic. This micrograph was taken from weld number 5 which was an E.T.P. butt weld. In contrast fig. 12. shows that the edge of an E.T.P. melt run (experiment number 8) was virtually free from porosity. The weld metal in this case was also free from porosity. In order to gain more evidence about the nature of the porosity, melt runs were also made with E.T.P. and D.H.P. plate with a shielding gas atmosphere containing 2 per cent hydrogen. The D.H.P. sample showed the characteristic herringbone type of porosity on solidification with elongated pores stretching from fusion line to the weld centre line. By contrast the E.T.P. sample produced a great deal of spluttering during welding and scattered spherical porosity on solidification.

3.1.2. THE EFFECT OF BASE MATERIAL

In order to extend the range of base materials in the survey, eight weld runs were made with O.F.H.C. copper plate under identical conditions to the eight runs made with D.H.P. in experiment numbers 1 to 16. This enabled a quarter replicate to be carried out comparing O.F.H.C. with E.T.P. The results of the welds are given in table 14 together with the complementary E.T.P. figures. Analysis of these data showed that the significant single factors were the same as those in the experiments involving E.H.C. copper, being similar in sign and magnitude. An estimate of the effect of water vapour content and base material can be made by considering the data from the 40 welds so far carried out. The differences between the mean densities for low and high water vapour levels for the three types of copper are given below: -

D.H.P.	1.08 g/cc
O.F.H.C.	1.62 g/cc
E.T.P.	2.22 g/cc.

From these figures it can be seen that the effect of water vapour on porosity increases progressively with D.H.P., O.F.H.C., and E.T.P.. The initial oxygen contents of the different grades of copper were 0.035 Wt.% for E.T.P. copper, 0.0003 Wt.% for O.F.H.C. copper and 0.0010 Wt.% for D.H.P., The latter also contained 0.04 Wt.% phosphorus.

3.1.3. THE INTERACTION OF WELDING SPEED AND WATER VAPOUR IN THE ARGON SHIELDING GAS

A series of weld melt runs were made in 3 mm thickness O.F.H.C. copper (300 mm square) sheet for four welding speeds

(2 - 8 mm/sec.) and five levels of water vapour (67 - 1340 volume parts per million) at a constant argon flow rate of 14.25 litres per minute. The 1340 v.p.m. mixture was made up as previously described however the other mixtures were obtained from British Oxygen Company (special gases division) with certificates of analysis which were guaranteed for one third of the cylinder pressure. In order to obtain full penetration runs the currents were varied from 265 - 365 amps in the knowledge that current had no significant effect on porosity. The results of these tests are plotted as density against water vapour content for the four speeds in figure 13. While in all cases the porosity increased with increasing water vapour content there is clearly a very marked speed effect. At any particular water vapour level the amount of porosity decreases as welding speed increases. There is a threshold level of water vapour for porosity which increases with speed, reaching over 500 v.p.m. at a speed of 8 mm/sec.

3.1.4. THE INTERACTION OF WATER VAPOUR IN THE ARGON SHIELDING GAS AND BASE MATERIAL

Melt weld runs were made in E.T.P., O.F.H.C. and D.E.P. copper plate (3 mm x 300mm x 300 mm) with argon water vapour mixtures containing 135, 260 and 540 v.p.m. water vapour at a welding speed of 4 mm/sec. and argon, water vapour flow rate of 14.25 litres per minute. A current of 325 amps and a voltage of 11 volts were used. In this section and the following welding sections a different batch of E.T.P. copper containing 0.028 wt %

oxygen was used. The results are plotted in terms of density and water content of the argon for the three materials in figure 14. In general the trends confirm the analysis of the 40 welds already described with a progressive increase of porosity at each water vapour level with change from D.H.P. to O.F.H.C. and E.T.P. However, there is a change of behaviour at the higher water vapour levels with E.T.P. copper since this material exhibits a drastic increase in porosity.

3.1.5. THE INTERACTION OF PULSE MATERIALS AND WELDING SPEED

Melt runs were made in E.T.P., O.F.H.C. and D.H.P. copper plate (3 mm x 300 mm x 300 mm) using an argon, 540 v.p.m. water vapour shielding gas at a flow rate of 14.25 l/min. The welding speed was varied in the range 2-8 mm/sec and currents in the range 265 to 365 amps were used with a voltage of 11 volts. To avoid repetition corresponding results already obtained in section 3.1.3. and 3.1.4. were again used in this section.

The results are plotted in terms of density and welding speed for the three materials in figure 15. It can be seen for all three materials that increasing the welding speed results in increased density. At all four speeds E.T.P. copper gives the lowest density values, however the densities of D.H.P. and O.F.H.C. copper are very similar except at the lowest speed of 2 mm/sec. when D.H.P. gives a higher density than O.F.H.C.

3.1.6. THE EFFECT OF WELDING SPEED ON THE COPPER-STEAM REACTION

In order to examine further the effect of speed upon the steam reaction, melt runs were made in E.T.P. copper (3 mm x 300 mm x 300 mm) using a 2 per cent hydrogen-argon shielding gas at 14.25 l/min for nine welding speeds between 4 and 20 mm/sec. The welding current was adjusted in the range 325 to 570 amps to maintain full penetration and a constant voltage of 11 volts was used throughout. During welding vigorous bubbling took place in the weld pool and the resulting weld metal showed the typical random spherical pores associated with the steam reaction. Vacuum fusion analysis of the weld metal confirmed that the oxygen content had been appreciably reduced below the initial level of 0.028 Wt.%. The weld metal oxygen contents are plotted against welding speed in figure 16. At low speeds the oxygen content was reduced from 0.028 to 0.012 Wt.% but with increasing speed the weld pool oxygen content rose to a value of 0.02 Wt.% at 10 mm/sec. Further increase in speed brought no further change so that the reduction of 0.008 Wt.% in the oxygen content must represent a limiting value.

3.1.7. THE INTERACTION OF WELDING SPEED AND WELD PREPARATION

This interaction was examined in the hope that it would elucidate the reason for the porosity encountered with butt welds. E.T.P. copper was chosen because of its being most sensitive to porosity and the argon flow rate was increased to 22 l/min. to ensure maximum coverage of the plate surface. Melt runs

and butt welds were made for welding speed of 2, 4, 6 and 8 mm/sec. and currents of 265 -365 amps, the shielding gas being pure argon. Again a total welded plate size of 3 mm x 300 x 300 mm was used and a constant voltage of 11 volts. Butt welds were prepared in the manner described in the factorial experiments. The results for both types of weld preparation are plotted as density and welding speed in figure 17. The melt runs remain sound for the four speeds whereas the butt welds show increasing porosity as the speed rises. This increased effect with higher speeds is the reverse of that encountered with the welding speed - water vapour interaction and suggests a different type of porosity mechanism. It is interesting to note that the densities of the E.T.P. butt welds in this section were considerably higher than those obtained in section 3.1.1. A different batch of E.T.P. having a lower initial oxygen content (0.028 Wt.% compared with 0.035 Wt.%) was used in this section. This emphasizes the deleterious effect of oxygen already mentioned.

3.2. THE OCCURRENCE OF NITROGEN POROSITY IN THE T.I.G. ARC WELDING OF COPPER

The statistically designed experiments revealed that butt welds produced in the absence of any added water vapour were porous in contrast to melt runs. The significant interaction of welding speed and weld preparation also indicated that the amount of porosity increased with increased welding speed. This suggests that butt welds involved entrainment from the arc atmosphere, the amount increasing with welding speed. This could obviously involve

water vapour but would certainly involve nitrogen. Although the published data for conventional melting conditions indicates no solubility up to 1400°C the recent work of Kobayashi (49) for M.I.G. welding suggests that nitrogen porosity can occur under arc welding conditions. Accordingly it was decided to investigate the occurrence of nitrogen porosity in the T.I.G. welding of copper.

3.2.1. POROSITY IN NITROGEN SHIELDED T.I.G. WELDING OF COPPER

Some preliminary experiments were conducted with nitrogen shielded T.I.G. arc welding of O.F.H.C. copper sheet because of the possibility of nitrogen porosity playing an important role in welding. Belt runs were made at speeds of 2, 4, 6 and 8 mm/sec. with currents of 265 - 365 amps, 11 volts, and nitrogen flow rates of 14.25 l/min. In order to conserve material, a smaller plate size of 3 mm x 300 mm x 114 mm was used throughout the nitrogen welding experiments.

As the work of Kobayashi (49) had suggested appreciable weld metal porosity was obtained. The results are plotted as density against welding speed in figure 16 where it can be seen that the extent of porosity decreases with increasing speed. This would appear to confirm that the nitrogen effect is a typical gas-metal reaction because the change with speed is similar to that obtained with water vapour, figure 13 and with hydrogen in Salter and Milner's work (50).

The morphology of the porosity differed quite considerably from the spherical porosity due to water vapour and the herringbone

porosity due to hydrogen as can be seen in the radiographs in figure 19. Macrosections from the weld metal also showed an unusual distribution with a clearly defined region of coarse porosity at the surface and fine porosity in the weld metal interior, figure 20. While there is little doubt that nitrogen porosity can be distinguished in its severe form with a 100 per cent nitrogen atmosphere, it might not be possible to identify it when it appears to a small extent. Thus porosity arising from small amounts of nitrogen entrained into the shielding gas might easily be confused with steam porosity. For this reason it was decided to conduct further experiments using T.I.G. and T.I.G. plus filler wire welding techniques to determine the effects of small additions, up to 1.0 per cent, of nitrogen to the argon shielding gas.

3.2.2. EFFECT OF SMALL NITROGEN ADDITIONS AND WELDING SPEED ON THE DENSITY OF T.I.G. WELDED COPPER

T.I.G. melt runs were produced on O.F.H.C. copper plate at welding speeds of 2 and 6 mm/sec. and currents of 250 and 315 amps respectively. A constant voltage of 11 volts and gas flow rate of 15 l/min was used throughout. Accurately calibrated rotameters were used to make up argon, nitrogen mixtures in the range 0 to 1.0 per cent nitrogen (super pure). The melt runs produced using these shielding gas mixtures were examined by radiography, metallography and density determinations. Figure 21 indicates clearly the effect of nitrogen and welding speed upon the density of O.F.H.C. copper melt runs. It can be seen that as little as

0.1 per cent nitrogen added to the argon shielding gas is sufficient to produce porosity at both welding speeds. For any given level of nitrogen in the argon, increasing the welding speed reduces the amount of porosity. Radiography and metallography revealed that the porosity was identical to that obtained in Figure 19(a) of the previous section.

In an attempt to confirm that the porosity in these welds was nitrogen gas, vacuum fusion analysis was carried out on a sample of the weld produced using 0.4 per cent nitrogen in argon at a speed of 2 mm/sec. 4.5622 g. of this weld metal was found to contain 0.13 cc of nitrogen. Assuming that all the porosity present in the weld metal accounted for the nitrogen the following calculation showed that 0.13 cc of nitrogen would be found in the weld metal:-

$$\text{density of copper} = 8.9 \text{ g/cc}$$

$$\text{density of weld} = 6.6 \text{ g/cc}$$

$$\% \text{ Unsoundness } = \underline{26.4\%}$$

$$\text{Wt. of sample used in analysis} = 4.56 \text{ g}$$

$$\therefore \text{ Vol.} = \underline{0.51 \text{ cc}}$$

Assuming all porosity is nitrogen at N.T.P.:-

$$\therefore \text{ Vol Nitrogen} = \frac{26.4}{100} \times 0.51 = 0.13 \text{ cc}$$

Unfortunately, the equipment used in vacuum fusion analysis measured nitrogen by difference and although the above strongly inferred that the porosity was due to nitrogen it was not direct evidence. For this reason advantage was taken of a special

technique available at The Welding Institute for analysis of gases in pores. The technique, which is described by Carter,⁽⁷⁰⁾ involved fracture of selected pores under high vacuum and analysis of the evolved gas by use of a small mass spectrometer. Two regions of a sample of the above mentioned weld metal were found to contain 91 and 94 per cent nitrogen.

3.2.3. EFFECT OF FILLER WIRE COMPOSITION AND SMALL NITROGEN ADDITIONS ON THE DENSITY OF T.I.G. WELDED COPPER

The previous section has shown that small nitrogen additions to the argon shielding gas cause nitrogen porosity in the weld metal. To investigate whether this porosity could be reduced by nitride forming elements two commercially available filler wires, nitrofil (containing 0.20 wt.% aluminium, 0.10 wt.% titanium) and argofil (containing 0.18 wt.% silicon, 0.23 wt.% manganese) were used to produce bead on plate runs on O.F.H.C. copper. The two wires represent sources of strongly and mildly denitriding additions respectively.

Nitrogen (super purity) was added to the argon shielding gas to make up mixtures in the range 0 to 1 per cent nitrogen using an overall flow rate of 15 l/min. A voltage of 12 volts was employed and a current in the range of 240 - 273 amps. A welding speed of 2 mm/sec. was used in conjunction with a wire feed speed of 20 mm/sec. at a feed angle of approximately 30°.

Using nitrofil sound welds were obtained throughout the nitrogen range whereas argofil resulted in a fall in density to a level of 8.5 g/cc. These results are illustrated in figure 22

where weld metal density is plotted against the nitrogen content of the shielding gas. Although the argofil welds were porous throughout the nitrogen range they contained less porosity than the corresponding O.F.H.C. T.I.G. welds shown in figure 21. This indicates that, to a limited extent, argofil also acts as a denitrider.

3.2.4. CONTROLLED ATMOSPHERE ARC MELTING OF O.F.H.C. COPPER IN AN ARGON NITROGEN ATMOSPHERE

It has been demonstrated so far in section 3.2. that nitrogen absorbed from the arc atmosphere resulted in porosity in the weld pool. Controlled atmosphere arc melting of copper in an argon nitrogen mixture has been carried out to investigate the effect of nitrogen in an arc melting situation. The experiments were carried out in an arc melting box which is described in detail in the next section. O.F.H.C. copper buttons were arc melted for periods of 0.5, 1, 2 and 4 minutes in an argon 1 per cent nitrogen (super purity) mixture at a flow rate of 10 litres per minute. A current of 300 amps and 11 volts were used for the four melts. The results of these experiments are given in table 15 together with the results of similar experiments using super pure argon as the shielding gas. The density measurements are shown against arcing time for the two atmospheres in figure 23. It can be seen that 1 per cent nitrogen reduces the density to about 0.3 g/cc compared with the sound melts in super pure argon.

3.3. THE STEAM REACTION IN COPPER UNDER ARC MELTING CONDITIONS

The T.J.G. welding experiments outlined in section 3.1. showed that the presence of water vapour in the arc atmosphere resulted in characteristic steam porosity in the weld metal. The extent of the porosity was dependent on, the water vapour content of the arc atmosphere, the oxygen content of the base material, the welding speed and interactions of these factors. In the case of B.P.P. copper the presence of hydrogen in the arc atmosphere resulted in the steam reaction occurring in the weld metal, the extent of this reaction decreasing with increased welding speed. These findings suggest very strongly that the occurrence of the steam reaction in the weld pool is a porosity producing reaction. Although the welding experiments gave a good insight into the factors affecting the extent of weld metal porosity they did not indicate the mechanism responsible for its formation. To elucidate this mechanism a series of arc melting experiments were carried out under controlled atmospheres. The technique involved the arc melting of copper buttons in a flow through system using atmospheres of known composition. After arc melting the buttons were analysed for hydrogen and oxygen and the porosity produced was assessed by radiography, metallography and density measurement.

3.3.1. EXPERIMENTAL TECHNIQUE

The arc melting experiments were carried out in a controlled atmosphere arc melting box, the essential features of which are shown schematically in figure 24(a). The box consisted of a

stainless steel casing, a copper anode and an adjustable tungsten electrode. These three components were all water cooled. The total volume of the box was 4.85 litres. A rotary pump and an oil diffusion pump enabled the box to be evacuated to a pressure of 1.316×10^{-7} atmosphere. Windows were attached to the front and side of the box for the purposes of illumination and viewing. The atmospheres under investigation were admitted into and out of the box through two attached valves. Direct current (electrode negative) was supplied by a Miller welding set and arc melting currents and voltages were measured using a dual pen Servoscribe recorder. A photograph of the arc melting box and associated equipment is shown in figure 24(b).

Initially it was proposed to carry out both flow through and closed box arc melts. After much effort it was decided that the closed box experiments were impracticable. This was mainly due to the fact that arcing in pure argon in a closed box resulted in melting of the thoriated tungsten electrode with resultant unstable arcing. In contrast when a flow through system was used the arc melting parameters were stable and much more control was available. Also copper buttons melted in a flow of pure argon were bright in appearance and chemically pure.

The object of the arc melting procedure was to provide a technique whereby buttons of copper could be arc melted under controlled atmospheres. To study the copper-steam reaction it was decided to use argon containing low levels of water vapour as the shielding gas. As in the welding experiments this represents

a practical problem which could be encountered in welding practice. For this purpose argon water vapour mixtures up to a maximum of 540 v.p.m. water vapour were obtained from B.O.C. special gases. A certificate of analysis was supplied with each of the gas cylinders and the water vapour level was guaranteed for one third of the cylinder pressure.

The melting procedure tried first, with the help of Howden & Milner's (34) work, was found to be successful. The procedure was initially to evacuate the arc melting box to a pressure of 1.316×10^{-7} atmosphere for fifteen minutes. After this period the atmosphere under investigation was admitted into the box to a pressure just over atmospheric. The box was then again evacuated to 1.316×10^{-7} atmosphere. This procedure was then repeated. After this second flush the atmosphere under investigation was admitted to a pressure just over atmospheric and the side valve on the box was opened to achieve a flow through the box. A constant flow rate into the box of 10 litres per minute was initially chosen and was found to give adequate shielding. The arc was then struck (by touching) against the water cooled base for half-a-minute before it was placed directly over the specimen to be melted. Arc melting times were measured by use of a stop clock. The specimen size used was kept at approximately 5.7 g. For this size the optimum current range to give a fully molten button was found to be 300-350 amps at a voltage of 11 volts. Below 300 amps the button was clearly not fully molten and above 350 amps the turbulence was so great that the button was severely dished. For the current range and

using a voltage of 11 volts and a flow rate of 10 l/min the box pressure was found to be constant at a value of 1.074 atmosphere. The thoriated tungsten electrode was adjusted manually and by this technique the current could be controlled to within ± 10 amps and the voltage to within ± 0.5 volts. The electrode diameter was 6 mm and care was taken to ensure that the end of the electrode was kept clean and at an included angle of 60° . During arc melting, with the aid of welding glass goggles, the molten buttons could be clearly observed through the front window of the box.

In the following experiments unless otherwise stated a current of 300 amps was used with a voltage of 11 volts. A constant flow rate of 10 l/min was also used. Pieces of copper were cut from the supplied 5 mm thickness sheet. Spectrographic analysis of this sheet as shown in table 16 revealed that the copper was of extremely high purity. The oxygen contents of the O.F.H.C. and E.T.F. copper were .0003 and .0340 wt.% respectively. Before arc melting the pieces of copper were prepared to give a weight of 5.7 g. ± 0.1 g. by filing, cleaning in dilute nitric acid, degreasing in inhibited and drying.

After arc melting the buttons were X-rayed and then density determinations were carried out. The buttons were then analysed for hydrogen (by vacuum hot extraction for 10 minutes at 1000°C) and oxygen (by vacuum fusion analysis for four minutes at 1300°C) using the Balzers exhalograph equipment. The maximum specimen size which would fit into the equipment was used because of the

anticipated low levels of hydrogen and oxygen (in the case of O.F.H.C.). This was found to be between 4 and 5 g. The specimens were prepared for analysis by light filing, degreasing in inhibisol and drying. Inhibisol was used as a degreasant since it was found to result in no detectable hydrogen contamination. As a result of the low levels of hydrogen anticipated from the water vapour atmospheres and the rapid solidification rate of the buttons (resulting from the water cooled hearth) it was assumed that the measured hydrogen and oxygen levels were equivalent to the levels in the molten pool immediately before solidification. Analysis for hydrogen was always carried out within about two hours of arc melting. To check whether hydrogen was lost by diffusion at room temperature, three identical buttons were produced. One was analysed immediately after arc melting, one was stored in liquid nitrogen and the other at room temperature. After two hours storage of the latter two buttons, it was found that there was no significant difference in the hydrogen contents of the three buttons.

As will be seen in the following sections the analysis technique gave consistent results for both hydrogen and oxygen determinations.

3.3.2. CLEANLINESS OF THE MELTING BOX ATMOSPHERE

In order to assess the cleanliness of the arc melting box atmosphere specimens of O.F.H.C. and E.T.P. copper were arc melted for periods of 0.5, 1, 2 and 4 minutes using a shielding

gas of super pure argon. The results of hydrogen and oxygen analysis and density measurements are given in table 17 with the melting conditions used. Analysis of the supplied material carried out by an independent laboratory revealed that O.P.H.C. and E.T.P. copper respectively contained 0.12 and 0.10 ml/100g (N.T.P.) hydrogen. It can be seen from table 17 that the arc melted buttons picked up little or no hydrogen from the super pure argon atmosphere. The oxygen analyses indicated that E.T.P. copper lost a small amount of oxygen (0.034 to 0.030 wt.%) and the O.P.H.C. copper did not pick up oxygen. In the case of E.T.P. copper there was also a slight decrease in density to a value of approximately 8.75 g/cc.

3.3.3. ARC MELTING UNDER ARGON WATER VAPOUR MIXTURES

Arc melted buttons were produced using argon 140, 230 and 540 v.p.m. water vapour mixtures. Melting periods of 0.5 to 4 minutes were used and the results are shown in table 18. The oxygen and hydrogen contents of the buttons are plotted against arcing time in figure 25 (a)-(e). It is clearly shown in figure 25 (a) and (c) that in the presence of argon water vapour mixtures the hydrogen level of O.P.H.C. copper increases with arcing time and water vapour level, whereas the oxygen level is unaffected. It is indicated in figure 25 (b)(d) and (e) that oxygen is removed from E.T.P. copper when water vapour is present in the arc atmosphere. The amount removed increases with arcing time and with the level of water vapour in the argon. The hydrogen level of E.T.P. copper increases as the oxygen is removed.

The results of a further set of similar experiments are given in table 19. Equal weights of O.P.H.C. and E.T.P. were used to

produce 5.7 g. buttons using 140 and 190 v.p.m. water vapour in argon mixtures. The oxygen and hydrogen contents of the buttons are shown in figure 25 (f) and (g). The trends of decreasing oxygen and increasing hydrogen levels are again indicated in these figures.

3.3.4. EFFECT OF INCREASING THE ARC MELTING CURRENT

Using an argon 100 v.p.m. water vapour mixture O.F.H.C. buttons were melted for 1, 2 and 4 minutes using an increased current of 350 amps and a voltage of 11 volts. The results of these experiments are shown in table 20. The same general trends for oxygen and hydrogen contents were obtained; however, as indicated in figure 26 the hydrogen level was increased as a result of using an increased current.

3.3.5. REPRODUCIBILITY OF EXPERIMENTAL TECHNIQUE

In order to check the reproducibility of the experimental procedure three O.F.H.C. buttons were arc melted under identical conditions. The three buttons were arc melted for 4 minutes at 300 amps using an argon 100 v.p.m. water vapour mixture. The hydrogen and oxygen levels of the three buttons are shown to be in good agreement in table 21.

3.3.6. ARC MELTING COPPER TITANIUM ALLOYS UNDER AN ARGON, WATER VAPOUR ATMOSPHERE

To investigate the effect of a deoxidizing element on the copper steam reaction a copper, titanium alloy was produced. A master alloy of O.F.H.C. copper, 1.8 wt% titanium was made up by casting in an induction furnace under a protective stream of

argon. Analysis of the casting revealed that it contained 1 ml per 100 g. hydrogen. This level was reduced to 0.1 ml/100g. by heating under vacuum for three hours at 1000°C. Specimens from the casting were arc melted using currents of 300 and 350 amps and 11 volts in an argon 100 v.p.m. water vapour mixture. This experiment was repeated using an alloy of 0.12 Wt.% titanium under an atmosphere of argon 100 v.p.m. water vapour at a current of 300 amps. The alloy was made up by using the required weight of O.P.H.C. copper needed to dilute the master alloy.

The results of these experiments are listed in table 22. It can be seen that the oxygen content of the buttons was extremely low in all cases. For a current of 300 amps figure 27 indicates that decreasing the titanium level by a factor of approximately ten had only a slight effect on the button hydrogen content. For the corresponding conditions the hydrogen levels were higher than those obtained in the absence of titanium. Again from table 22 it is clear that increasing the current results in increased button hydrogen contents.

3.3.7. ARC MELTING COPPER ALUMINIUM ALLOYS UNDER AN ARGON WATER VAPOUR ATMOSPHERE

A master alloy of O.P.H.C. copper, 1.3 Wt.% aluminium was made up in the manner described in the previous section. Specimens from the casting were arc melted using a current of 300 amps and 11 volts in an argon 130 v.p.m. water vapour mixture. This experiment was repeated using an alloy of 0.1 Wt.% aluminium. The alloy was made up by using the required weight of O.P.H.C. copper needed to dilute the master alloy.

Again the alloy containing 1.3 Wt.% aluminium gave an increased

hydrogen content over O.F.H.C.. However, reducing the aluminium content to 0.1 wt% resulted in hydrogen contents similar to those obtained for O.F.H.C. under similar conditions. These results are illustrated in table 23.

3.3.8. GENERAL BUTTON MELTING CHARACTERISTICS

O.F.H.C. buttons were bright clean and were rounded in shape. The presence of water vapour in the arc atmosphere resulted in a slight oxide skin on the top surface of these buttons. The central region of the button surface which had been directly under the arc was extremely clean and bright. This point is highlighted in the scanning electron micrographs of figure 28, for an O.F.H.C. button melted for 3 minutes in argon, 100 v.p.m. water vapour. The light oxide skin and the clean central region are shown in figure 28 (a) and (b) at magnifications of 6,500 and 8,000 respectively.

E.T.P. buttons on the other hand were much flatter and less bright in appearance. The bright spot mentioned above was also not present in this case.

With respect to button shape it is interesting to note at this stage the melting characteristics of the E.T.P. button arc melted in argon, 540 v.p.m. water vapour (figure 25(e)). At a period between 3 and 4 minutes of arcing the button changed from the flat type characteristic of E.T.P. to a rounded type characteristic of O.F.H.C.. This would be expected since as shown in figure 25(e), after 4 minutes the oxygen level of the button was lowered to a level approaching that of the O.F.H.C. arc melted buttons. It appears

that the removal of oxygen from the E.T.P. button results in an increase in surface tension. This point will be further highlighted in a following section when the densities of the buttons are considered.

3.3.9. CALCULATION OF "APPARENT" EQUILIBRIUM CONSTANTS UNDER ARC MELTING CONDITIONS

The work of Allen and Hewitt ⁽¹⁵⁾ described in the literature review showed that the equation:

$$[H]_{\text{Helt}} = A \sqrt{\frac{p_{H_2O}}{[O]}}$$

held for molten copper under atmospheres of various water vapour pressures. The 'A' value was found to increase as the temperature was increased. (Fig. 8) Using the results of hydrogen and oxygen contents of buttons which reached an "apparent" equilibrium after 4 minutes arcing, 'A' values were calculated from Allen & Hewitt's ⁽¹⁵⁾ equation. These results are indicated in table 24.

For C.P.M.C. copper, E.T.P. copper and an alloy of these two, the 'A' values ranged between 0.051 - 0.068. According to Allen and Hewitt ⁽¹⁵⁾ (extrapolating their values in figure 8) this corresponds to a temperature range of 1500 - 1700°C.

3.3.10. BUTTON TEMPERATURE MEASUREMENT

In order to measure the temperature of the pool directly, a platinum, platinum 13% rhodium thermocouple was inserted into a copper button as it was arc melted at 300 amps and 11 volts. The thermocouple was protected by a silica sheath. In spite of this whenever the thermocouple was placed in the region of the arc, it was "burnt" out. After several attempts a temperature within the range 1400 - 1450°C was measured. It must be stressed

however, that to measure this temperature the thermocouple was placed in the edge and not the bulk of the specimen and it would thus be anticipated that the bulk button temperature would be at least 1450°C .

It was shown in the previous section that the copper-steam reaction temperature was in the range $1500 - 1700^{\circ}\text{C}$ and it thus appears that this reaction occurs within the bulk of the button.

Further evidence for this is shown in the micrographs of figure 29. The micrographs were taken from an E.T.P. button are melted for 2 minutes at 300 amps and 11 volts in an argon 230 v.p.m. water vapour mixture. The micrographs are typical of the bulk of the specimen. Randomly distributed spherical pores and the copper-cuprous oxide eutectic associated with the grain boundaries are shown in figure 29(a) and figure 29(b) shows that some of these pores are associated with the copper-cuprous oxide eutectic.

3.3.11. E.T.P. COPPER ARC MELTED IN AN ARGON-HYDROGEN ATMOSPHERE

It has already been shown that the presence of water vapour in the arc atmosphere results in the removal of oxygen from E.T.P. copper arc melted buttons. Thus hydrogen from the dissociated water vapour must be diffusing into the molten button. In order to substantiate this an argon, hydrogen mixture was used to arc melt E.T.P. copper for periods of 0.5, 1, 2 and 4 minutes. The results of these experiments are given in table 25 and shown in figure 30 with the included results for super pure argon and

230 and 540 v.p.m. argon water vapour mixtures. The argon hydrogen mixture of 280 v.p.m. hydrogen was made by mixing streams of pure argon with an argon 2 per cent hydrogen mixture. Accurately calibrated rotameters were used in the mixing process.

Assuming full dissociation, the argon 540 v.p.m. water vapour mixture would give 540 v.p.m. hydrogen. It can be seen from figure 30 that the argon, 280 v.p.m. hydrogen mixture also reduces the oxygen content of E.T.P. copper. The levels of oxygen after four minutes arcing were 0.0018 and 0.0012 Wt.% for the argon, hydrogen and argon, water vapour mixtures respectively.

3.3.12. POROSITY IN ARC MELTED BUTTONS

The amount of porosity present in the arc melted buttons was assessed by careful density measurement. The density results for the arc melted buttons are shown in figure 31(a) - (m). In the O.F.H.C., O.F.H.C., titanium and O.F.H.C., aluminium alloys the density in all cases was between 8.7 and 8.9 g/cc and arcing time had little effect. In the case of the E.T.P. and E.T.P./O.F.H.C. buttons as shown in figure 31(b), (c), (e), (f) and (g), the densities were much lower but increased with arcing time. This is consistent with the fact that with increasing arcing time the oxygen content of the E.T.P. buttons approaches that of the O.F.H.C. buttons. X-ray radiography of the arc melted buttons revealed that the porosity was present as scattered spherical pores.

3.3.13. O.F.H.C. COPPER ARC MELTED IN ARGON HYDROGEN AND ARGON OXYGEN ATMOSPHERES

To investigate further the copper steam reaction O.F.H.C.

copper was arc melted for periods of 1, 2 and 4 minutes using gas mixtures of argon, 153 v.p.m. hydrogen and argon, 77 v.p.m. oxygen. As in the previous section the mixtures were made up by using accurately calibrated rotameters mixing super pure argon with mixtures of argon containing 2 per cent of hydrogen and oxygen respectively. Hydrogen and oxygen analyses were carried out for the samples melted in the argon, hydrogen and argon, oxygen mixtures respectively. The experimental conditions and results are given in table 26 and the hydrogen and oxygen values are plotted in figure 32. For comparison the hydrogen and oxygen analyses obtained for O.F.H.C. melted in argon, 140 v.p.m. water vapour are also included in figure 32. Assuming full dissociation 140 v.p.m. water vapour would result in 140 v.p.m. hydrogen and 70 v.p.m. oxygen. From figure 32 it is clear that 153 v.p.m. hydrogen and 77 v.p.m. oxygen result in higher hydrogen and oxygen contents.

4. DISCUSSION

The discussion is divided into four sections. In the first three sections the occurrence of steam and nitrogen porosity are considered under welding and arc melting conditions. The fourth section considers the practical significance of the results in copper welding.

4.1. THE OCCURRENCE OF STEAM POROSITY IN T.I.G. WELDED COPPER

The welding experiments represent a considerable advance in the understanding of the effects of welding and material variables on porosity formation in the T.I.G. welding of copper. It must be stressed however, that while the results of this section are quantitative they only give limited insight into the mechanism of steam porosity formation.

It has been shown that the presence of water vapour in the welding arc results in randomly distributed spherical porosity in the weld metal similar to that obtained in practice. Analysis of variance of the factorial experiments revealed that four of the six selected factors significantly affected weld metal porosity. Increasing water vapour in the argon, and oxygen in the base material increased the porosity whereas welding at increased welding speed reduced the amount of porosity. Porosity was also decreased by carrying out melt runs instead of butt welds and the significance of the results involving butt welds will be discussed in Section 4.3. Significant two factor interactions involving the significant single factors were also investigated and gave increased

information about steam porosity formation.

As shown by Ludwig ⁽²⁴⁾ dissociation of molecular gases is complete at temperatures of 10,000°C. Thus in the welding arc water vapour by dissociation represents a source of both hydrogen and oxygen. Both gases, assisted by plasma jets, are then capable of diffusing into the weld pool where they will react to produce steam porosity. Clearly if oxygen is already present in the weld metal, as in the case of E.T.P. copper, the formation of steam porosity will be enhanced. In all cases involving steam porosity, increasing welding speed reduced the level of porosity. At higher welding speeds the gas-metal contact time between the arc atmosphere and the molten weld pool is shorter and thus the time available for steam porosity formation is reduced. A study of the interaction of welding speed and water vapour in the shielding gas emphasized this point. For each of the water vapour levels considered, the density of O.F.H.C. copper melt runs, as shown in figure 13, was increased by increasing the welding speed. Since O.F.H.C. copper was used in these experiments it is clear, from the high water vapour (1340 v.p.m.) low speed (2 mm/sec) result (density of approximately 5.3 g/cc), that the steam reaction in the weld pool results from the diffusion of both hydrogen and oxygen from the arc atmosphere. This factor will be further discussed in section 4.2. The effect of welding speed on the copper-steam reaction was also emphasized by carrying out E.T.P. copper melt runs using an argon 2 per cent hydrogen shielding gas

(figure 16). In the range of welding speeds 4 to 10 mm/sec. the amount of oxygen removed decreased as the welding speed was increased. This again indicates that the steam reaction in the weld pool, is time dependent. It is interesting to note however, that in the welding speed range 10 to 20 mm/sec. the amount of oxygen removed (approximately 0.008 wt.%) remained constant. This indicates that within this range the steam reaction occurs but to a limited extent. Since the steam reaction occurs even at a speed as high as 20 mm/sec. it appears that the controlling factor is the reaction of hydrogen and oxygen to produce steam porosity in the weld metal and not the supply of hydrogen from the arc atmosphere.

The factorial analysis and the study of the interactions involving base material, water vapour and welding speed indicated generally that D.H.P. copper gave sounder welds than O.F.H.C. copper. This is a result of the phosphorus "tying up" oxygen in the weld pool and thus inhibiting the occurrence of the steam reaction. Since the levels of hydrogen produced assuming full dissociation of the water vapour in the arc would be extremely low then hydrogen porosity would not occur.

The effects on porosity of increasing current and inert gas flow rate were very slight and did not arise as significant single factors. In the case of welding current this was probably due to the fact that at a particular welding speed only a narrow range of current was practical and all the other variables considered

this range was too narrow. The effect of current will again be considered in section 4.2. Increasing the shielding gas flow rate also had no significant effect on porosity. The low end of the range was restricted since extremely low flow rates would result in excessive weld metal oxidation. In the range considered however, it is interesting to remember some of the work of Salter and Milner.⁽⁴²⁾ In a study of the oxygen-titanium system they also found that increasing the shielding gas flow rate had no significant effect on the rate of absorption of oxygen. This was explained on the basis of extremely high plasma jet velocities present in the welding arc. These velocities were of the order of 10^5 mm/sec. Clearly the plasma jet velocity nullifies possible effects due to increased shielding gas velocities.

Summarising the results so far discussed it is clear that porosity can occur in the T.I.G. arc welding of copper by the occurrence of the steam reaction in the weld pool. The nature of the porosity was randomly distributed spherical pores typical of that observed in welding practice. The extent of the steam porosity is increased by increased water vapour content of the arc atmosphere, increased oxygen content of the base material and decreased welding speed.

4.2. THE COPPER-STEAM REACTION UNDER ARC MELTING AND ARC WELDING CONDITIONS

The aim of this work was to elucidate the mechanism responsible for the occurrence of steam porosity in the T.I.G. welding of copper. This was achieved by arc melting copper buttons

under controlled atmospheres.

The results indicated that E.T.P. copper arc melted in argon, water vapour atmospheres lost considerably more oxygen than the equivalent melts in a super pure argon atmosphere. If sufficient water vapour was present (540 vpm) and sufficient arcing time used (4 minutes) the E.T.P. copper was converted to a level approaching that of O.F.H.C. copper (0.0012 wt%).

The hydrogen content of E.T.P. copper generally increased with increased water vapour in the argon. When O.F.H.C. copper was arc melted in argon, water vapour its hydrogen content increased with increased arcing time and increased water vapour in the argon. The oxygen content of O.F.H.C. copper buttons generally increased with respect to the initial oxygen content (0.0003 wt%) but only to a maximum level of 0.0007 wt%. For any given argon water vapour mixture the oxygen level did not increase significantly in the arcing time periods considered. It appears that both E.T.P. and O.F.H.C. coppers attain an equilibrium state in the button as a whole and that this equilibrium state is dominated by the supply of hydrogen from the water vapour present in the arc atmosphere. The fact that water vapour was a predominant source of hydrogen is in agreement with the findings of Salter. (71) In a study of hydrogen absorption in the arc melting of steel he showed that the absorption of hydrogen from argon, water vapour atmospheres closely followed that from the equivalent argon hydrogen atmospheres, (assuming that a given volume of water vapour was equivalent to the same

volume of hydrogen).

Using the equation of Allen and Hewitt ⁽¹⁵⁾ and measured apparent equilibrium hydrogen and oxygen button contents 'A' values were calculated. For an arc melting current of 300 amps and extrapolating Allen and Hewitt's ⁽¹⁵⁾ data (figure 8), these values corresponded to a reaction temperature of 1500 - 1700°C. To maximise the accuracy of extrapolation a regression analysis was carried out on Allen and Hewitt's ⁽¹⁵⁾ 'A' values over the temperature range 1090 - 1350°C. The regression coefficient was found to be 0.996 and the reaction temperature given by the equation: -

$$\text{Temperature} = (1008 + 10,286 \times 'A')^{\circ}\text{C}.$$

The minimum (0.051) and maximum (0.068) 'A' values thus correspond to a temperature range of 1533 - 1707°C.

Direct temperature measurement revealed that the bulk button temperature was at least 1450°C. Using hydrogen solubility, temperature data from Howden and Milner's ⁽³⁴⁾ work calculations have been made in section 8.1 to compare the measured hydrogen button contents with those expected at 2000°C. Assuming full dissociation of the water vapour the measured hydrogen contents correspond closely to the solubilities at 2000°C.

It appears then that the copper-steam reaction reaches an apparent equilibrium state corresponding to a temperature of the order of 1500 - 1700°C. Further evidence for this was illustrated in the micrographs of figure 29(a) and (b). These indicated that the spherical porosity was distributed throughout the bulk of the button and that some of these pores were associated with the copper, cuprous oxide eutectic structure. However it also appears that

there is a region directly under the arc at a temperature of 2000°C. In the case of copper Howden and Lilner (34) estimated that the temperature of the hot spot corresponded to 1650°C. However, their maximum current used was 200 amps and their arc melted specimens weighed approximately 9 g. Clearly using a smaller arc melted button and a higher current results in a higher hot spot temperature and also a higher overall button temperature. At a higher current the electromagnetic stirring forces within the button would also be more vigorous and thus the overall button temperature would be higher. In a detailed study of CO₂ welding of steel Pollard and Lilner (39) showed that thermodynamic equilibrium was attained corresponding to the hot spot temperature of 2300°C. Although the present investigation has shown that the apparent equilibrium temperature is below the hot spot temperature, the hydrogen and oxygen required for the reaction are supplied from the hot spot directly under the electrode. Evidence confirming the existence of the hot spot was shown clearly in the scanning electron micrographs of figure 28.

The general mechanism of steam porosity formation is now evident and can best be illustrated by considering E.T.P. copper arc melted in an argon, water vapour atmosphere. The high temperatures present in the arc result in dissociation of water vapour to produce hydrogen and oxygen. Two volumes of hydrogen will be produced for every one volume of oxygen. Hydrogen and oxygen, assisted by plasma jets, will diffuse into the hot spot directly under the arc. As pointed out by Salter (71) hydrogen will diffuse at a rate considerably in excess of oxygen. At 0°C and 1 atmosphere pressure

the diffusivity of hydrogen is considerably in excess of that of oxygen. (72) ($1.31 \text{ cm}^2/\text{sec.}$ compared with $0.189 \text{ cm}^2/\text{sec.}$).

Although these conditions are far removed from an arc melting situation they give a rough indication of the relative diffusivities. When the hydrogen has diffused into the hot spot it will be rapidly circulated by electromagnetic forces within the molten pool where it will react with oxygen to produce steam porosity. As oxygen is continually removed by this process the amount of hydrogen will increase to maintain a constant hydrogen-oxygen ratio in the button. If hydrogen diffuses into the hot zone under the arc then presumably oxygen will also. However, since hydrogen diffuses much more rapidly than oxygen, after any given arc melting period considerably more hydrogen will have diffused into the button and the net effect is thus removal of oxygen from the E.T.P. copper button.

It is now interesting to consider the mechanism for a similar situation involving O.F.H.C. copper. The results show that the hydrogen level again increases, however the oxygen level is only marginally increased. This is again in agreement with the fact that hydrogen is more mobile and the net effect is thus a build up of hydrogen and a final equilibrium hydrogen, oxygen ratio dominated by the supply of hydrogen into the button.

In order to further investigate the steam reaction O.F.H.C. copper was arc melted in an argon 153 v.p.m. hydrogen mixture and an argon 77 v.p.m. oxygen mixture. These levels are approximately equivalent to a fully dissociated argon 140 v.p.m. water vapour mixture. The button hydrogen content was again in agreement with the hydrogen solubility at $2,000^\circ\text{C}$ (calculation in section 3.1.).

It is interesting to note however that the hydrogen level was higher than that obtained with the argon 140 v.p.m. water vapour mixture. Also for the argon, hydrogen atmosphere the hydrogen level was constant for the four arcing times whereas in the case of the argon water vapour mixture the maximum hydrogen content was attained after 2 minutes arcing. This again indicates that in the case of argon water vapour, both hydrogen and oxygen diffuse into the molten button. The argon 77 v.p.m. oxygen atmosphere again gave only a slight increase in the button oxygen content. The calculation in section 0.2 shows that, for this level of oxygen and a temperature of 2027°C , the free energy of formation of cuprous oxide is + 164, 746 Joule/mole oxygen. Thus even though oxygen diffuses into the copper, cuprous oxide will not be formed and the button oxygen content will remain at a low level. On the basis of this calculation it would be anticipated that E.T.P. copper arc melted in pure argon (an extremely low oxygen partial pressure) would lose oxygen by the decomposition of cuprous oxide. This loss of oxygen did not occur to any appreciable extent and the reason must be the difficulty of nucleating oxygen porosity. However, as soon as water vapour is added to the argon, hydrogen is supplied to the button and oxygen is removed as steam.

The calculation in section 8.3 indicates that, for the copper-steam reaction at 2027°C the partial pressure of hydrogen in equilibrium with an argon, 230 v.p.m. water vapour atmosphere would be extremely low (7×10^{-7} atmosphere). This hydrogen partial pressure would not be sufficient to account for the levels measured in the copper buttons. Clearly then the hydrogen is supplied by dissociation of water vapour in the arc.

The effect of deoxidising elements was investigated by arc melting copper titanium and copper aluminium alloys in an argon 100 v.p.m. water vapour mixture. Generally the presence of these deoxidising elements increased the level of hydrogen in the solidified buttons. The reason for this is that both are strongly deoxidising and tie up any oxygen present in the molten button and prevent steam formation. Thermodynamically titanium and aluminium oxides are both more stable than steam at temperatures up to 2200°C. During arc melting of these alloys a tenacious oxide skin was formed and both alloys were "sluggish" in the molten form compared with the much more fluid pure copper melts. During arc melting it was observed, however that in a small area under the arc the oxide skin was broken up and this is the region at which hydrogen would diffuse into the molten button. Since all the oxygen was tied up by the deoxidising elements the buttons could thus absorb a higher level of hydrogen. This explains why deoxidising elements effectively prevent steam porosity formation. If the oxygen was free to react with the hydrogen, steam porosity would be formed. However, since the oxygen is tied up steam porosity will not be formed and also hydrogen porosity will not result because of the low levels of hydrogen present.

The density values given in figure 31 follow a general trend. The O.F.H.C. and deoxidised alloys vary little in density with arcing time. This is because of the low concentrations of oxygen present in all these buttons and hence the amount of steam produced is low. In contrast the densities of the E.T.F. buttons varied markedly with arcing time. The density increased with arcing time for all the argon water vapour levels. The greatest increase in density was observed when the high water vapour level, 540 v.p.m.

was used. This was because the oxygen was removed with arcing time and thus the density increased until it approached that of O.F.H.C. buttons when the oxygen level had fallen to O.F.H.C. level.

In summarising the arc melting experiments then it appears that the steam reaction occurs in the body of the molten arc melted button and proceeds to an apparent equilibrium state appropriate to its temperature. Hydrogen and oxygen are supplied by dissociation of water vapour in the arc, however the supply of hydrogen exceeds that of oxygen and is the controlling factor in the attainment of equilibrium.

It is now worth considering the findings of the welding experiments involving the steam reaction. Generally speaking E.T.P. copper melt runs carried out in argon water vapour mixtures lost oxygen, the amount being greater at lower welding speeds. This is in agreement with the fact that water vapour removed oxygen from E.T.P. arc melted buttons, the amount removed increasing with arcing time. It was shown that increased oxygen in the base material significantly increased weld metal porosity and this obviously enhanced the formation of steam porosity in the weld pool. In the case of O.F.H.C. copper welded in argon water vapour atmospheres it was clearly shown that for any given water vapour level increasing welding speed reduced the level of porosity. At higher welding speeds the gas-metal contact time is decreased and although hydrogen might be diffusing into the weld pool there is insufficient oxygen present to produce steam porosity. In contrast at low welding speeds there is sufficient time for both oxygen and hydrogen

diffusion and hence the steam reaction occurs in the weld pool. Analysis of G.F.H.C. melt runs showed that oxygen was picked up during welding compared with arc melting. This is because oxidation of the weld pool by the atmosphere is likely in a welding situation and any oxygen gained in this way would obviously enhance the steam reaction.

Generally speaking then there is good agreement between the welding and arc melting studies. The two studies together explain the mechanism responsible for steam porosity formation and the main factors affecting the extent of its occurrence.

4.3. THE OCCURRENCE OF NITROGEN POROSITY IN ARC WELDED COPPER

The welding experiments revealed that it was much more difficult to produce sound butt welds than sound melt runs. It was also shown that in the case of butt welds the amount of porosity increased with increased welding speed. This suggests that joint set up is extremely important, and that another mechanism is responsible for porosity formation. The mechanism must be associated with the greater likelihood of atmospheric ~~cont~~ainment in butt welds particularly at higher welding speeds. If this is the case then as well as steam porosity it became apparent from the work of Kobayashi ⁽⁴⁹⁾ that nitrogen might also be a possible source of porosity.

The results of figure 18 showed clearly that welding in a nitrogen atmosphere resulted in extensive porosity. Like steam and hydrogen porosity the level produced in melt runs decreased with increased welding speeds. This is again a result of the shorter gas-metal contact time at increased welding speeds and

suggests that the absorption of nitrogen by copper is a typical gas-metal reaction. Radiography (figure 19(a)) and metallography (figure 20) of the nitrogen porosity revealed that its distribution was extremely interesting. Fine porosity was associated with the base of the weld and coarse porosity at the weld surface especially at the edges of the weld bead. The appearance of the weld bead suggested that a vigorous "nitrogen boil" had occurred. As mentioned in the literature review it is well known that nitrogen is virtually insoluble in copper even at 1400°C , however as pointed out by Ahmes and Eahn ⁽⁶⁶⁾ the presence of an arc results in the formation of atomic nitrogen. In the welding arc extremely high temperatures of the order of $20,000^{\circ}\text{C}$ are present and as pointed out by Ludwig ⁽²⁴⁾ most molecular gases, including nitrogen, are fully dissociated at temperatures of the order of $10,000^{\circ}\text{C}$. It appears then that nitrogen dissociated to produce nitrogen atoms can produce porosity in copper welding. As soon as the weld pool begins to cool down the liberation of nitrogen will occur extremely vigorously as would appear to have been the case in figure 20. As well as the distribution of the porosity it is interesting to note that the porosity is spherical, the larger pores being associated with the edge of the weld metal. The radiographs in figure 19 show clearly that different gases produce different shapes of porosity in O.T.F.C. copper. Water vapour, like nitrogen produces spherical porosity. Hydrogen on the other hand produces the characteristic "herringbone" porosity. The differing porosity morphologies can be explained by considering the stage at which the porosity is formed which is related to the solubility of the

particular gas in copper. Nitrogen as pointed out has virtually no solubility in copper, thus nitrogen bubbles are formed in the molten weld pool at an early stage and these are "frozen in" by the solidification front. Steam porosity is similar to nitrogen porosity, hydrogen and oxygen react in the molten weld pool to produce steam porosity which has no solubility in copper. Thus again spherical gas bubbles are entrapped in the solidification front. Hydrogen on the other hand has considerable solubility in both liquid and solid copper. Thus hydrogen porosity will not be produced until sufficient hydrogen segregation has occurred to produce a pressure high enough to nucleate porosity. This build up of hydrogen will occur in the last liquid to solidify, the dendrite areas and thus "herringbone" porosity is formed. With respect to hydrogen porosity it is worth remembering the work of Salter and Lilner. ⁽⁵⁰⁾ They found that hydrogen produced different shaped porosity in different metals. In copper the porosity was "herringbone", in aluminium it was rounded pores and in nickel it was centre line. These different forms of porosity are illustrated schematically in figure 33. The solubility of hydrogen in aluminium, copper and nickel as a function of temperature is given in table 27 from Smithells. ⁽¹¹⁾ The most important factor in terms of porosity formation is the change in solubility during solidification. Using the figures in table 27 the ratios of the solubilities of hydrogen in liquid and solid of each of these three metals, at their melting points, is given in table 28. The solubility ratio decreases from aluminium to copper to nickel. In other words solid aluminium will retain

less hydrogen at the melting point than will solid copper or solid nickel. Thus on solidification the porosity will be formed at different stages for each of the three metals. In the case of aluminium the porosity will form at the liquid-solid interface and thus rounded pores will be trapped in the solidification front. In the case of nickel the porosity will form towards the end of the solidification process and thus centre line porosity will result. It appears that copper is an intermediate case and thus "herringbone" porosity is a form of porosity intermediate between rounded pores and centre line porosity. In inert gas arc welding these solubility ratios will be exaggerated especially in the case of aluminium. As shown by Howden and Hilner (34) the presence of an arc results in hydrogen solubilities very much in excess of calculated solubilities in the absence of an arc. Nitrogen in copper will be an extreme case of a large difference between liquid and solid solubility and thus the porosity will be formed at a very early stage i.e., at the edge of the weld pool since this is the first weld region to solidify. The porosity, as observed, would also be rounded pores.

Considering nitrogen porosity it is interesting to know how much nitrogen added to argon will give rise to porosity formation. This question was answered in figure 21 where it was shown that as little as 0.1 per cent nitrogen was sufficient to give considerable porosity. Again increasing the welding speed for any particular nitrogen level resulted in an increase in weld metal density. Analysis of the gas present in these pores revealed that it was predominantly nitrogen. This proves beyond doubt that in an arc welding situation nitrogen can cause porosity in copper. It might

be argued that the nitrogen is physically entrapped in the weld metal rather than rejected from the solidifying weld metal. However, the pore analysis revealed predominantly nitrogen and physical entrapment of the atmosphere would have resulted in pores containing predominantly argon. Arc melting studies also revealed that an argon 1.0 per cent nitrogen mixture resulted in porous buttons compared with the sound buttons in pure argon. The amount of porosity was considerably less than that obtained in the equivalent welding experiment illustrated in figure 21. This was probably a result of the fact that the arc melted buttons were a much bigger mass than the weld pools involved and thus the supersaturation of nitrogen would be much lower in the former case. Also in a welding situation motion of the electrode is involved and the nucleation of porosity would be enhanced.

A level of nitrogen as low as 0.1 per cent could be picked up by entrainment of the atmosphere especially in the case of butt welds. Since nitrogen porosity has been shown to be spherical it would be difficult to distinguish it from steam porosity. It has been shown conclusively that nitrogen porosity can be eliminated by using a filler wire containing powerful denitrifying elements. (Nitrofil) On the other hand use of a filler wire containing deoxidising elements and only mildly denitrifying elements (argofil) results in porous welds. This clearly shows that if there is any danger of nitrogen or steam porosity then a filler wire containing aluminium and titanium, which are both denitrifying and deoxidising elements, should be used. Comparing the densities in figures 21

and 22 it is clear that argofil acts as a mild denitrider. This fact is confirmed by reference to figure 34 from Elliott and Gleiser. (73) This figure shows that silicon and manganese are mild denitriders in comparison with titanium and aluminium.

In conjunction with the present work Lammas and Jordan (74) have investigated the occurrence of nitrogen porosity in the H.I.G. welding of copper. Generally their findings have substantiated those of Kobayashi (49) and of the present work. Lammas and Jordan (74) carried out bead on plate (D.H.P.) runs using argofil and nitrofil welding wires. Using nitrofil the welds were sound throughout the range 0 to 100 per cent nitrogen. However using argofil wire extensive porosity resulted. Again the morphology of the porosity was spherical and it was concentrated mainly at the edge of the weld bead. The lowest level of nitrogen used by Lammas and Jordan (74) was 1.0 per cent and this resulted in a considerable decrease in density of the argofil weld metal. This is indicated in their results which are given in figure 35. Again this figure illustrates the important effect of welding speed. Up to a nitrogen level of 8 per cent, increasing the welding speed from 4 to 8 mm/sec. resulted in sound argofil weld metal.

4.4. PRACTICAL SIGNIFICANCE FOR WELDING OF COPPER

It has been demonstrated that the porosity encountered in the inert gas arc welding of copper can be reproduced in laboratory experiments. The presence of water vapour or nitrogen in the welding arc results in the formation of spherical porosity in the weld

metal. At low welding speeds, less than 100 v.p.m. water vapour and 0.1 per cent nitrogen (1000 v.p.m.) contamination of the argon shielding gas are sufficient to produce considerable porosity. These are levels which could occur in practice. It has been shown for any level of contamination that the amount of porosity produced in melt runs is reduced by increasing the welding speed. Steam porosity is enhanced by the presence of oxygen in the base material and is retarded by the presence of deoxidising elements which effectively tie up oxygen in the base material.

Using a shielding gas of super pure argon it has been shown that sound melt runs can be obtained for the grades of copper considered. Under the same conditions however, it was much more difficult to produce sound butt welds particularly at high welding speeds. In the case of butt welds entrainment of the atmosphere is more likely and will involve both water vapour and, to a greater extent, nitrogen. It has been demonstrated that nitrogen porosity can be completely eliminated by use of a filler wire containing small amounts of powerful denitrifying elements. The use of a filler wire containing powerful deoxidising and mildly denitrifying elements on the other hand did not eliminate nitrogen porosity. It is clear then that both nitrogen and steam porosity could be eliminated by the use of filler wires containing small amounts of aluminium and/or titanium which are both strongly denitrifying and strongly deoxidising elements. The filler wires commonly used in the inert gas (argon) arc welding of copper are those containing powerful deoxidising elements. However these wires do not completely eliminate

the porosity and the radiographic standards are below those achieved in steel welding. It appears then that the porosity which is not removed by these filler wires is a result of nitrogen entrainment. Nitrofil welding wire was developed primarily for the nitrogen arc welding of copper, however its use in argon arc welding would eliminate both steam and nitrogen porosity.

5. CONCLUSIONS

1. Porosity can occur in T.I.G. arc welding of copper by the occurrence of the steam reaction in the weld pool.
2. The extent of steam porosity is increased by, increased water vapour content of the arc atmosphere, increased oxygen content of the base material and decreased welding speed.
3. The steam reaction occurs in the body of the weld pool and proceeds to an apparent equilibrium state appropriate to its temperature. The hydrogen and oxygen are supplied by the dissociation of water vapour in the arc atmosphere. In the case of E.T.P. copper oxygen is also supplied by the parent metal.
4. Porosity can occur in T.I.G. arc welding of copper by rejection from solution of nitrogen that has been absorbed by the weld pool from the arc atmosphere.
5. The level of porosity increases progressively as the nitrogen content of the shielding gas increases to approximately 0.4 per cent, the apparent optimum level, but it is appreciable at levels as low as 0.1 per cent.
6. Nitrogen porosity can be eliminated by addition to the weld pool of filler wire containing small amounts of denitriding elements such as titanium and aluminium.
7. The porosity associated with weld fit up-butt welds instead of melt runs - is due to nitrogen entrained into the arc atmosphere.

6. RECOMMENDATIONS FOR FURTHER WORK

It is considered that two principle areas require further work: -

1. Welding and arc melting studies of the steam reaction for other metals, including nickel, iron and alloys of these with copper. This would give greater insight into the mechanism and the effect of material upon it.
2. A further study of the effect of filler wire composition on the occurrence of nitrogen porosity in both the T.I.G. and M.I.G. arc welding of copper. It would be interesting to know the minimum amount of aluminium and/or titanium necessary to eliminate nitrogen porosity.

7. ACKNOWLEDGEMENTS

The author wishes to thank Dr. M. F. Jordan for his supervision and lively interest throughout this investigation. Thanks are also due to Professor W. O. Alexander, Head of the Department of Metallurgy and Professor R. H. Thornley, Head of the Department of Production Engineering for providing laboratory facilities. The author is indebted to the International Copper Research Association, for whom the work was carried out under contract. Finally the author wishes to thank the academic and technical staff of the University for their help throughout the project.

8. APPENDIX

8.1. COMPARISON OF MEASURED FINAL O.F.H.C. COPPER HYDROGEN CONTENTS WITH THE EQUILIBRIUM HYDROGEN SOLUBILITY AT 2000°C

The hydrogen solubility data from Howden and Milner (43) shows that for a hydrogen partial pressure of 0.01 atmosphere the hydrogen solubility is 3.1 ml./100g.

Using Sievert's law: -

$$[H]_{\text{melt}} = K_{2000^{\circ}\text{C}} \sqrt{0.01}$$

$$\therefore 3.1 = K_{2000^{\circ}\text{C}} \times 0.1$$

$$\text{and } K_{(2000^{\circ}\text{C})} = 31$$

Assuming full dissociation of an argon, 100 v.p.m. water vapour mixture at an arc melting pressure of 816 mm. mercury,

then, partial pressure of hydrogen =

$$\frac{100 \times 10^{-6} \times 816}{760} \text{ - Atmosphere} = \underline{1.074 \times 10^{-4} \text{ Atmosphere}}$$

Thus the anticipated hydrogen solubility at 2000°C is given by,

$$[H]_{2000^{\circ}\text{C}} = 31 \times 1.03 \times 10^{-2} = \underline{0.32 \text{ ml./100g.}}$$

This is in good agreement with the measured hydrogen solubility,

$$\underline{[H]_{\text{measured}} = 0.34 \text{ ml./100g.}}$$

Using the same method the following hydrogen solubilities have been calculated at 2000°C and compared with the measured button hydrogen contents:

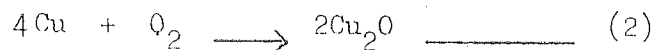
ARC MELTING ATMOSPHERE	CALCULATED HYDROGEN SOLUBILITY AT 2000°C ml./100g.	MEASURED FINAL BUZZON HYDROGEN CONTENT ml./100g.
Argon, 100 v.p.m. water vapour	0.32	0.34
Argon, 140 v.p.m. water vapour	0.38	0.35
Argon, 190 v.p.m. water vapour	0.44	0.36
Argon, 230 v.p.m. water vapour	0.49	0.49
Argon, 153 v.p.m. hydrogen	0.40	0.53

8.2. FREE ENERGY OF FORMATION OF CUPROUS OXIDE FOR AN ARGON, 77 v.p.m. OXYGEN ATMOSPHERE AT 2027°C

The effect of oxygen pressure on the free energy of formation of a metallic oxide can be calculated using Van't Hoff's isotherm.

$$\text{Thus } \Delta G_T = \Delta G_T^0 + RT \log_e \frac{P_{\text{PRODUCTS}}}{P_{\text{REACTANTS}}}$$

Assuming that the activity of pure solids is unity then for the reaction,



equation - (1) simplifies to;

$$\Delta G_T = \Delta G_T^0 - RT \log_e P_{\text{O}_2} \quad \text{_____} \quad (3)$$

Where P_{O_2} = Partial pressure of oxygen

$$= \frac{77 \times 10^{-6} \times 816}{760} \text{ atmosphere}$$

$$= \underline{8.27 \times 10^{-5} \text{ atmosphere}}$$

Using free energy data from Elliott and Gleiser (73) for reaction _____ (2)

$$\underline{\Delta G_{2027^\circ\text{C}}^0 = 15,068 \text{ Joule per mole oxygen}}$$

Substituting in _____ (3)

$$\Delta G_{2027^\circ\text{C}} = -15,068 - 19.15 \times 2300 \log_{10} (8.27 \times 10^{-5})$$

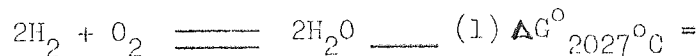
$$\Delta G_{2027^\circ\text{C}} = -15,068 + 179,814$$

$$\therefore \Delta G_{2027^\circ\text{C}} = \underline{+ 164,746 \text{ Joule per mole oxygen}}$$

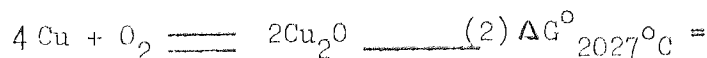
8.3. PARTIAL PRESSURE OF HYDROGEN IN EQUILIBRIUM WITH THE COPPER-STEAM REACTION FOR AN ARGON, 230 v.p.m. WATER VAPOUR MIXTURE AT A TEMPERATURE OF 2027°C

Using free energy data from Elliott and Gleiser (73)

for the reactions:-

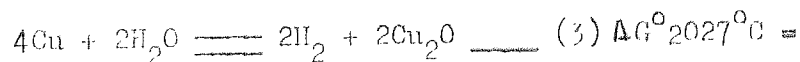


-235,141 Joule per mole oxygen.



-15,068 Joule per mole oxygen.

Subtracting, (2) _____ (1)



220,073 Joule per mole oxygen.

For reaction - (3) assuming that the activity of pure solids is unity, the equilibrium constant is given by:-

$$K_{2027^{\circ}\text{C}} = \frac{P_{\text{H}_2}^2}{P_{\text{H}_2\text{O}}^2}$$

Using Van't Hoff's isotherm for equilibrium conditions,

$$\Delta G^{\circ}_{2027^{\circ}\text{C}} = -RT \log_e \frac{P_{\text{H}_2}^2}{P_{\text{H}_2\text{O}}^2}$$

thus

$$220,073 = -19.15 \times 2300 \times \log_{10} \frac{P_{\text{H}_2}^2}{P_{\text{H}_2\text{O}}^2}$$

$$\therefore \log_{10} \frac{P_{\text{H}_2}}{P_{\text{H}_2\text{O}}} = -2.50 \text{ and } \frac{P_{\text{H}_2}}{P_{\text{H}_2\text{O}}} = 0.00316$$

The partial pressure of water vapour for an argon, 230 v.p.m. water vapour mixture is given by: -

$$\begin{aligned} P_{\text{H}_2\text{O}} &= \frac{230 \times 10^{-6} \times 816}{760} \text{ atmosphere} \\ &= \underline{2.47 \times 10^{-4} \text{ atmosphere}} \end{aligned}$$

thus: -

$$\frac{P_{\text{H}_2}}{2.47 \times 10^{-4}} = 0.00316$$

$$\therefore \underline{P_{\text{H}_2} = 7.8 \times 10^{-7} \text{ atmosphere}}$$

9. REFERENCES

- (1) N.P. Inglis and G.R. Nichie.
"Welding of copper and its alloys, difficulties, possible improvements and their economic implications."
International Research and Development Co.Ltd. IRD 67-62.
- (2) I.D. Johnson.
The Welding Journal, 1970, 49 (2), 55s - 60s.
- (3) Welding of Copper, Revere Copper and Brass,
1947 Edition New York.
- (4) I.T. Hook,
The Welding Journal, 1937, 16 Research Supplement, 7 -31.
- (5) A.F. Young,
The Welding Journal, 1941, 20 (11), 513 - 521.
- (6) J.T. Vreeland,
The Welding Journal, 1938, 17 (7), 20 - 40.
- (7) C.E. Swift,
The Welding Journal, 1935, 14 (1), 26 - 29.
- (8) E. Cook and E. Davies,
Trans. Inst. Welding, 1947, 10 105, 178 - 192.
- (9) F.E. Garriott,
The Welding Journal, 1947, 26 (10), 907 - 915.
- (10) J. Wegrzyn,
British Welding Journal, 1967, 14 (5), 233 - 238.
- (11) C.J. Smithells,
"Metals Reference Book", 1967, 2, 4th Edition,
London, Butterworths.
- (12) E.A. Taylor and A.H. Burn,
1965 Proceedings, 2nd Commonwealth Welding Conference, 224 - 229
- (13) J.F. Lancaster,
"The Metallurgy of Welding Soldering and Brazing",
London 1965, Allen & Urwin.
- (14) A.J. Phillips,
Trans. A.I.D.M.E. 1947, 171, 17-46.
- (15) V.P. Allen and T. Hewitt,
Journal Institute of Metals, 1933, 51, 257 - 275.
- (16) "Inert Gas Arc Welding",
Institute of Welding, 1966, 57-64.

- (17) "Selection of Shielding Gases for the Gas Shielded Arc Welding of Copper and its Alloys",
Welding in the World, 1973, 11 (3/4), 50 - 55.
- (18) J.G. Young,
British Welding Journal, 1961, 8. 7, 349 - 353.
- (19) J.K. Clews,
British Welding Journal, 1961, 8.7, 353 - 359.
- (20) J.B. Wilkinson, G.R. Salter and D.R. Pilner,
British Welding Journal, 1960, 7, 78 - 87.
- (21) C.E. Jackson,
The Welding Journal, 1960, 39, 129s - 140s.
- (22) G. Den Ouden,
"Physical Properties of the Arc Column",
Lausanne, Annual Assembly of the International Institute
of Welding, 1970, 3 - 7.
- (23) H. Edels,
"Properties and Theory of the Electric Arc."
Proceedings of the Institution of Electrical Engineers,
1961, Vol. 108, Part A, No. 37, 55 - 69.
- (24) H.C. Ludwig,
The Welding Journal, 1959, 38, 206s - 300s.
- (25) H.H. Olson,
Phys. Fluids, 1949, 2, 260.
- (26) H. Maecker,
Z. Physik, 1955, 141, 198 - 216.
- (27) J.B. Wilkinson & D.R. Pilner,
British Welding Journal, 1960, 7, 115 - 128.
- (28) H. Christensen & J. Chipman,
Welding Research Council Bulletin, 1953, No. 15.
- (29) I.K. Pokhodyna & I.M. Prumin,
Avto Svarka, 1958, 5, 14 - 24.
- (30) G.R. Belton, T.J. Moore, & E.B. Tankins,
The Welding Journal, 1963, 42, 289s - 297s.
- (31) H. Christensen, V. de L. Davies, K.Gjermundsen.
British Welding Journal, 1965, 12, 54 - 75.
- (32) D.H. Rabkin,
British Welding Journal, 1959, 6, 132 - 137.
- (33) R.L. Apps & D.R. Pilner,
British Welding Journal, 1963, 10, 348 - 350.

- (34) D.G. Howden & D.R. Hilner,
British Welding Journal, 1963, 10, 304 - 316.
- (35) D.T. Babcock,
The Welding Journal, 1941, 20, 189s - 197s.
- (36) G.E. Claussen,
The Welding Journal, 1949, 28, 12 - 24.
- (37) E.C. Rollason & E. Bishop,
J.I.S.I. 1948, 158, 161 - 168.
- (38) H. Christensen,
The Welding Journal, 1949, 28, 373s - 380s.
- (39) P. Pollard & D.R. Hilner,
J.I.S.I. 1971, 209, 291 - 300.
- (40) R. Woods & D.R. Hilner,
The Welding Journal, 1971, 50, 163s - 173s.
- (41) J. Campbell,
Iron & Steel Institute Publication, 1967, 110, 19 - 26.
- (42) G.R. Salter & D.R. Hilner,
British Welding Journal, 1960, 7, 89 - 100.
- (43) D.G. Howden & D.R. Hilner,
British Welding Journal, 1963, 10, 395 - 398.
- (44) P.D. Blake & H.W. Jordan,
J.I.S.I. 1971, 209, 197 - 200.
- (45) J.F. O'Brien & H.W. Jordan,
Metal Construction, 1971, 3, 299 - 303.
- (46) T. Kobayashi, T. Kuwana & Y. Kitachi,
Welding in The World, 1967, 5 (2), 59 - 72.
- (47) E. Uda & T. Uda,
Transactions of National Research Institute for Metals,
1968, 10 (2), 79 - 91.
- (48) G.R. Pease, R.W. Brien & F.E. Legrand,
The Welding Journal, 1958, 37, 354s - 360s.
- (49) T. Kobayashi,
International Conference on the Welding and Fabrication
of Non-Ferrous Metals, 1972, Eastbourne, Paper 7.
- (50) G.R. Salter and D.R. Hilner,
British Welding Journal, 1965, 12, 222 - 228.
- (51) V.I. Galinich & V.J. Podgaetskii,
Avtó Svarka, 1961, 2, 34 - 32.

- (52) J.F. Wallace & R.J. Kissling,
Foundry, 1962, 90 (12), 36 - 39.
- (53) J.F. Wallace & R.J. Kissling,
Foundry, 1963, 91 (1), 64 - 68.
- (54) N.P. Allen,
Journal of the Institute of Metals, 1930, 43, 81 - 124.
- (55) A. Sieverts & M. Kruhbhaar,
Z. Physik Chem. 1910, 74, 277 - 307.
- (56) W. Eichenauer & A. Pebler,
Z. Metallkunde, 1957, 48, 373 - 378.
- (57) A. Sieverts,
Z. Physik Chem. 1911, 77, 591 - 613.
- (58) P. Röntgen & F. Höller.
Metallwirtschaft, 1934, 13, 81 - 97.
- (59) H.B. Bever & C.F. Floe,
Trans. A.I.M.E., 1944, 156, 149.
- (60) C.F. Floe & J. Chipman,
Trans. A.I.M.E., 1941, 143, 287 - 300.
- (61) T.F. Pearson, W.A. Baker & F.C. Child,
Institute of British Foundrymen, 1948, Paper 904.
- (62) P.H. Bartle,
British Welding Journal, 1963, 10, 367 - 373.
- (63) E.A. Taylor & D.C. Moore,
I.I.I. Hynoch - Private Communication.
- (64) E. Davies & C.A. Terry,
British Welding Journal, 1954, 1 (2), 53 - 64.
- (65) I. Onishi & T. Okui,
Jap. Weld. Soc., 1956, 25, 506 - 511.
- (66) B.N. Ames & H.A. Kahn,
Trans. American Foundrymen's Association, 1947, 55, 558 - 573.
- (67) D.R. Milner,
British Welding Journal, 1956, 3, 542 - 545.
- (68) O.I. Davies,
"Statistical Methods in Research and Production",
Oliver and Boyd, 1967.
- (69) R.W. Ralph & R.P. Jordan,
Institute of Welding, London Autumn Conference Proceedings,
1967, 27 - 34.

- (70) R.W. Carter,
Part I. Welding Institute Research Bulletin, October 1972,
13 (10), 307 - 308.
Part II. Welding Institute Research Bulletin, November 1972,
13 (11), 332 - 335.
- (71) G.R. Salter,
British Welding Journal, 1963, 10, 316 - 325.
- (72) L.S. Darken & R.W. Curry,
"Physical Chemistry of Metals",
London 1953, McGraw Hill.
- (73) J.F. Elliott & H. Gleiser,
"Thermochemistry for Steelmaking",
1960, 1, Pergamon Press, London - Paris.
- (74) J. Lammaas & H.F. Jordan,
University of Aston Final Year Project,
Dept. of Metallurgy, January 1973.

Metal	Thermal Conductivity Cgs units at 20°C
Copper	0.94
Aluminium	0.57
Iron	0.17
Nickel	0.21
Magnesium	0.40

TABLE 1 Thermal Conductivity of some
Pure Metals.
After Smithells (11)

Material to be Welded	Filler Wire	B.S.2901: Part 2 designation
Phosphorus deoxidised copper	Copper+0.25% Mn+0.25% Si Copper+0.25% Ti+0.25% Al	C.7 C.8 (for nitrogen arc welding)
Tough-pitch, high conductivity copper Zinc-deoxidised copper	Copper+0.02% B None, or if required, should match parent alloy	C.21
Aluminium brass	Aluminium brass (1.8 to 2.3% Al, 0.02 to 0.06% As)	C.15
Admiralty brass	Admiralty brass (1.0 to 1.5% Sn)	C.14
"Cupro-nickels" 95/5 Cu-Ni alloy	95/5 alloy (+0.2 to 0.5% Ti+Mn+Fe)	C.19
80/20 Cu-Ni alloy	80/20 alloy (+0.2 to 0.5% Ti+Mn+Fe)+	C.17
90/10 Cu-Ni alloy	90/10 alloy (+0.5% Ti)	
70/30 Cu-Ni alloy	70/30 alloy (+0.5% Ti+Mn+Fe)	C.18
Phosphor-bronze	Copper+4.5 to 6.0% Sn+0.4% P (max.) Copper +6.0 to 7.5% Sn+0.4% P (max.)	C.10 C.11 Select C.10, C.11 to match composition of parent alloy.
7% aluminium bronze	Copper+7% Al	C.12
10% aluminium bronze	Copper+10% Al	C.13
Aluminium bronze (Alloy D*)	"Alloy E"* (8 to 10% Al, 1.5 to 3.5% Fe, 4 to 7% Ni)	C.20
Nickel-aluminium bronze	"Alloy E"*	C.20
Silicon bronze	Everdur (Cu+2.75 to 3.25% Si +0.75 to 1.25% Mn)	C.9

TABLE 2 Recommended filler wires for the copper base alloys. After Institute of Welding Publication "Inert Gas Arc Welding" (12)

* A.S.T.N. Specification B.171

+ Alternatively, the 70/30 alloy may be used.

Element	ionization energy (eV)	Element	ionization energy (eV)
H	13.53	P	10.9
(H ₂)	15.6	S	10.30
He	24.5	A	15.68
B	8.26	K	4.32
C	11.22	Ca	6.09
(CO)	14.1	Ti	6.81
(CO ₂)	14.4	In	7.41
N	14.48	Fe	7.83
(N ₂)	15.51	Ni	7.61
O	13.55	Cu	7.68
(O ₂)	12.5	Zn	9.36
F	17.34	Zr	6.92
Na	5.12	Ho	7.35
Mg	7.61	Sn	7.30
Al	5.96	W	8.1
Si	8.12	Pb	7.38

Table 3. The ionization energy of some metals and gases.

After DEN OUDEN (22)

Gas	Temperature of arc column close to cathode °C
Alkali metal vapour	4,000
Alkaline earth vapour	5,000
Iron vapour	6,000
Argon (200 amp)	20,000
Argon (500 amp)	30,000

Table 4. Temperature of the arc column in various gases.

After Lancaster. (13)

Gas	dissociation energy (eV)
H ₂	4.48
N ₂	9.76
O ₂	5.08
CO	11.11
CO ₂	16.56

TABLE 5 The dissociation energy of some gases.
After DEN OUDEN (22)

Metal	Current Amps	Hydrogen Content of Liquid metal ml / 100 g.		Hydrogen to Form bubbles %
		In 1% Hydrogen Atmosphere (with arc)	At M.P. under 1 atmosphere Hydrogen	
Iron	150	4.25	30.2	50
Nickel	120	5.0	39	60
Copper	150	2.0	5.2	6.8
Aluminium	100	3.75	0.7	0.04

Table 6. Hydrogen concentration for
bubble formation in liquid.
After Howden & Milner (34)

Metal	Current amps	Hydrogen %	Hydrogen under static conditions %
Aluminium	150 a.c.	< 0.3	0.04
Copper	220 d.c.	0.7-1.0	6.8
Nickel	130 d.c.	25-30	60
Magnesium	145 a.c.	< 0.3	100

TABLE 7 Hydrogen required to initiate porosity.
After Salter and Milner (50)

SOLID COPPER										Ref
TEMP. °C	300	400	500	600	700	800	900	1000	1083	
SOLUBILITY	0.01	0.05	0.11	0.21	-	-	-	-	-	(56)
ml.N.T.P./100g	-	0.06	0.16	0.31	0.49	0.72	1.08	1.57	2.10	(57)
	-	-	-	0.11	0.27	0.53	0.89	1.34	1.90	(58)
LIQUID COPPER										
TEMP. °C	1083	1100	1150	1200	1250	1300	1350	1400	1500	
SOLUBILITY	6.0	6.3	7.3	8.3	9.3	10.3	11.1	12.0	13.3	(57)
ml.N.T.P./100g	5.1	5.4	6.3	7.2	8.3	9.2	10.4	11.8	-	(58)
	5.4	5.7	-	7.3	-	9.4	-	-	-	(59)

TABLE 8 Solubility of Hydrogen in Solid
and Liquid Copper.
After Smithells ⁽¹¹⁾

Experiment No.	Level of Variables	Experiment No.	Level of Variables
1	All low	17	b d
2	e f	18	a e
3	a b d f	19	c d
4	a b d e	20	b d e f
5	a c d f	21	c d e f
6	a c d e	22	b e
7	a b	23	b f
8	a c e f	24	a f
9	a c	25	a b c e
10	b c d e	26	a d
11	b c d f	27	a d e f
12	b c e f	28	c e
13	b c	29	a b c f
14	d e	30	a b c d e f
15	d f	31	a b c d
16	a b e f	32	c f

TABLE 9 Half Replicated Factorial Experiment

The order of experiments is random.

Letter stated = high level

Not stated = low level.

- a. Current
- b. Water vapour in Argon
- c. Argon flow rate
- d. Welding speed
- e. Weld preparation
- f. Base material.

Factor Involved	Level	
	Low	High
Base Material	D.H.P.	E.T.P.
Water Vapour in Argon	0	0.0005 g/l
Argon flow rate	7.5 l/min	22.0 l/min
Weld preparation	Butt weld	Melt run
Welding current*	(350 amps 225 amps)	(380 amps 275 amps)
Welding voltage	11.5	11.5
Welding speed	1 mm/sec	8 mm/sec

TABLE 10 EXPERIMENTAL VARIABLES AND LEVELS USED
IN THE HALF REPLICATED EXPERIMENT

Tungsten electrode size. 6mm dia, Tip angle 60°

* Two levels of current needed to give full penetration welds at high and low levels of welding speed.

EXP NO.	WATER VAPOUR g/litre	FLOW RATE l/min	WELDING SPEED mm/s	WELD PREP'N	BASE MAT'L	CURRENT Amps	OXYGEN CONTENT OF WELD Wt.%	DENSITY OF WELD g/cc
1	-	7.5	1	Butt	DHP	225	0.0018	8.71
2	-	7.5	1	Melt	ETP	225	0.0362	8.15
3	0.0005	7.5	8	Butt	ETP	380	0.0281	7.09
4	0.0005	7.5	8	Melt	DHP	380	0.0015	8.84
5	-	22.0	8	Butt	ETP	380	0.0441	6.41
6	-	22.0	8	Melt	DHP	380	0.0020	8.93
7	0.0005	7.5	1	Butt	DHP	275	0.0022	7.31
8	-	22.0	1	Melt	ETP	275	0.0360	8.92

TABLE 11 Summary of Results of Weld Metal Density and Oxygen Content for the half replicate experiment.

EXP NO.	WATER VAPOUR g/litre	FLOW RATE l/min	WELDING SPEED mm/s	WELD PREP'N	BASE MAT'L	CURRENT Amps	OXYGEN CONTENT OF WELD Wt.%	DENSITY OF WELD g/cc
9	-	22.0	1	Butt	DHP	275	0.0013	8.78
10	0.0005	22.0	8	Melt	DHP	350	0.0014	8.91
11	0.0005	22.0	8	Butt	ETP	350	0.0245	6.00
12	0.0005	22.0	1	Melt	ETP	225	0.0134	6.27
13	0.0005	22.0	1	Butt	DHP	225	0.0020	7.23
14	-	7.5	8	Melt	DHP	350	0.0026	8.93
15	-	7.5	8	Butt	ETP	350	0.0395	6.14
16	0.0005	7.5	1	Melt	ETP	275	0.0130	5.35

TABLE 11 Continued

EXP NO.	WATER VAPOUR g/litre	FLOW RATE l/min	WELDING SPEED mm/s	WELD PREP'N	BASE MAT'L	CURRENT Amps	OXYGEN CONTENT OF WELD Wt. %	DENSITY OF WELD g/cc
17	0.0005	7.5	8	Butt	DHP	350	0.0054	7.86
18	-	7.5	1	Melt	DHP	275	0.0019	8.83
19	-	22.0	8	Butt	DHP	350	0.0026	8.84
20	0.0005	7.5	8	Melt	ETP	350	0.0248	5.85
21	-	22.0	8	Melt	ETP	350	0.0361	8.91
22	0.0005	7.5	1	Melt	DHP	225	0.0019	7.72
23	0.0005	7.5	1	Butt	ETP	225	0.0173	5.06
24	-	7.5	1	Butt	ETP	275	0.0320	8.60

TABLE 11 Continued

EXP NO.	WATER VAPOUR g/litre	FLOW RATE l/min	WELDING SPEED mm/s	WELD PREP'N	BASE MAT'L	CURRENT Amps	OXYGEN CONTENT OF WELD Wt.%	DENSITY OF WELD g/cc
25	0.0005	22.0	1	Melt	DHP	275	0.0024	7.10
26	-	7.5	8	Butt	DHP	380	0.0018	8.91
27	-	7.5	8	Melt	ETP	380	0.0340	8.91
28	-	22.0	1	Melt	DHP	225	0.0033	8.87
29	0.0005	22.0	1	Butt	ETP	275	0.0100	4.93
30	0.0005	22.0	8	Melt	ETP	380	0.0284	6.60
31	0.0005	22.0	8	Butt	DHP	380	0.0035	7.21
32	-	22.0	1	Butt	ETP	225	0.0379	8.81

TABLE 11 Continued

Factor or Interaction	Significance Level	Factor or Interaction	Significance Level
Water Vapour	1%	Vapour-Speed	1%
Flow Rate	N.S.	Vapour-Preparation	N.S.
Welding Speed	1%	Oxygen content-Vapour	1%
Weld Preparation	1%	Flow-Speed	10%
Base Material (Oxygen content)	1%	Flow-Preparation	1%
Current	N.S.	Flow-Oxygen Content	2.5%
Current-Vapour	N.S.	Speed-Preparation	1%
Current-Flow	1%	Speed-Oxygen content	1%
Current-Speed	5%	Preparation-Oxygen Content	5%
Current-Preparation	N.S.		
Current-Oxygen Content	2.5%		
Vapour-Flow	10%		

TABLE 12 Significance Levels of the Effect of Single Factors and Interactions on Weld Metal Density.

N.S. Not Significant

Variable	Difference of Means; Low to High g/cc
Water Vapour	- 1.65
Base Material	- 1.31
Weld Preparation	+ 0.57
Welding speed	+ 0.23
Welding Current	+ 0.03
Flow rate	+ 0.03

TABLE 13 EFFECT OF SINGLE FACTORS ON WELD METAL DENSITY

EXP NO.	WATER VAPOUR g/litre	FLOW RATE l/min	WELDING SPEED mm/sec	WELD PREP'N	BASE MAT'L	CURRENT Amps	WELD OXYGEN Wt.%	DENSITY g/cc
1 ¹	-	7.5	1	B	OFHC	225	0.0010	8.66
2	-	7.5	1	M	ETP	225	0.0362	8.15
3	0.0005	7.5	8	B	ETP	380	0.0281	7.09
4 ¹	0.0005	7.5	8	M	OFHC	380	0.0007	8.91
5	-	22.0	8	B	ETP	380	0.0441	6.41
6 ¹	-	22.0	8	M	OFHC	380	0.0010	8.94
7 ¹	0.0005	7.5	1	B	OFHC	275	0.0045	5.56
8	-	22.0	1	M	ETP	275	0.0360	8.92
9 ¹	-	22.0	1	B	OFHC	275	0.0013	8.84
10 ¹	0.0005	22.0	8	M	OFHC	350	0.0012	8.96
11	0.0005	22.0	8	B	ETP	350	0.0245	6.00
12	0.0005	22.0	1	M	ETP	225	0.0134	6.27
13 ¹	0.0005	22.0	1	B	OFHC	225	0.0032	5.50
14 ¹	-	7.5	8	M	OFHC	350	0.0015	8.96
15	-	7.5	8	B	ETP	350	0.0395	6.14
16	0.0005	7.5	1	M	ETP	275	0.0130	5.35

TABLE 14 Summary of Weld Metal Density and Oxygen Content for $\frac{1}{2}$ Replicated Experiment with OFHC and ETP Copper.

B = Butt Weld

M = Melt Run

CURRENT AMPS	VOLTAGE VOLTS	ARC TIME MINS.	NITROGEN IN ARGON PER CENT	DENSITY g/cc
300	11	0.5	0	8.93
300	11	1.0	0	8.93
300	11	2.0	0	8.93
300	11	4.0	0	8.94
300	11	0.5	1.0	8.41
300	11	1.0	1.0	8.41
300	11	2.0	1.0	8.16
300	11	4.0	1.0	8.30

TABLE 15

Results of density determinations of O.F.H.C. copper buttons are melted in argon and argon 1 per cent nitrogen atmospheres at a flow rate of 10 litres per minute.

ELEMENT	O.F.H.C.	E.T.P.
	Wt. % ELEMENT	Wt. % ELEMENT
PH	< .01	< .01
LEAD	< .005	< .005
IRON	< .01	< .01
NICKEL	< .01	< .01
ZINC	< .01	< .01
LANGANESE	ND	ND
SILICON	ND	ND
MAGNESIUM	ND	ND
TITANIUM	ND	ND
PHOSPHORUS	< .001	< .001
ALUMINIUM	ND	ND
ARSENIC	< .005	< .005
ANTHONY	< .001	< .001
BISMUTH	< .001	< .001
BERYLLIUM	TRACE	TRACE
CADMIUM	ND	ND
CARBON	ND	ND
CHROMIUM	ND	ND
COBALT	ND	ND
SILVER	< .001	< .001
SULPHUR	ND	ND
TELLURIUM	< .001	< .001
ZIRCONIUM	< .001	< .001

TABLE 16

Results of spectrographic analysis
of O.F.H.C. and E.T.P. copper
used in arc melting experiments.

ARCING TIME (Mins)	CURRENT (Amps)	VOLTAGE (Volts)	MATERIAL	DENSITY g/cc	OXYGEN Wt.%	HYDROGEN ml/100g
0.5	300	11	OFHC	8.93	.0003	.16
1.0	300	11	OFHC	8.93	.0004	.15
2.0	300	11	OFHC	8.93	.0004	.16
4.0	300	11	OFHC	8.94	.0003	.16
0.5	300	11	ETP	8.73	.0303	.13
1.0	300	11	ETP	8.75	.0333	.14
2.0	300	11	ETP	8.76	.0316	.14
4.0	300	11	ETP	8.75	.0306	.14

TABLE 17 Results of oxygen, hydrogen and density determinations for OFHC and ETP copper arc melted in super purity argon.

ARCING TIME (mins)	WATER VAPOUR (VM)	CURRENT (Amps)	VOLTAGE (Volts)	MATERIAL	DENSITY (g/cc)	OXYGEN (wt.%)	HYDROGEN (ml/100g)
0.5	140	300	11	OFHC	8.66	.0006	.08
1.0	140	300	11	OFHC	8.65	.0007	.31
2.0	140	300	11	OFHC	8.76	.0007	.39
4.0	140	300	11	OFHC	8.73	.0007	.35
0.5	140	300	11	ETP	8.06	.0253	.11
1.0	140	300	11	ETP	8.13	.0278	.12
2.0	140	300	11	ETP	8.23	.0167	.14
4.0	140	300	11	ETP	8.27	.0100	.16
1	230	300	11	OFHC	8.68	.0006	.45
2	230	300	11	OFHC	8.69	.0005	.48
4	230	300	11	OFHC	8.67	.0004	.49
1	230	300	11	ETP	7.75	.0299	.37
2	230	300	11	ETP	7.96	.0212	.38
4	230	300	11	ETP	8.05	.0070	.39
1	540	300	11	ETP	7.94	.0264	.28
2	540	300	11	ETP	8.02	.0135	.41
4	540	300	11	ETP	8.88	.0012	.40

TABLE 18

Results of oxygen, hydrogen and density determination for OFHC and ETP copper arc melted in argon water vapour mixtures.

ARCING TIME (Mins)	WATER VAPOUR (VFH)	CURRENT (Amps)	VOLTAGE (Volts)	MATERIAL	DENSITY (g/cc)	OXYGEN (Wt.%)	HYDROGEN (ml/100g)
0.5	140	300	11	ETP/OFHC	8.07	0.0117	0.16
1.0	140	300	11	ETP/OFHC	8.29	0.0124	0.28
2.0	140	300	11	ETP/OFHC	8.32	0.0088	0.39
4.0	140	300	11	ETP/OFHC	8.74	0.0019	0.40
1.0	190	300	11	ETP/OFHC	8.19	0.0153	0.18
2.0	190	300	11	ETP/OFHC	8.37	0.0069	0.40
4.0	190	300	11	ETP/OFHC	8.80	0.0009	0.36

TABLE 19

Results of oxygen, hydrogen and density determinations for equal weights of ETP and OFHC copper arc melted in argon water vapour mixtures.

ARCING TIME (Mins)	WATER VAPOUR (VPM)	CURRENT (Amps)	VOLTAGE (Volts)	MATERIAL	DENSITY (g/cc)	OXYGEN (Wt.%)	HYDROGEN (ml/100g)
1.0	100	350	11	OFHC	8.70	0.0008	0.15
2.0	100	350	11	OFHC	8.75	0.0004	0.50
4.0	100	350	11	OFHC	8.72	0.0005	0.54

TABLE 20

Results of oxygen, hydrogen and density determinations for OFHC buttons arc melted in an argon water vapour mixture at an increased current.

ARCING TIME (Mins)	WATER VAPOUR (VPM)	CURRENT (Amps)	VOLTAGE (Volts)	MATERIAL	OXYGEN Wt.%	HYDROGEN ml/100g
4.0	100	300	11	O.F.H.C.	0.0003	0.38
4.0	100	300	11	O.F.T.C.	0.0003	0.34
4.0	100	300	11	O.P.H.C.	0.0003	0.34

TABLE 21 Oxygen and hydrogen contents of three O.F.H.C. melts carried out under identical conditions

ARCING TIME (mins)	WATER VAPOUR (VPE)	CURRENT (Amps)	VOLTAGE (Volts)	MATERIAL	DENSITY (g/cc)	OXYGEN (Wt.%)	HYDROGEN (ml/100g)
1.0	100	300	11	OFHC	8.81	0.0001	0.64
2.0	100	300	11	1.81	8.79	0.0001	0.59
4.0	100	300	11	Wt% Ti	8.80	0.0001	0.69
1.0	100	300	11	OFHC	8.90	0.0001	0.52
2.0	100	300	11	0.12	8.84	0.0001	0.48
4.0	100	300	11	Wt% Ti	8.84	0.0001	0.53
1.0	100	350	11	OFHC	8.88	0.0001	0.88
2.0	100	350	11	1.81	8.81	0.0001	0.77
4.0	100	350	11	Wt% Ti	8.90	0.0001	0.77

TABLE 22 Results of oxygen, hydrogen and density determinations for copper titanium alloys arc melted in argon water vapour mixtures.

ARCING TIME (Mins)	WATER VAPOUR (VPH)	CURRENT (Amps)	VOLTAGE (Volts)	MATERIAL	DENSITY	OXYGEN Wt. %	HYDROGEN ml/100g
1.0	130	300	11	OFHC/ 1.3 wt%Al	8.77	.0002	.56
2.0	130	300	11	--	8.74	.0002	.54
4.0	130	300	11	--	8.76	.0002	.56
1.0	130	300	11	OFHC/ 0.13 wt%Al	8.93	.0003	.33
2.0	130	300	11	--	8.91	.0004	.30
4.0	130	300	11	--	8.94	.0004	.33

TABLE 23 Results of oxygen, hydrogen and density determinations for copper aluminium alloys are melted in an argon water vapour mixture.

WATER VAPOUR IN ARGON ATMOSPHERE	CURRENT (Amps)	MATERIAL	OXYGEN CONTENT Wt. %	HYDROGEN CONTENT (mgH ₂ /100g)	'A' VALUE
150.3 x 10 ⁻⁶	300	OFHC	0.0007	0.0315	0.068
247.0 x 10 ⁻⁶	300	OFHC	0.0004	0.0441	0.056
579.8 x 10 ⁻⁶	300	ETP	0.0012	0.0360	0.052
204.0 x 10 ⁻⁶	300	ETP/OFHC	0.0009	0.0324	0.068
107.4 x 10 ⁻⁶	300	OFHC	0.0003	0.0342	0.057
107.4 x 10 ⁻⁶	300	OFHC	0.0003	0.0306	0.051
107.4 x 10 ⁻⁶	300	OFHC	0.0003	0.0306	0.051

TABLE 24 Calculation of Apparent Equilibrium constants under arc melting conditions using the equation of Allen and Hewitt. (15)

$$[H] = A \sqrt{\frac{p_{H_2O}}{[O]}}$$

where [H] = button hydrogen content mg. Hydrogen/100g
 [O] = button oxygen content, Wt. %
 p_{H₂O} = partial pressure of water vapour (atmosphere)

ARCING TIME (Mins)	HYDROGEN IN ARGON (V.P.H.)	CURRENT (Amps)	VOLTAGE (Volts)	MATERIAL	OXYGEN Wt.%
0.5	280	300	11	ETP	.0222
1.0	280	300	11	ETP	.0148
2.0	280	300	11	ETP	.0057
4.0	280	300	11	ETP	.0018

TABLE 25 Oxygen contents of ETP copper are
melted in an argon, hydrogen mixture.

ARCING TIME (Mins)	HYDROGEN IN ARGON (VPL)	OXYGEN IN ARGON (VPL)	CURRENT (Amps)	VOLTAGE (Volts)	MATERIAL	OXYGEN (Wt.%)	HYDROGEN (ML/100g)
0.5	153	-	300	11	OFHC	-	0.51
1.0	153	-	300	11	OFHC	-	0.52
2.0	153	-	300	11	OFHC	-	0.52
4.0	153	-	300	11	OFHC	-	0.53
0.5	-	77	300	11	OFHC	0.0009	-
1.0	-	77	300	11	OFHC	0.0009	-
2.0	-	77	300	11	OFHC	0.0013	-
4.0	-	77	300	11	OFHC	0.0011	-

TABLE 26 Hydrogen and oxygen contents of OFHC copper arc melted in argon, hydrogen and argon, oxygen mixtures.

ALUMINIUM		COPPER		NICKEL				
TEMP °C	SOL. ml/100g	TEMP °C	SOL. ml/100g	TEMP °C	SOL. ml/100g			
S {	350	0.0012	S {	300	.01	S {	300	2.0, 2.4, 2.5,
	400	0.0028, 0.0050		400	.05, .06,		400	2.5, 3.2, 3.7,
	500	.011, .013,		500	.11, .16,		500	3.3, 4.2, 4.9,
	600	.030, .026,		600	.21, .31, .11,		600	4.3, 5.4, 6.1,
	660	.050, .036,		700	.49, .27,		700	5.6, 6.7, 7.2,
+		800	.72, .53,	800	7.0, 8.0, 8.4,			
L {	660	.69, .43,	900	1.08, 0.89,	S {	900	8.5, 9.5, 9.4,	
	700	.92, .63, .90,	1000	1.57, 1.34,		1000	10.0, 11.1,	
	750	1.23,	1083	2.1, 1.9,		1100	11.5, 12.7,	
	800	1.67, 1.23, 1.75,	+			1200	13.0, 14.3,	
	900	2.18, 2.75,	1083	6.0, 5.1, 5.4,		1300	15.9,	
	1000	3.51, 4.15,	1100	6.3, 5.4, 5.7,		1400	17.5, 18.8,	
			1150	7.3, 6.3,		1453	18.3,	
		1200	8.3, 7.2, 7.3,	+				
		L {	1250	9.3, 8.3,	L {	1453	39.2,	
			1300	10.3, 9.2, 9.4,		1500	40.9, 38.5,	
			1350	11.1, 10.4,		1570	38.8,	
			1400	12.0, 11.8,		1600	42.5, 40.3,	
			1500	13.3				

TABLE 27 Solubility of hydrogen at 1 atmosphere pressure in aluminium, copper and nickel over a range of temperatures.
(After Smithells (11))

+ Melting Point

S = Solid

L = Liquid

METAL	HYDROGEN SOLUBILITY RATIO 'R'	TYPE OF POROSITY
ALUMINIUM	R = 13.02	ROUND PORES
COPPER	R = 2.75	HERRINGBONE
NICKEL	R = 2.14	CLEFT LINE

TABLE 28

Hydrogen solubility ratios (R) for
aluminium, copper and nickel.

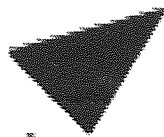
$$R = \frac{\text{mean hydrogen solubility in liquid at melting point}}{\text{mean hydrogen solubility in solid at melting point.}}$$



Aston University

Illustration removed for copyright restrictions

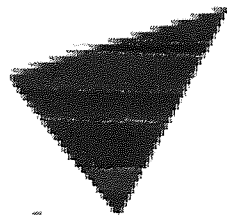
Fig. 1. Schematic representation of the three
different regions of the electric arc.
After Den Ouden (22)



Aston University

Illustration removed for copyright restrictions

Fig. 2. Dissociation in molecular gas
at 1 atm pressure.
After Ludwig ⁽²⁴⁾



Aston University

Illustration removed for copyright restrictions

Fig. 3. Total thermal conductivity of
some representative gases as a function
of temperature (calculated).
After Ludwig ⁽²⁴⁾



Aston University

Illustration removed for copyright restrictions

Fig. 4. Temperature distribution in a
200 amp argon-shielded tungsten/copper
arc.

After Olsen (25)



Aston University

Illustration removed for copyright restrictions

Fig. 5. Hydrogen solubility/temperature curves.
After Howden and Milner (34)

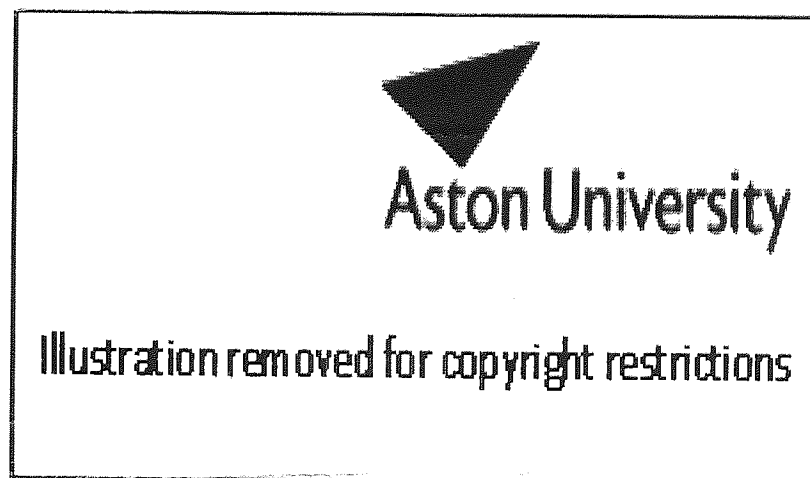


Fig. 6. Model of gas absorption in T.I.G. arc
welding showing the high temperature zone
under the arc and convective forces in
the weld pool.
After Howden and Milner (34)

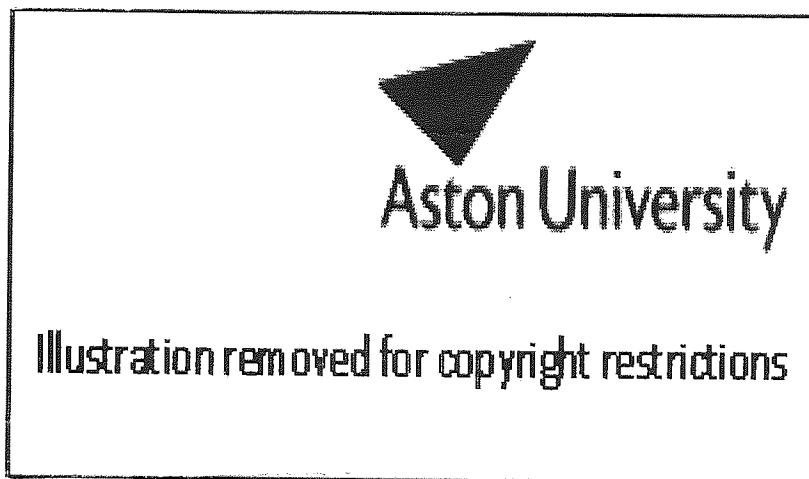


Fig 7. Relationship of weld metal Nitrogen content and shielding gas composition in the metal inert gas arc welding of mild steel.
After Blake and Jordan ⁽⁴⁴⁾

TEMPERATURE °C	1090	1150	1250	1350
'A' VALUE	0.0085	0.014	0.022	0.034

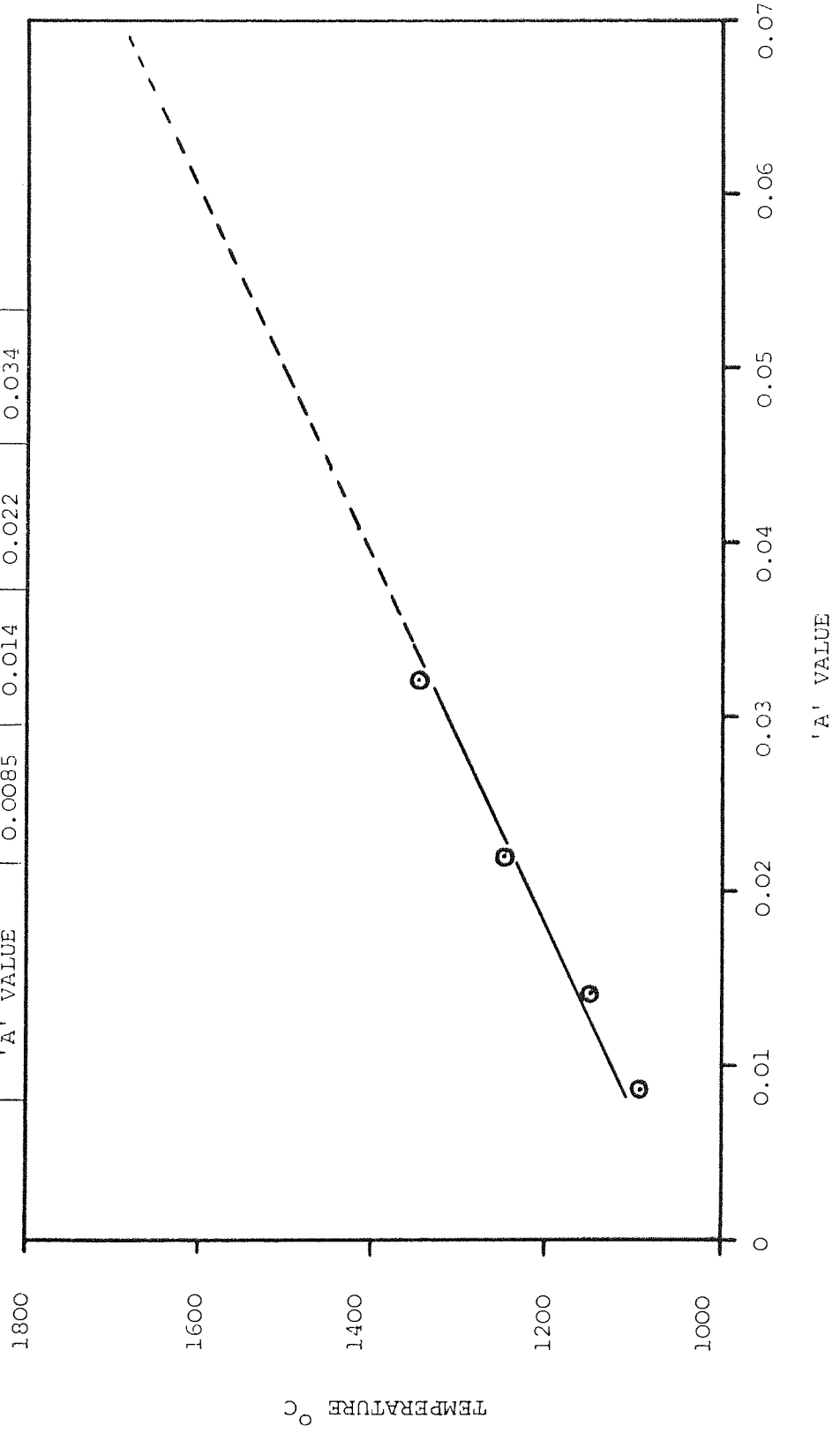


Figure 8 Plot of 'A' Value against temperature using the data of Allen and Hewitt (15)

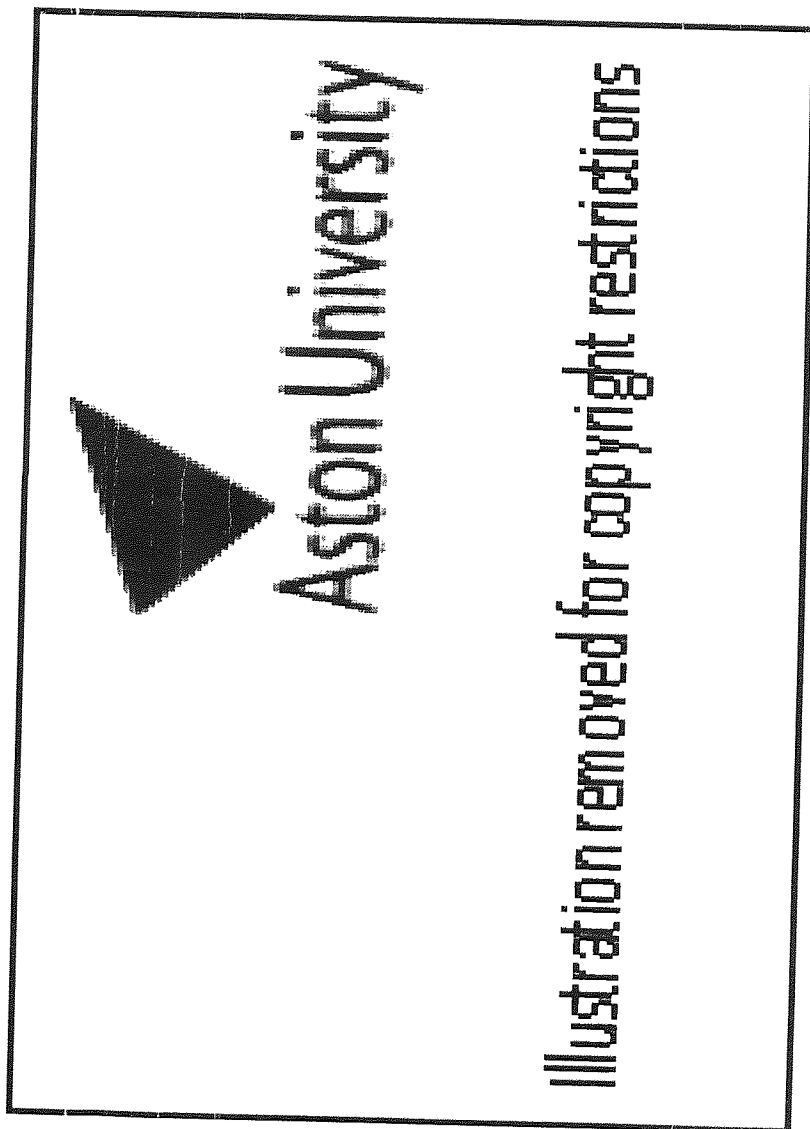
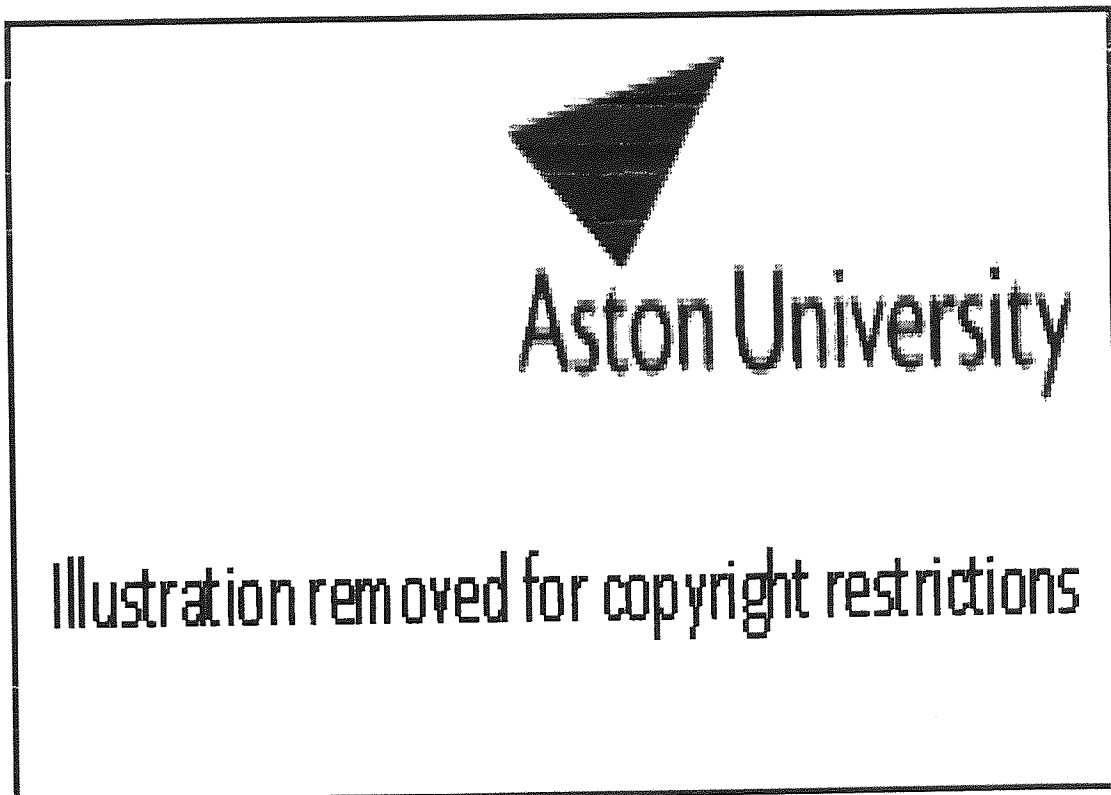
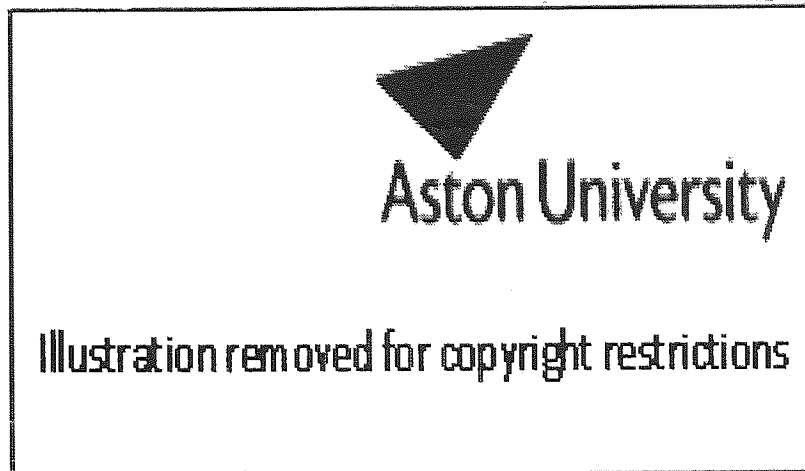


Figure 9

Effect of welding speed and hydrogen on the density of copper melt runs.

After SALTER and MILNER (50)



- Figure 10 (a) Effect of titanium on the porosity in O.F.H.C. bead on plate runs using shielding gases of Argon Nitrogen mixtures.
- (b) Effect of titanium on weld metal Nitrogen content of O.F.H.C. bead on plate runs using shielding gases of Argon Nitrogen mixtures.

After Kobayashi (49)

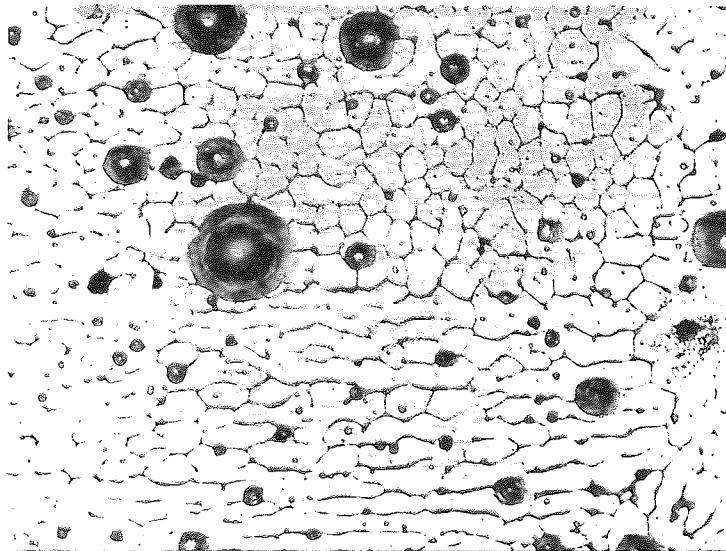


Figure 11: Micrograph showing weld metal porosity in E.T.P. weld number 5.

MAGNIFICATION: - x 300
ETCHANT: - ALCOHOLIC FERRIC
CHLORIDE

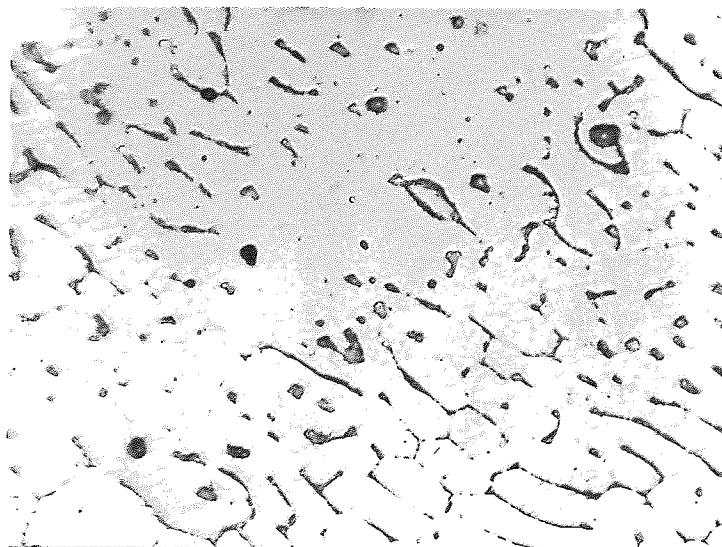
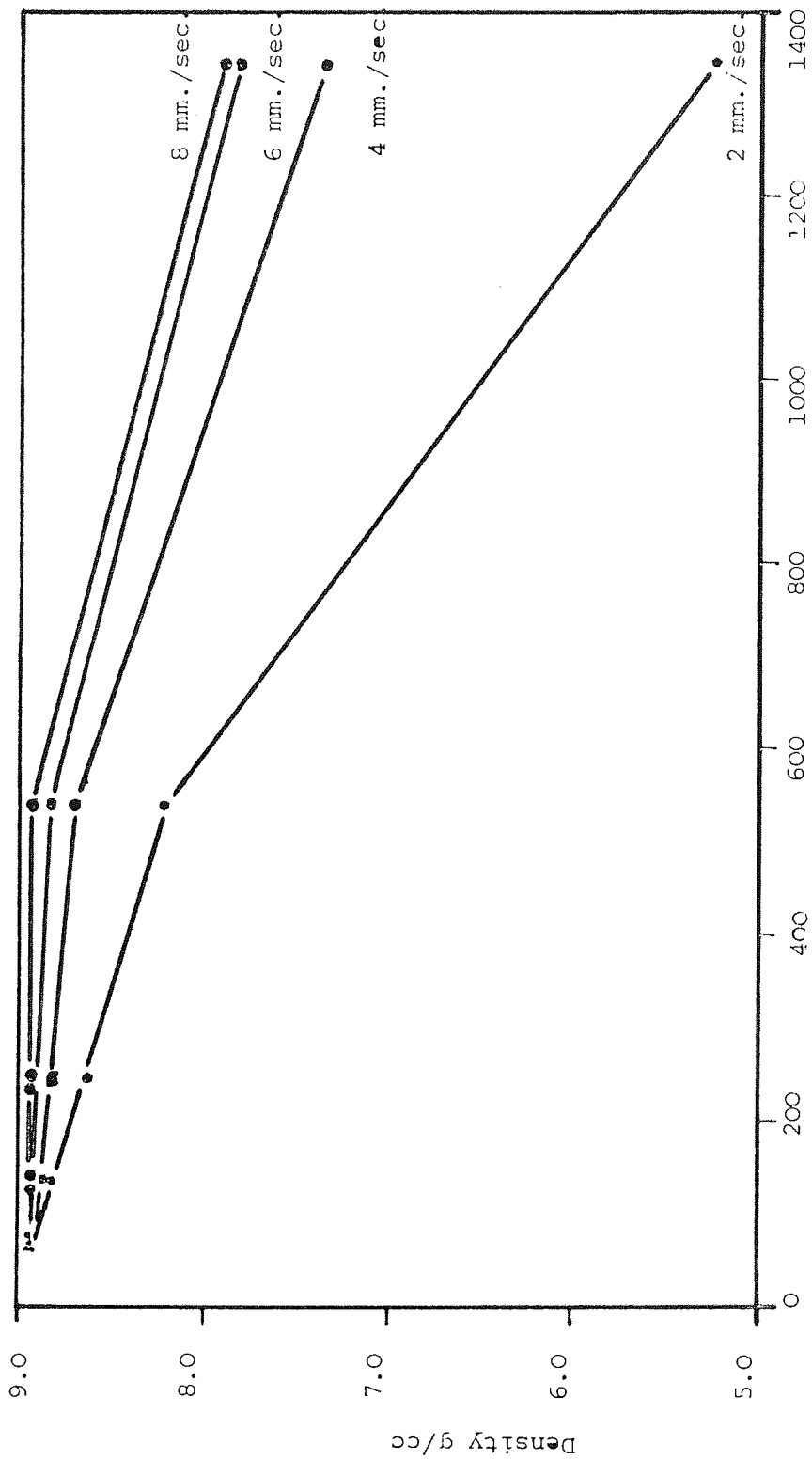


Figure 12: Micrograph showing edge of weld metal in E.T.P. weld number 8.

MAGNIFICATION: - x 300
ETCHANT: - ALCOHOLIC FERRIC
CHLORIDE



WATER VAPOUR IN ARGON v.p.m.

Figure 13 Effect of welding speed and water vapour content of shielding gas on the density of O.F.H.C. copper weld metal.

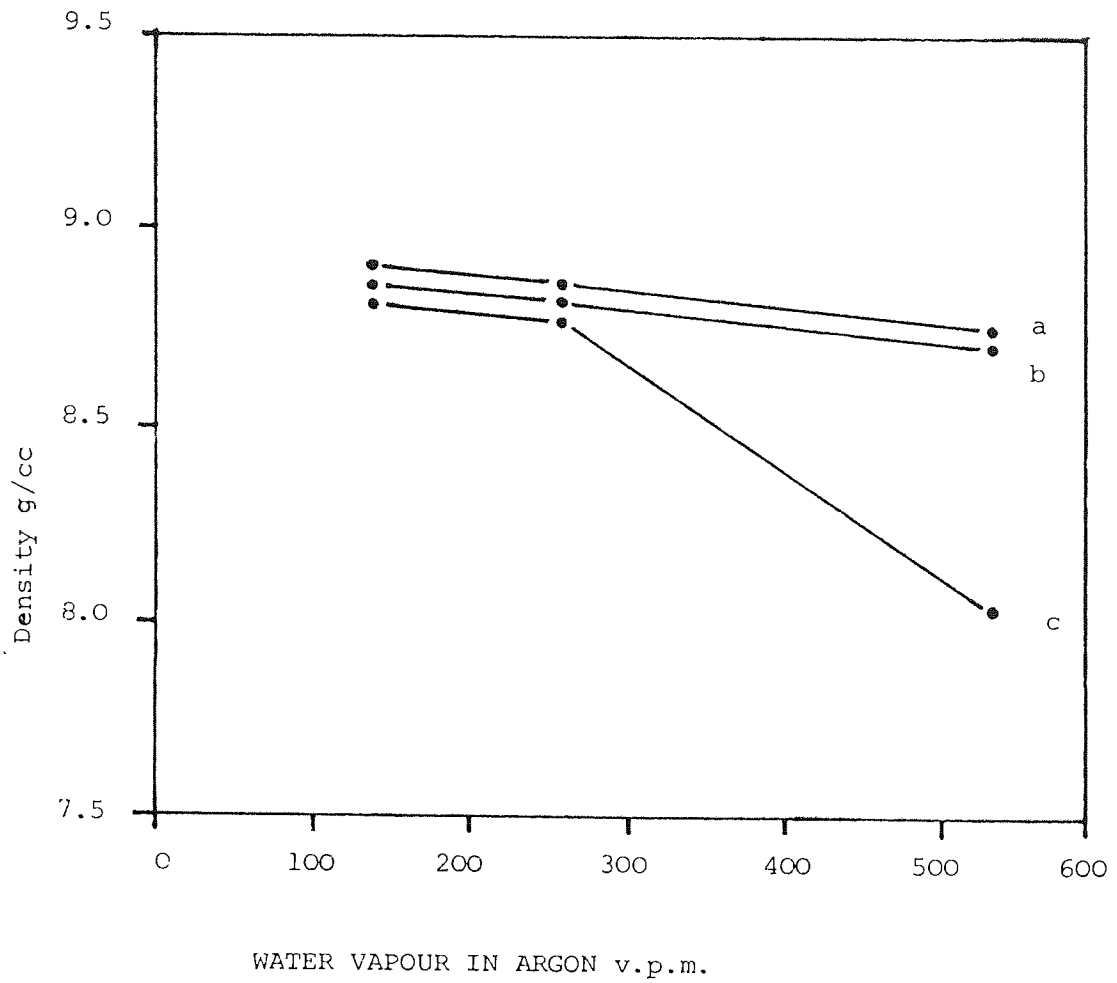


Figure 14 Effect of base material and water vapour content of shielding gas on weld metal density at a constant welding speed of 4 mm.per second.

- (a) D.H.P
- (b) O.F.H.C.
- (c) E.T.P.

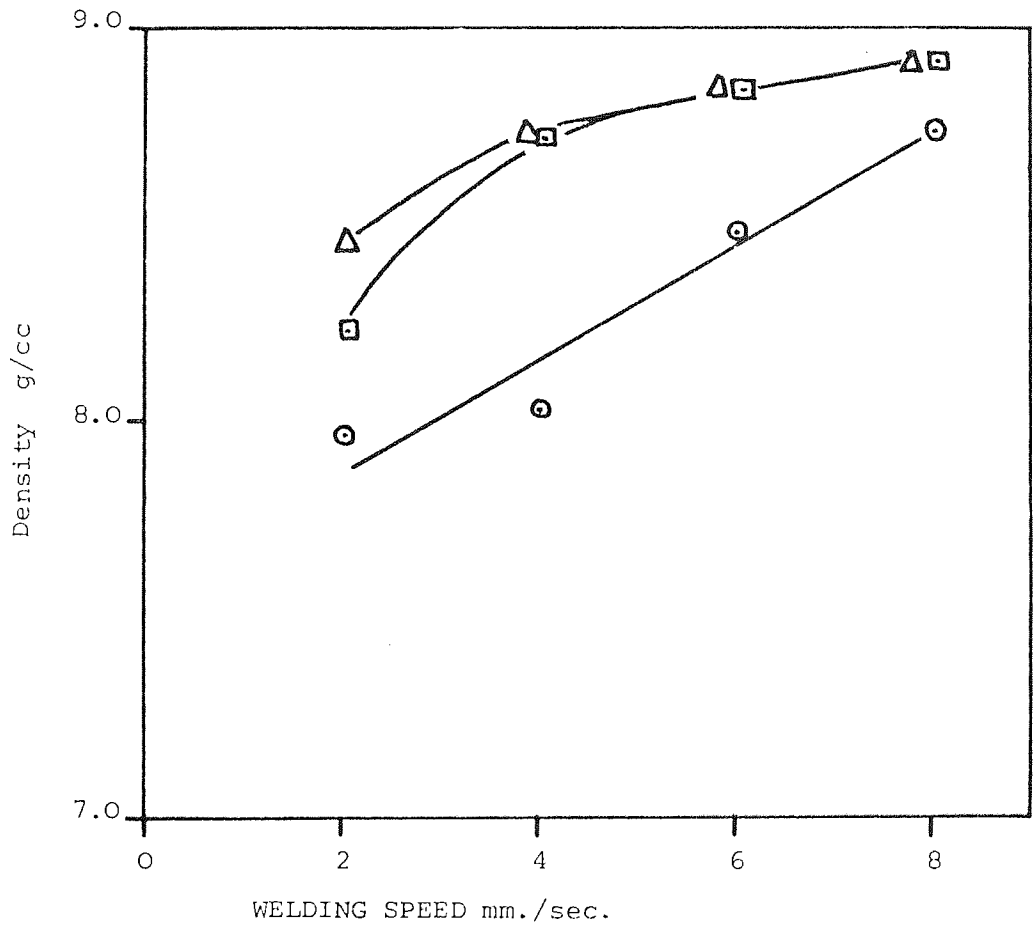


Figure 15 Effect of welding speed and base material on weld metal density, using a shielding gas of argon, 540 vpm water vapour

- △ D.H.P.
- ▣ O.F.H.C.
- ⊙ E.T.P.

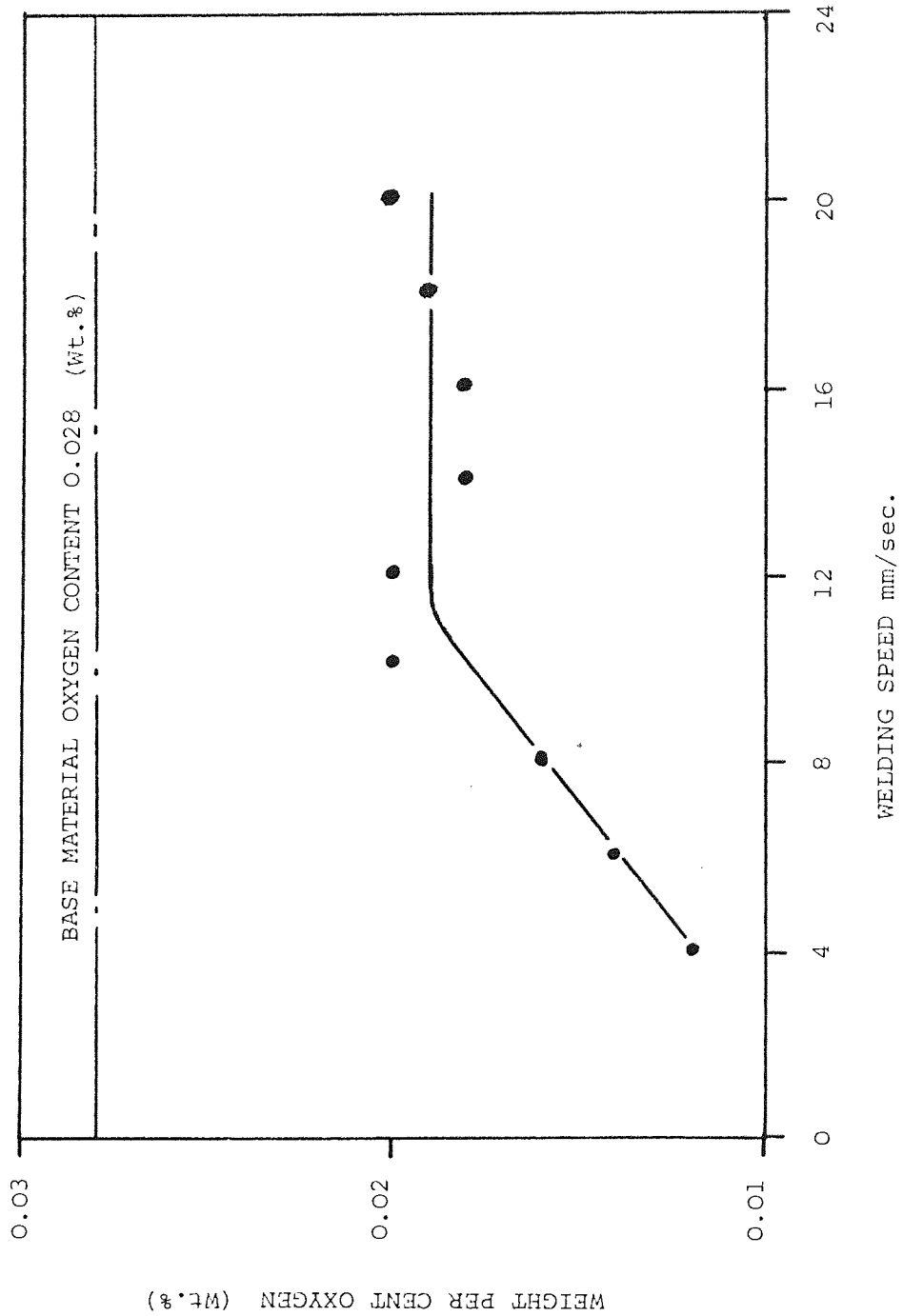


Figure 16

Effect of welding speed on weld metal oxygen content using a shielding gas of argon containing 2 per cent hydrogen.

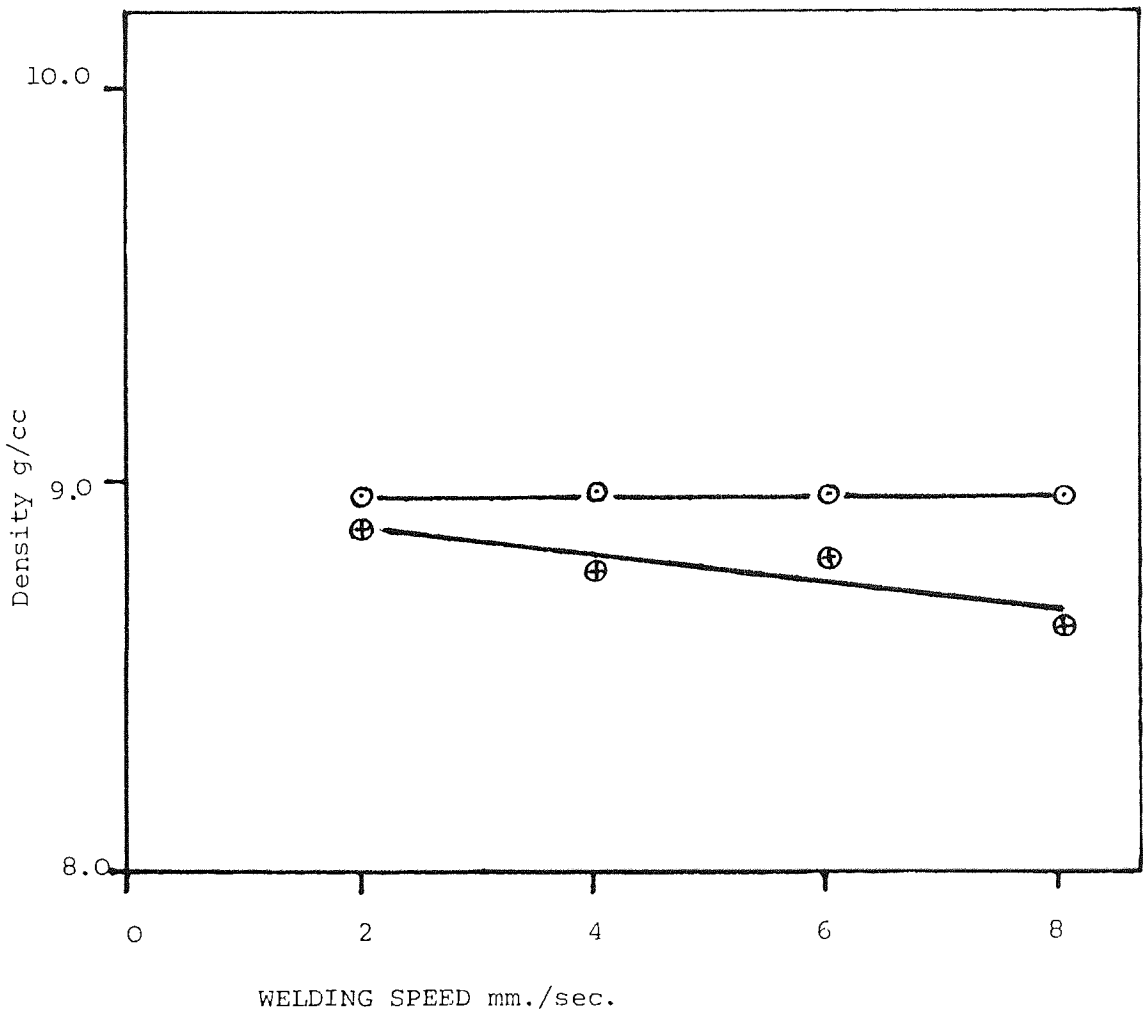


Figure 17 Effect of welding speed on density of E.T.P. copper

- ⊙ Melt runs
- ⊕ Butt welds.

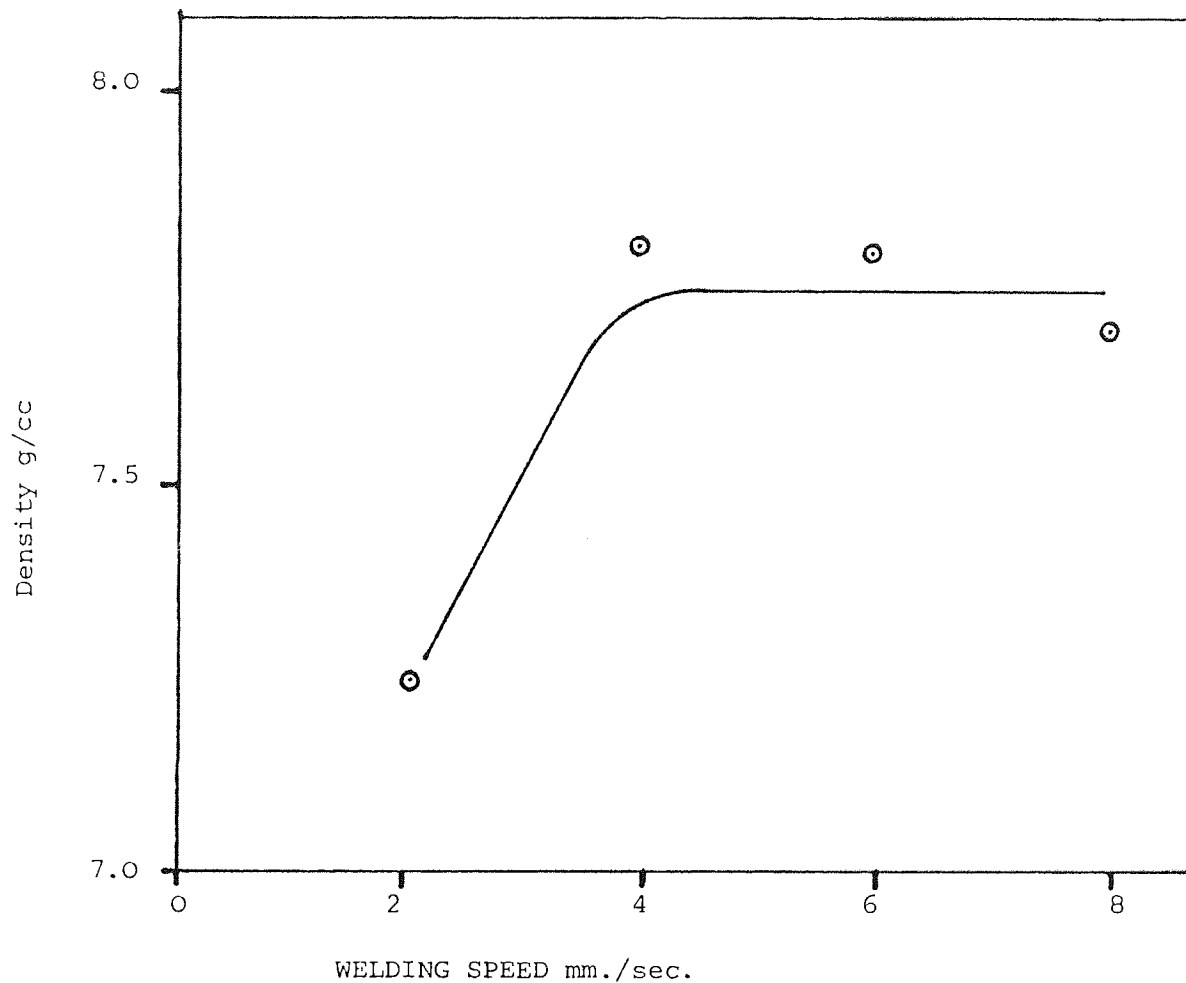
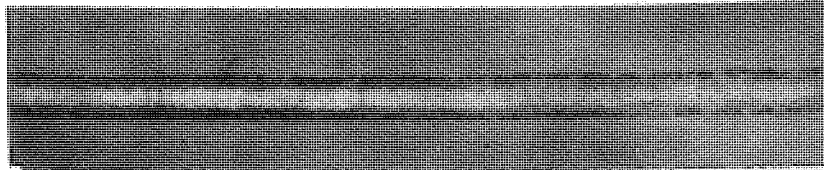
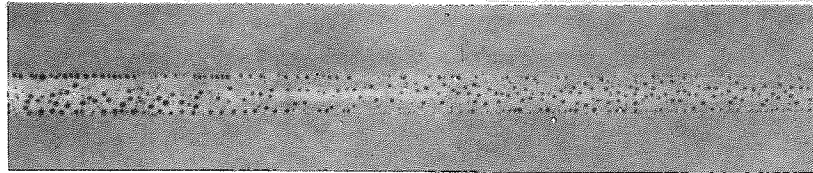


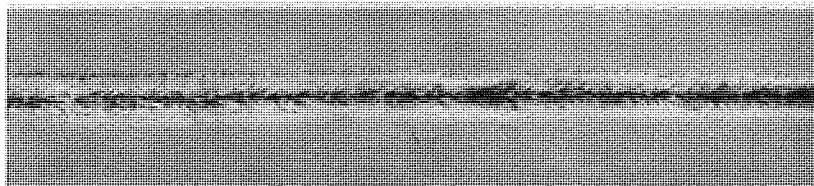
Figure 18 Effect of welding speed on the density of O.F.H.C. copper weld metal using a commercial purity nitrogen shielding gas.



a



b



c

Figure 19 Porosity produced in O.F.H.C. copper using shielding gases of:

- a) Commercial purity nitrogen
- b) Argon + water vapour
- c) Argon + hydrogen

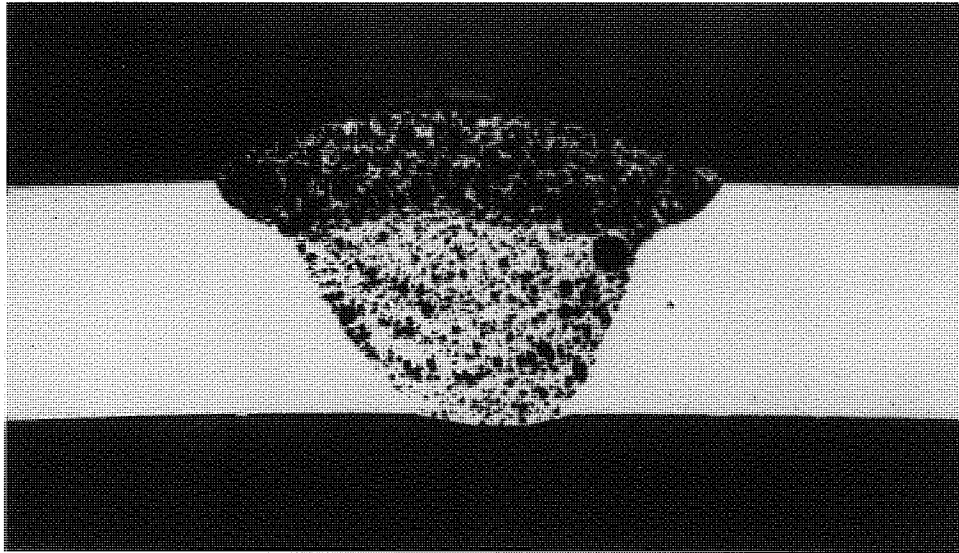


Figure 20 Porosity in O.F.H.C. copper weld metal
using commercial purity nitrogen
shielding gas.

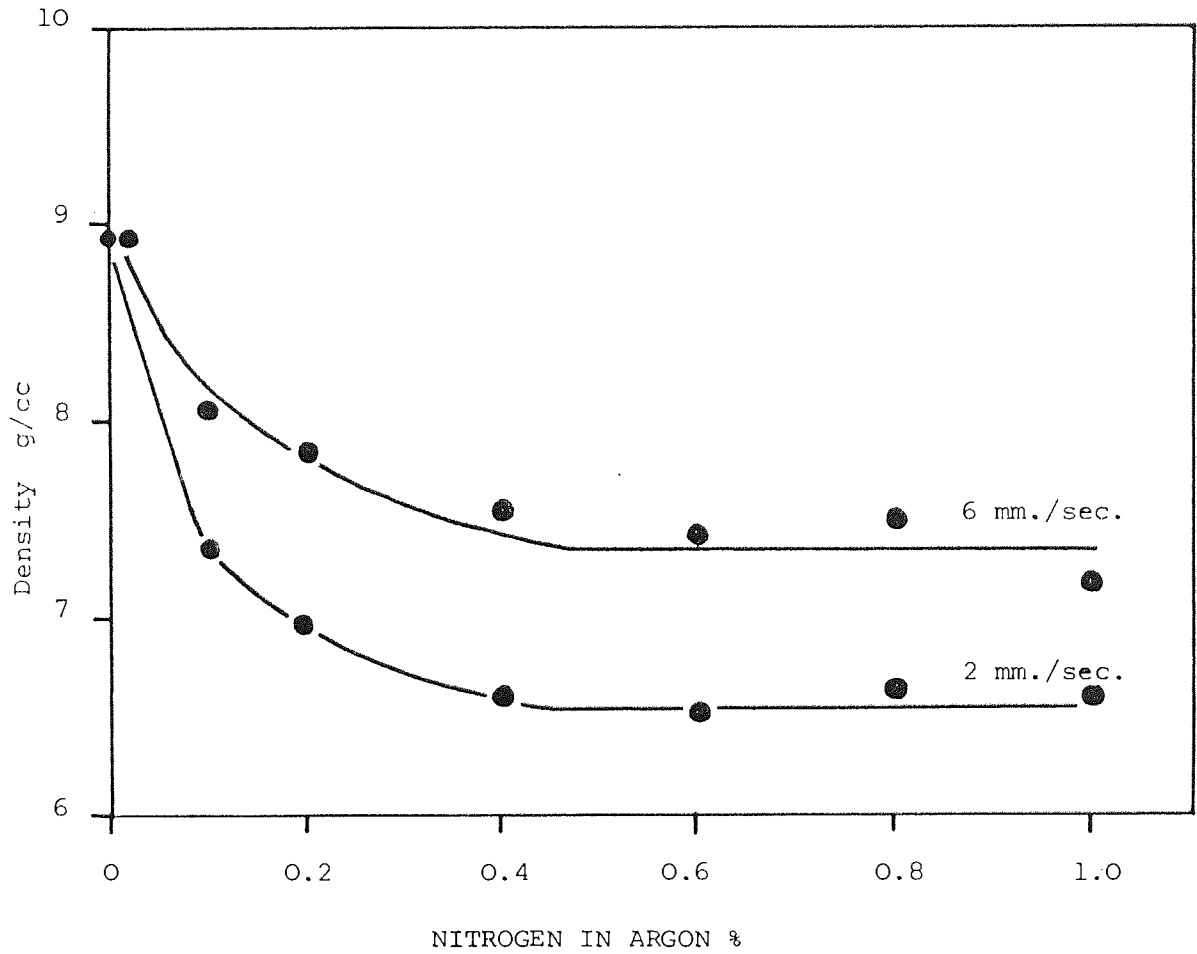


Figure 21 Effect of welding speed and nitrogen content of the argon shielding gas on the density of O.F.H.C. melt runs.

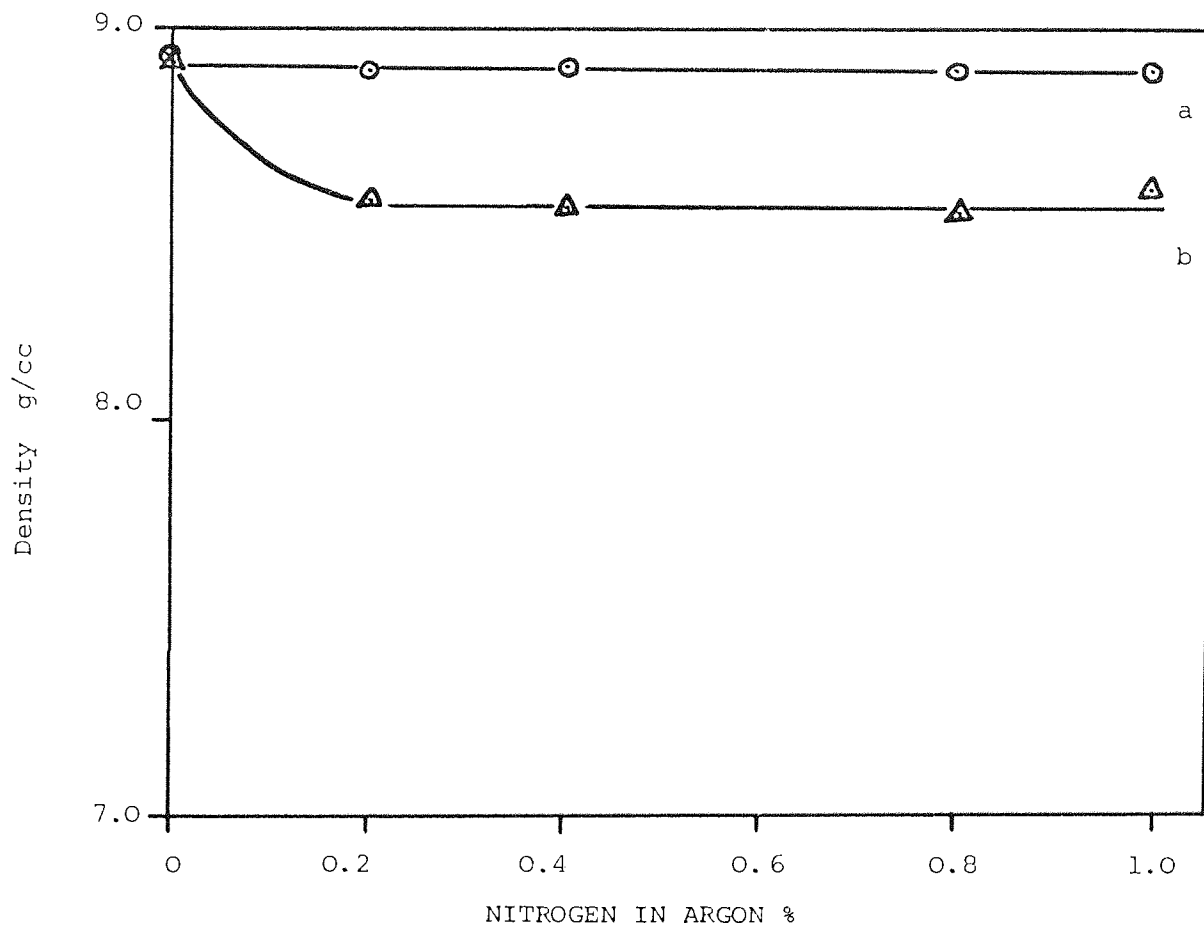


Figure 22 Effect of nitrogen content of the shielding gas on the density of O.F.H.C. T.I.G. + filler bead on plate runs using filler wires:-

(a) Nitrofil

(b) Argofil.

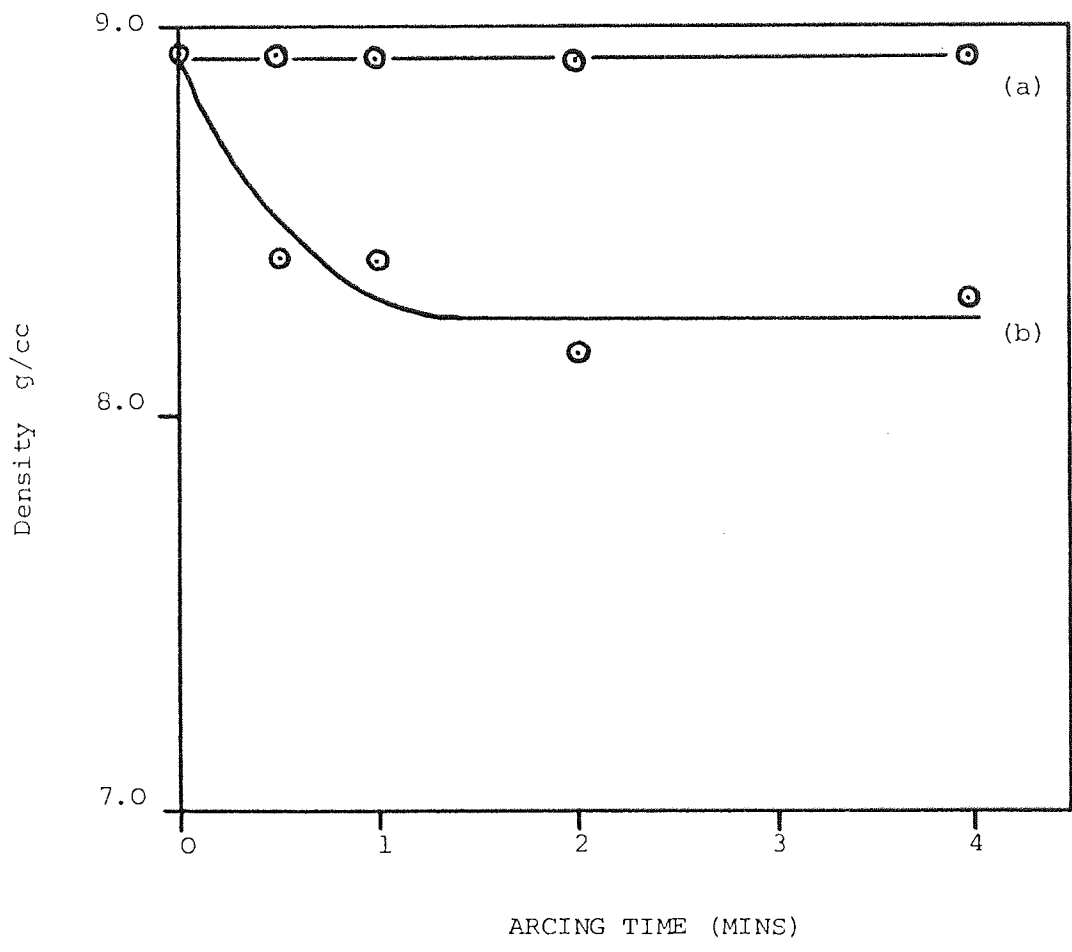


Figure 23 Density of O.F.H.C. copper buttons arc melted for varying times in atmospheres of;

(a) argon

(b) argon, 1 per cent nitrogen.

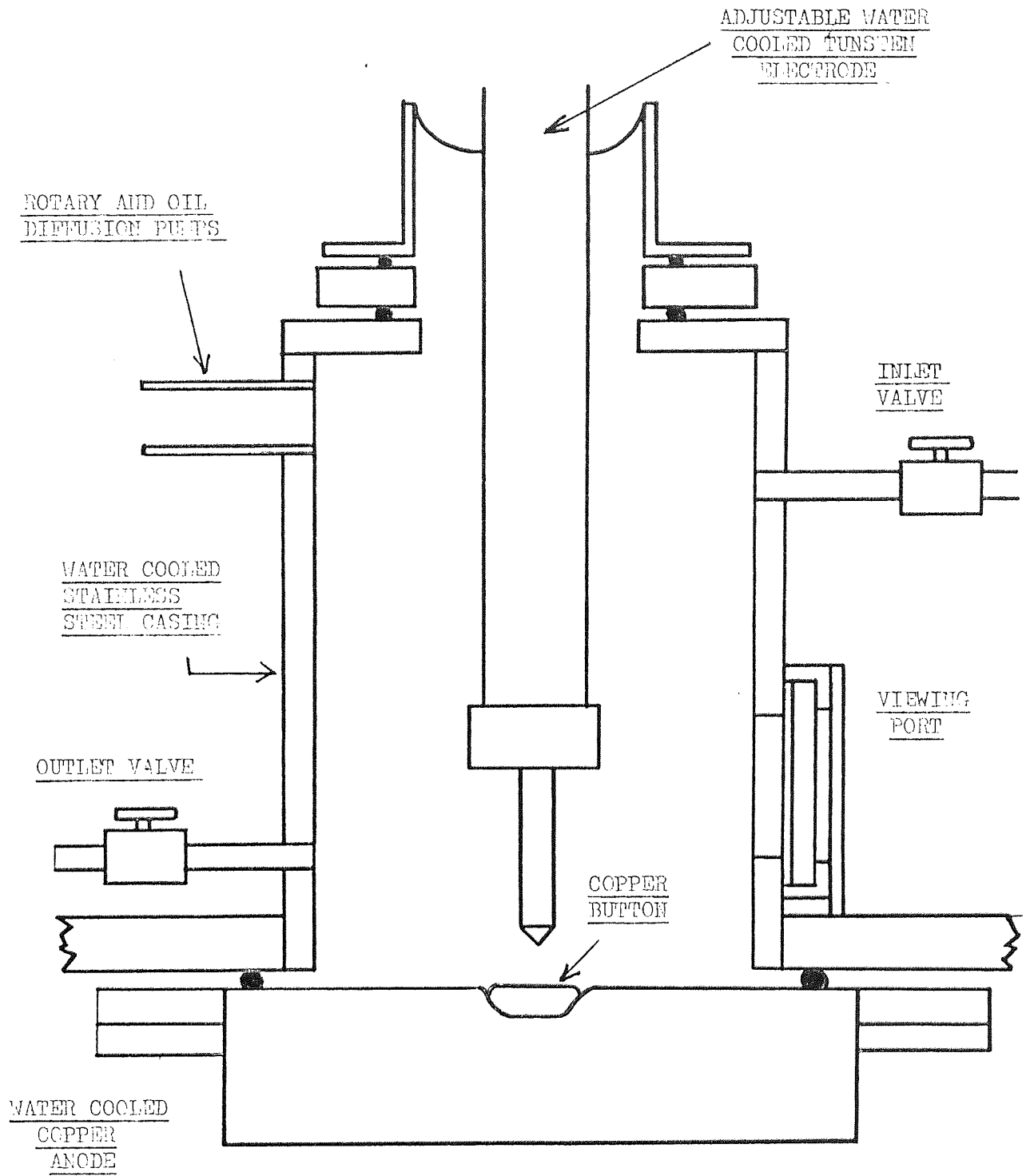


Figure 24 (a): Schematic representation showing the essential features of the controlled atmosphere arc melting box.

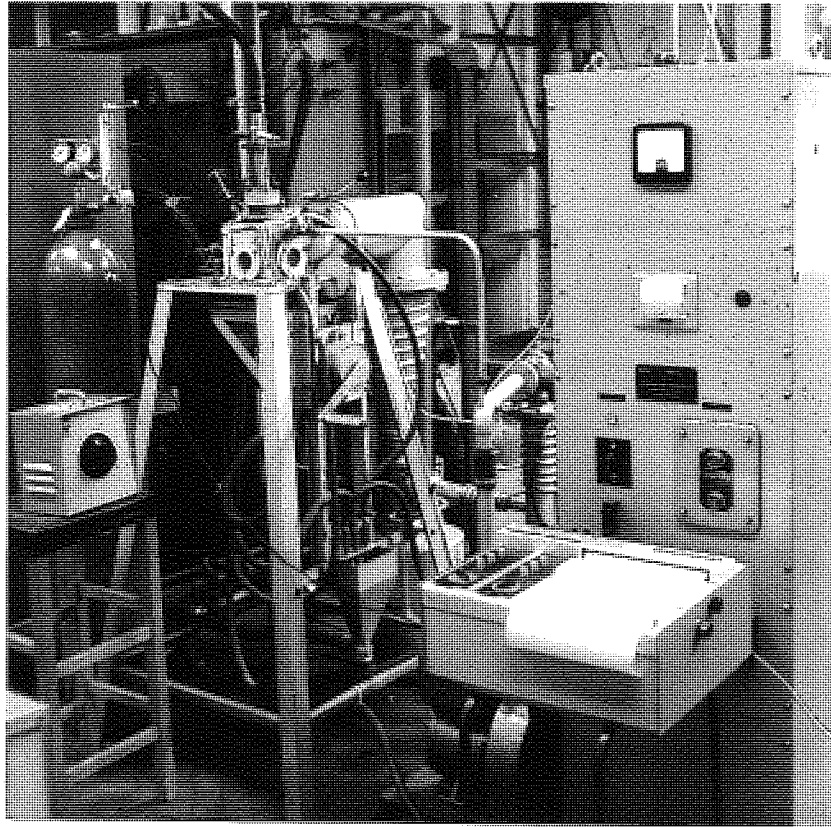
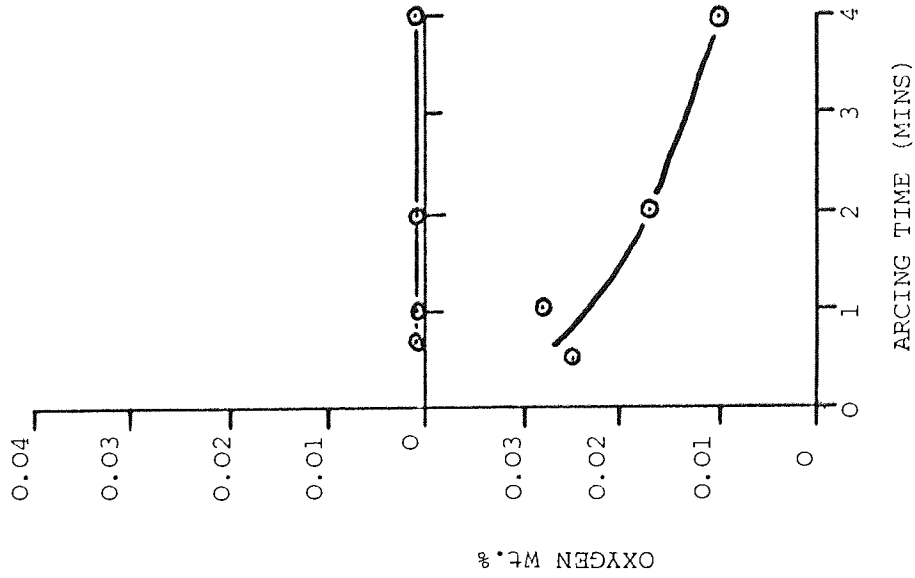
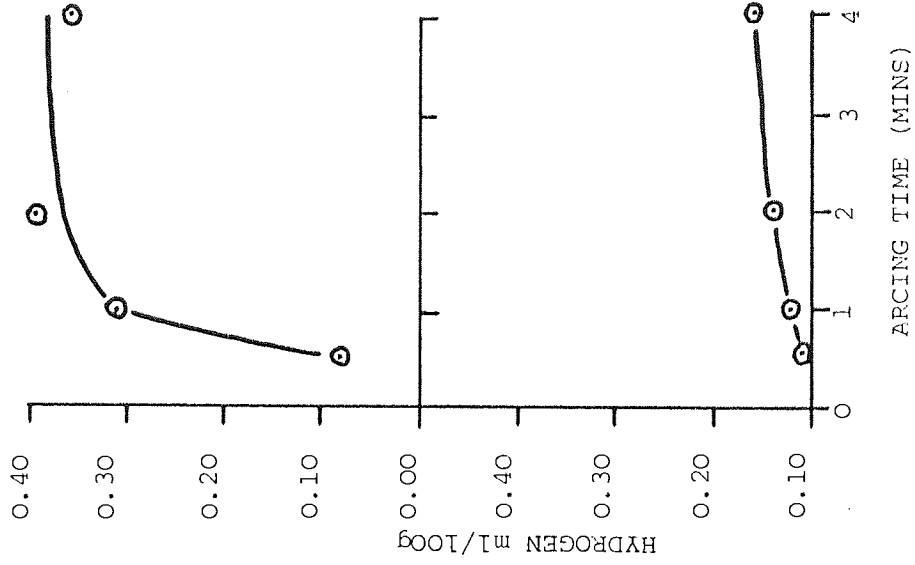


FIGURE 24(b): Arc melting equipment showing (from right to left) vacuum pumping control panel, recorder, arc melting box and welding set control box.



-(a) -



-(b) -

Figure 25

Oxygen and hydrogen contents of O.F.H.C. and E.T.P. copper arc melted in argon water vapour mixtures;

(a) O.F.H.C. arc melted at 300 amps in an argon, 140 v.p.m. water vapour mixture.

(b) E.T.P. arc melted at 300 amps in an argon, 140 v.p.m. water vapour mixture.

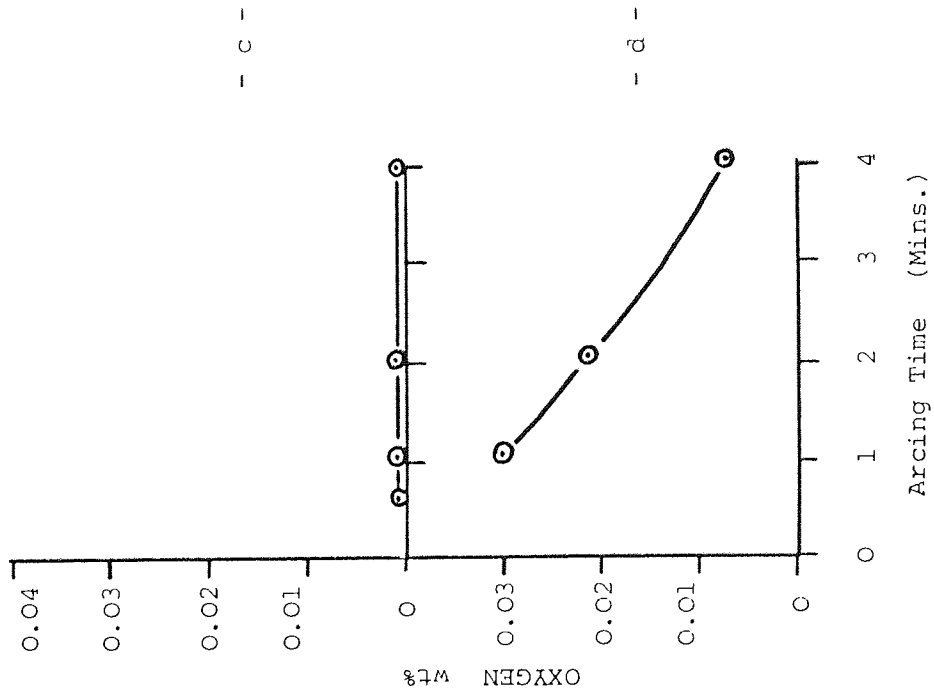
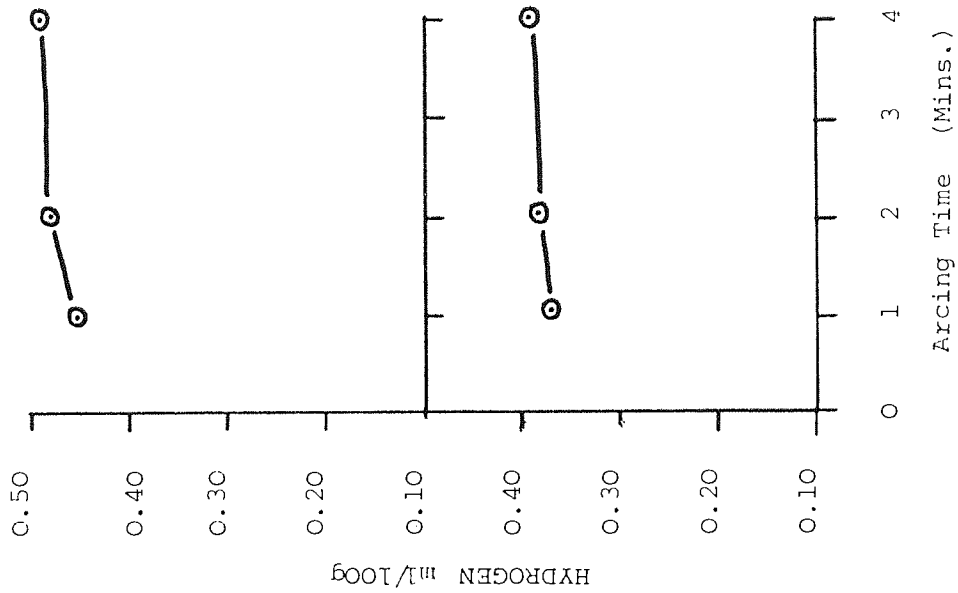
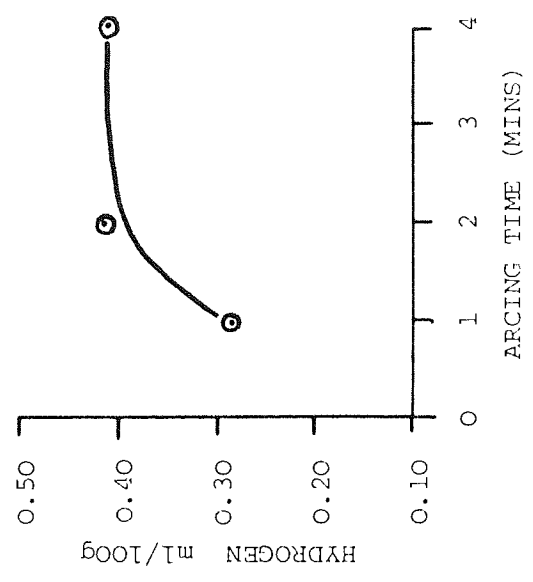


Figure 25 Continued

- (c) OFHC arc melted at 300 Amps in an argon 230 v.p.m. water vapour mixture
- (d) ETP arc melted at 300 Amps in an argon, 230 v.p.m. water vapour mixture



- e -

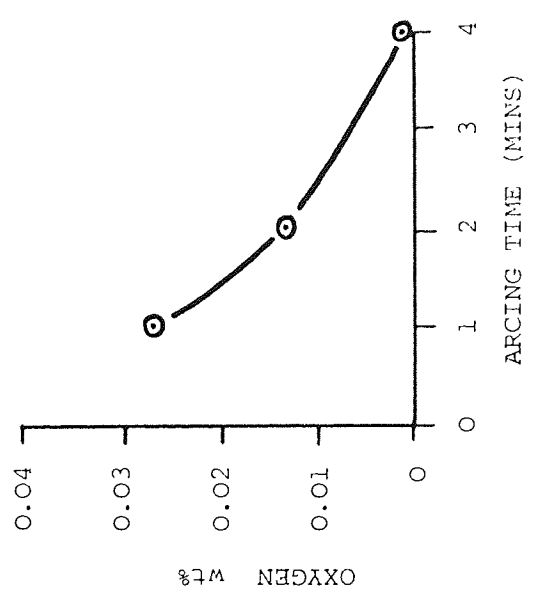


Figure 25 Continued

(e) ETP arc melted at 300 amps in an argon, 540 v.p.m. water vapour mixture

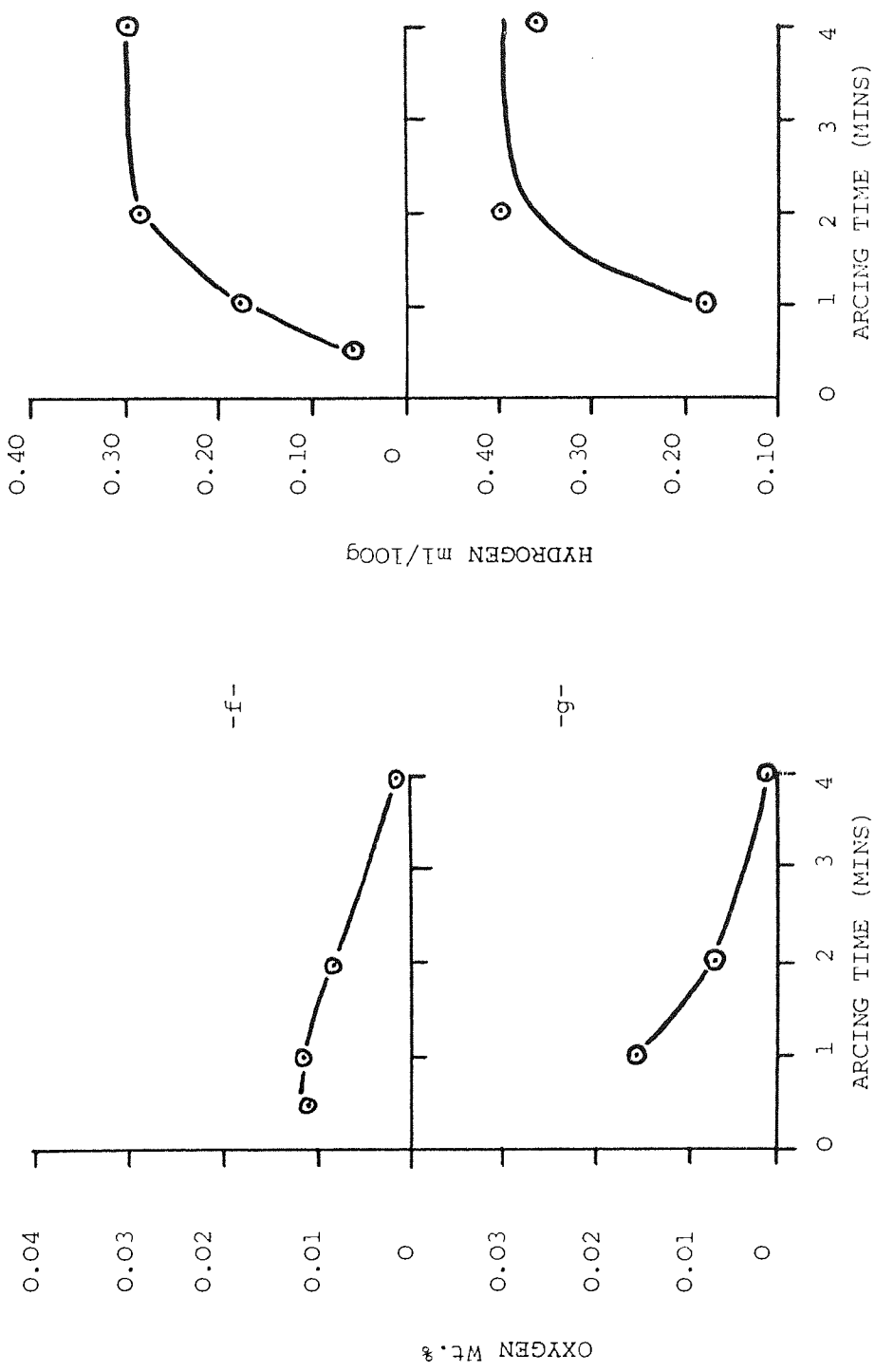
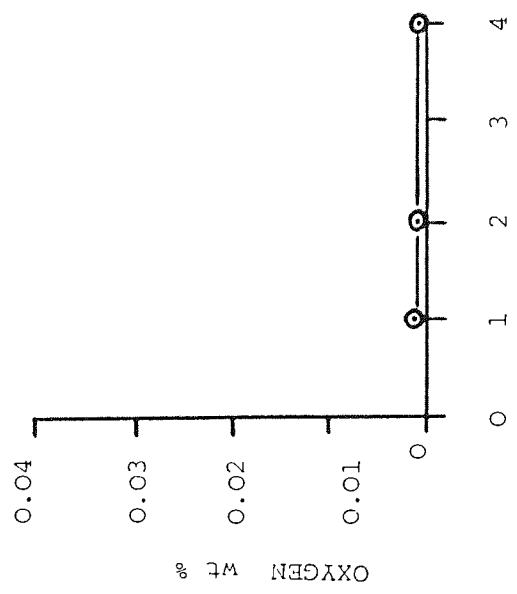
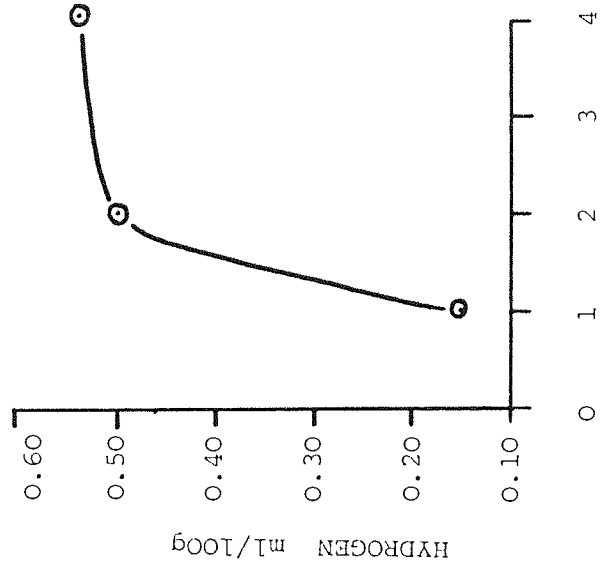


Figure 25 continued (f) O.F.H.C./E.T.P. alloy arc melted at 300 Amps in an argon, 140 vpm water vapour mixture
 (g) O.F.H.C./E.T.P. alloy arc melted at 300 Amps in an argon, 190 vpm water vapour mixture.



Arcing Time (Mins.)

Arcing Time (Mins.)

Figure 26

Oxygen and hydrogen contents of OFHC copper arc melted at a current of 350 Amps in an argon, 100 v.p.m. water vapour mixture

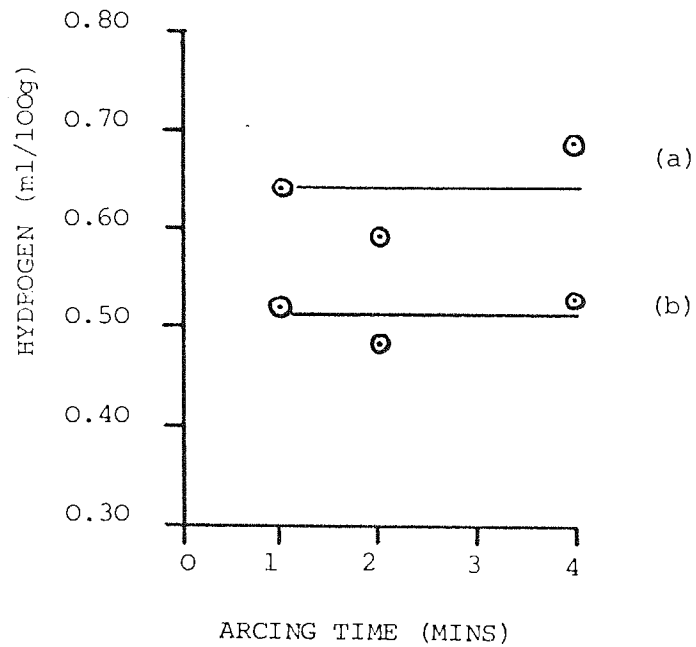


Figure 27 Hydrogen contents of copper titanium alloys;

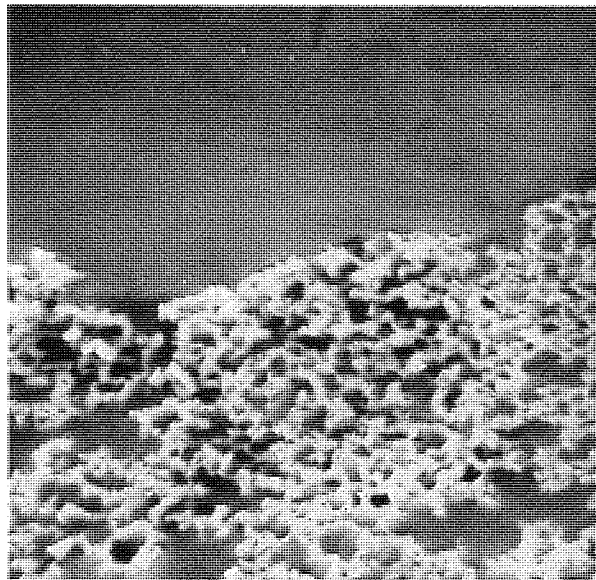
(a) Copper, 1.8 Wt.% titanium arc melted in an argon, 100 vpm water vapour mixture.

(b) Copper, 0.12 Wt.% titanium arc melted in an argon, 100 vpm water vapour mixture.



(a)

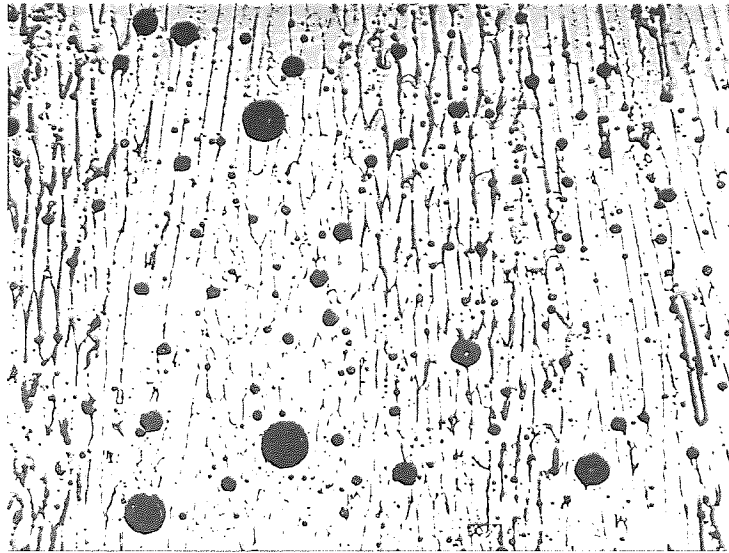
MAG. X6,500



(b)

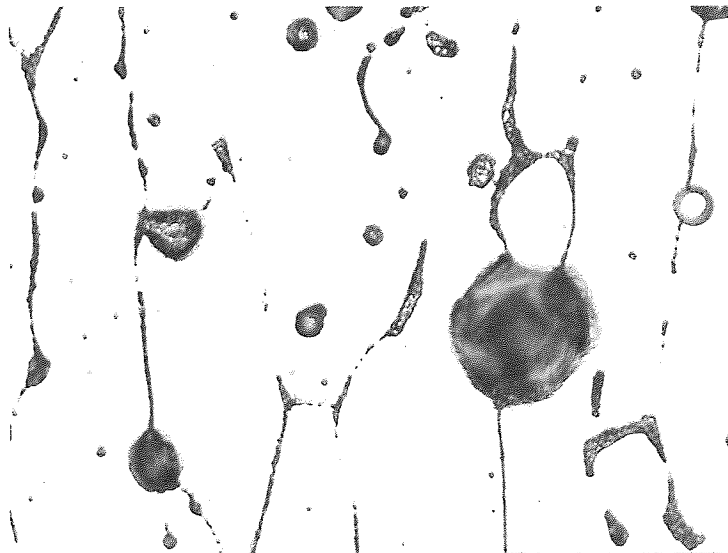
MAG. X8,000

FIGURE 28(a) (b): The bright central zone and light oxide skin of O.F.H.C. copper arc melted in argon, 100 v.p.m. water vapour for 3 minutes at 300 amps.



(a)

MAG. X75



(b)

MAG. X400

FIGURE 29: E.T.P. copper arc melted for 2 minutes at 300 amps and 11 volts in an argon, 230 v.p.m. water vapour mixture. (a) shows the distribution of the porosity and (b) shows that some of the pores are associated with the Cu-Cu₂O eutectic.

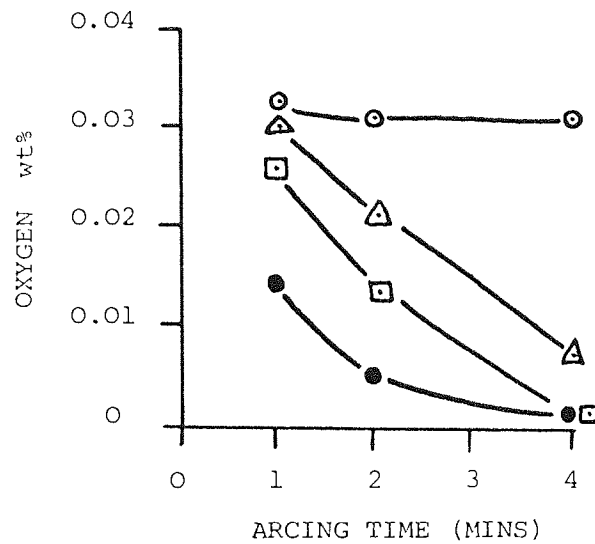


Figure 30 Oxygen contents of E.T.P. copper arc melted in:

- ⊙ super purity argon
- △ argon, 230 vpm water vapour
- ◻ argon, 540 vpm water vapour
- argon, 280 vpm hydrogen.

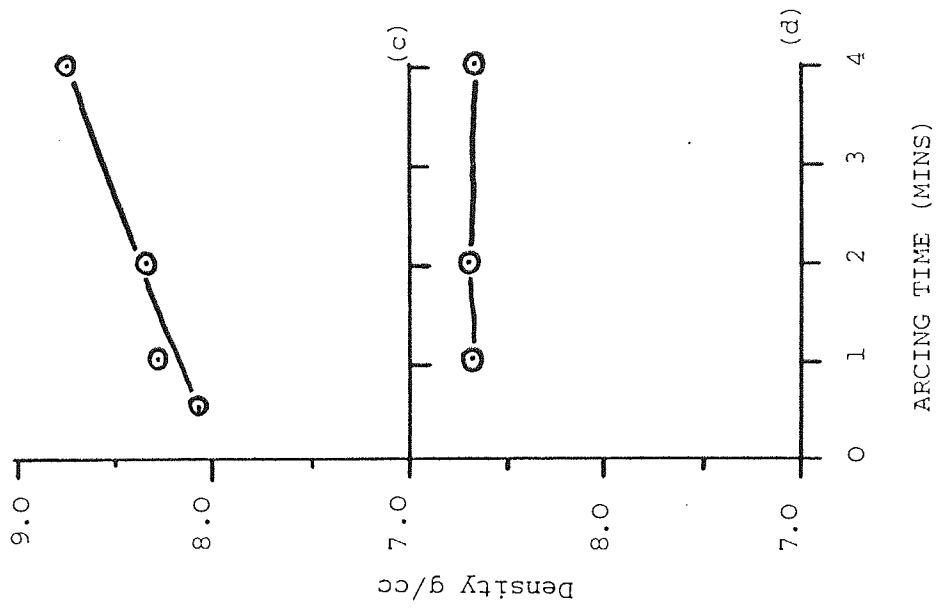
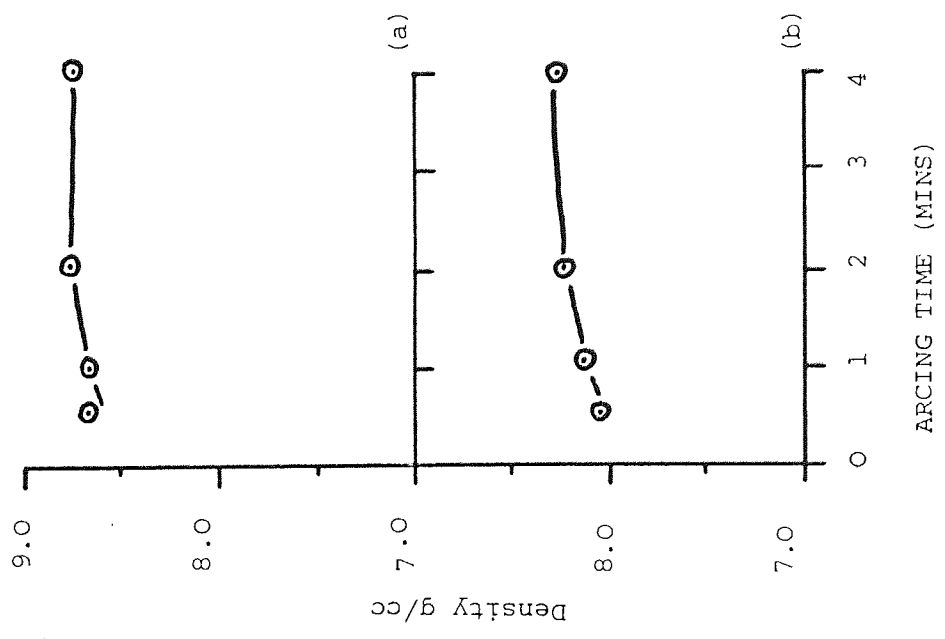
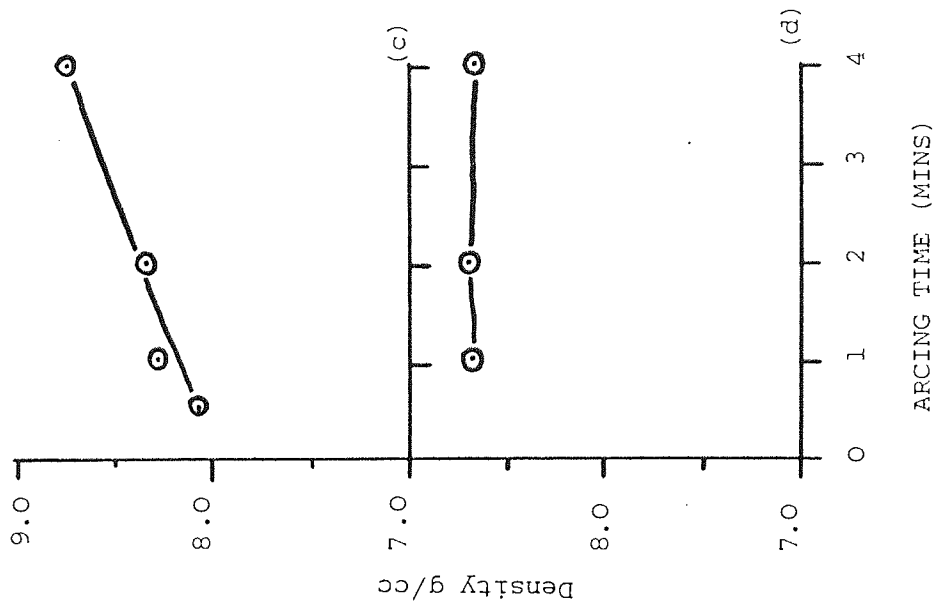
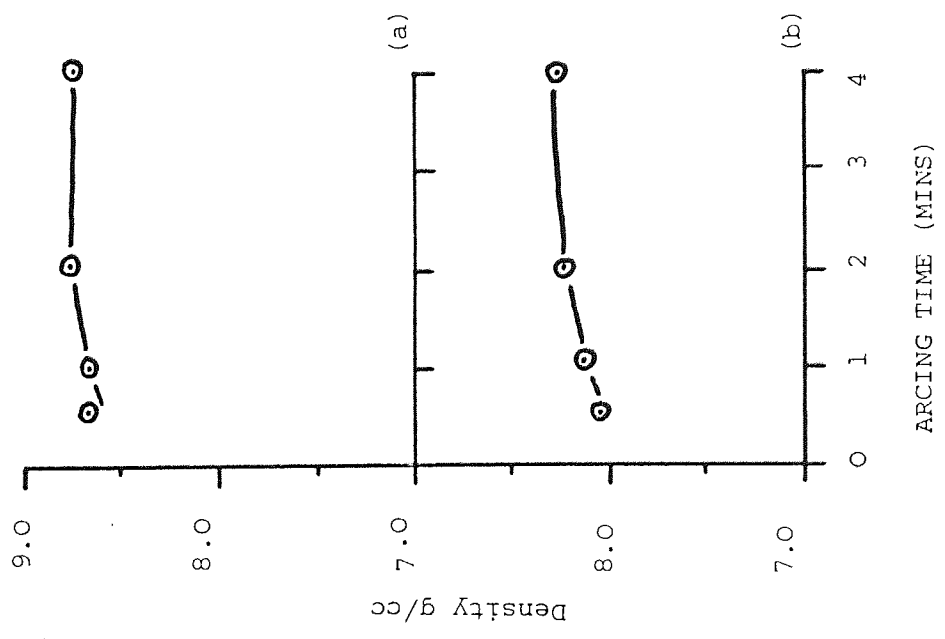


Figure 31 Density values of arc melted copper buttons;

- (a) O.F.H.C. arc melted at 300 amps using argon, 140 vpm water vapour
- (b) E.T.P. arc melted at 300 amps using argon, 140 vpm water vapour
- (c) Equal weights of O.F.H.C. and E.T.P. arc melted at 300 amps using argon, 140 vpm water vapour.
- (d) O.F.H.C. arc melted at 300 amps using argon, 230 vpm water vapour.

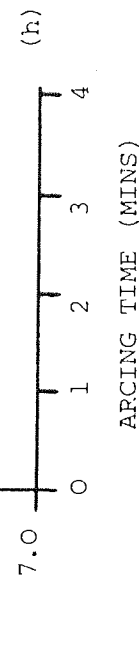
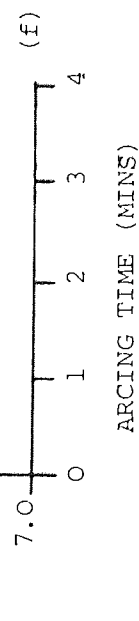
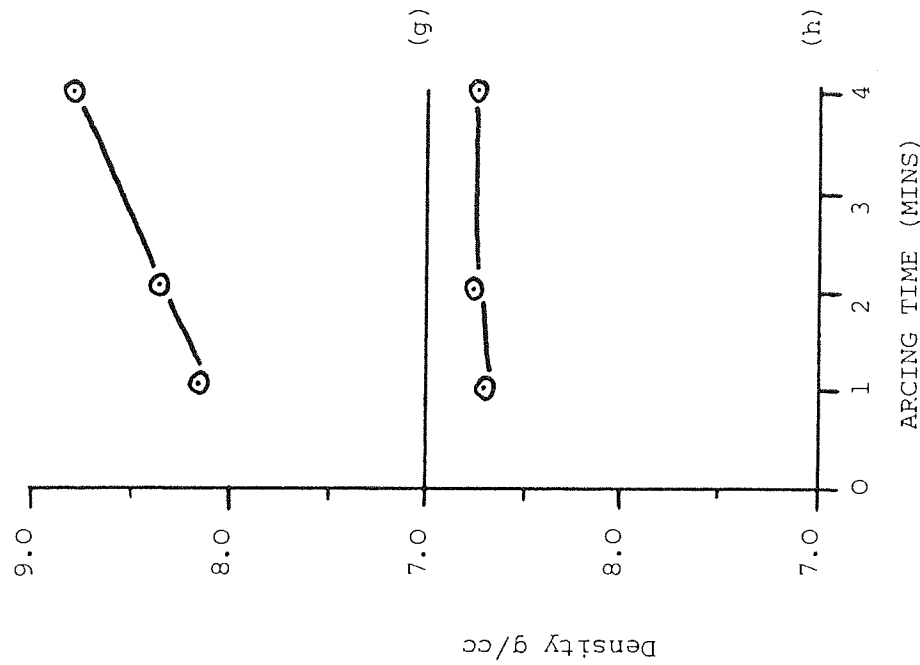
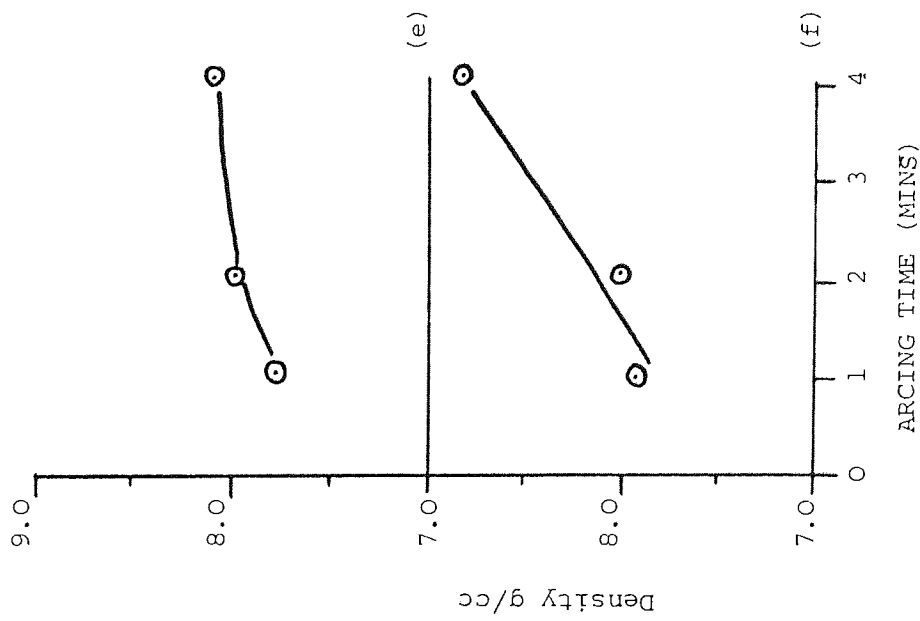


Figure 31 Continued;

- (e) E.T.P. arc melted at 300 amps using argon, 230 vpm water vapour
- (f) E.T.P. arc melted at 300 amps using argon, 540 vpm water vapour
- (g) Equal weights of O.F.H.C. and E.T.P. arc melted at 300 amps, using argon, 190 vpm water vapour
- (h) O.F.H.C. arc melted at 350 amps using argon, 100 vpm water vapour.

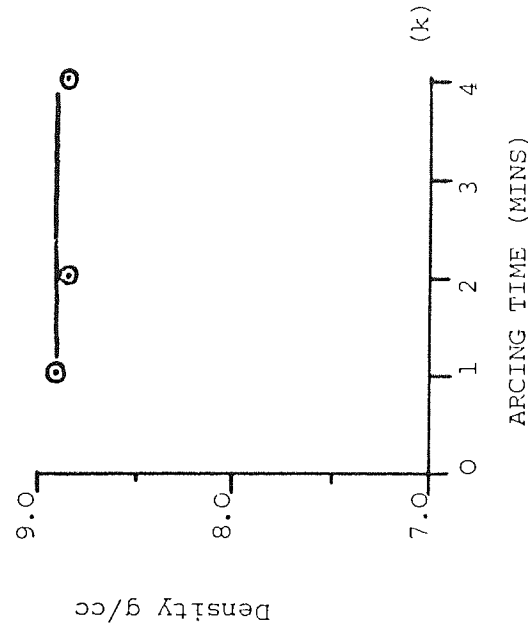


Figure 31 Continued:

- (i) O.F.H.C., 1.8 Wt.% titanium arc melted at 350 amps using argon,
100 vpm water vapour
- (j) O.F.H.C., 1.8 Wt.% titanium arc melted at 300 amps using argon,
100 vpm water vapour
- (k) O.F.H.C., 0.12 Wt.% titanium arc melted at 300 amps using argon,
100 vpm water vapour.

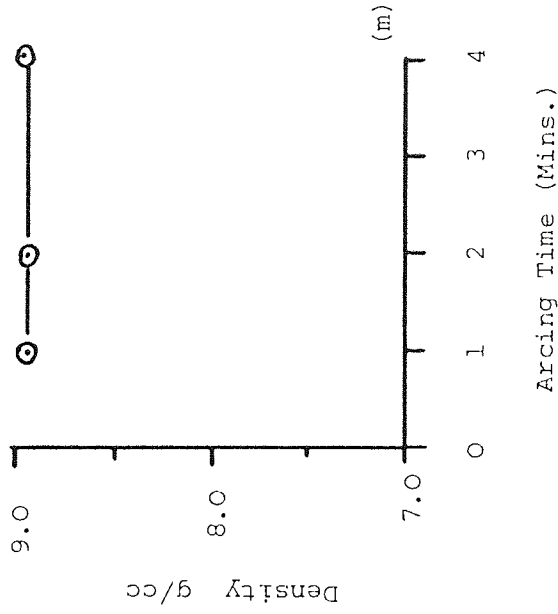
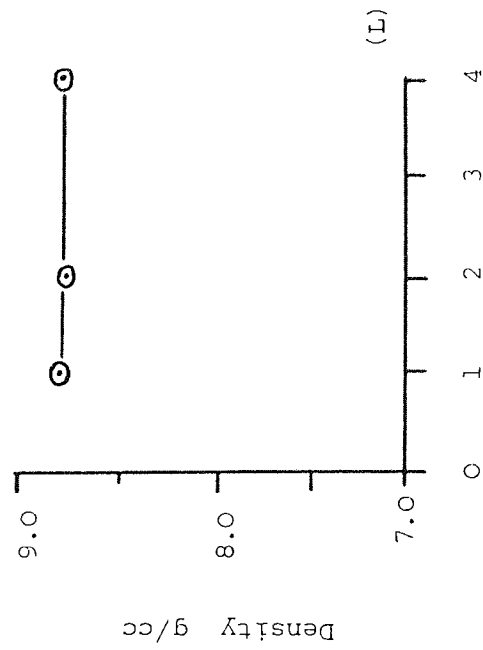


Figure 31 continued

(L) OFHC, 1.0 wt % aluminium arc melted at 300 Amps using argon, 130 v.p.m. water vapour

(m) OFHC 0.10 wt% aluminium arc melted at 300 Amps using argon, 130 v.p.m. water vapour

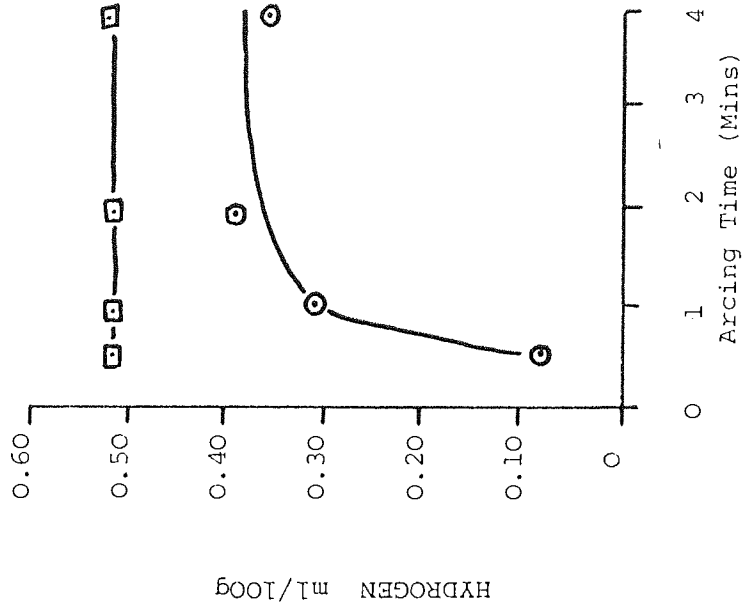
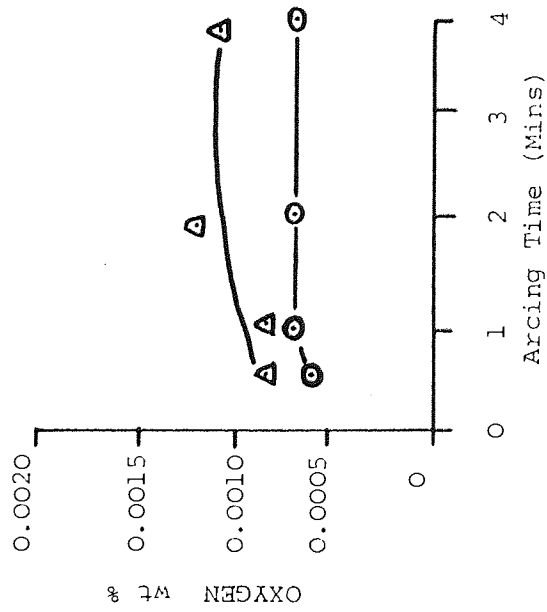


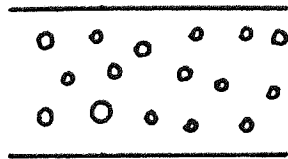
Figure 32

Oxygen and hydrogen contents of OFHC copper arc melted in:

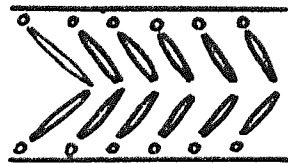
○ Argon, 140 v.p.m. water vapour

△ Argon, 77 v.p.m. oxygen

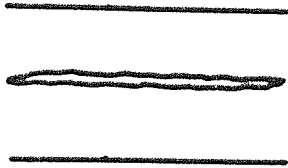
□ Argon, 153 v.p.m. hydrogen



Rounded Pores
in Aluminium



Herringbone
in Copper



Centre Line
in Nickel

Figure 33

Typical morphologies of porosity produced by welding aluminium, copper and nickel in argon hydrogen atmospheres.



Aston University

Illustration removed for copyright restrictions



Aston University

Illustration removed for copyright restrictions

FIGURE 34 The standard free energies of formation of the nitrides per pound-mole (or gramme-mole) of N_2 (gas).
After Elliott and Gleiser⁽⁷³⁾

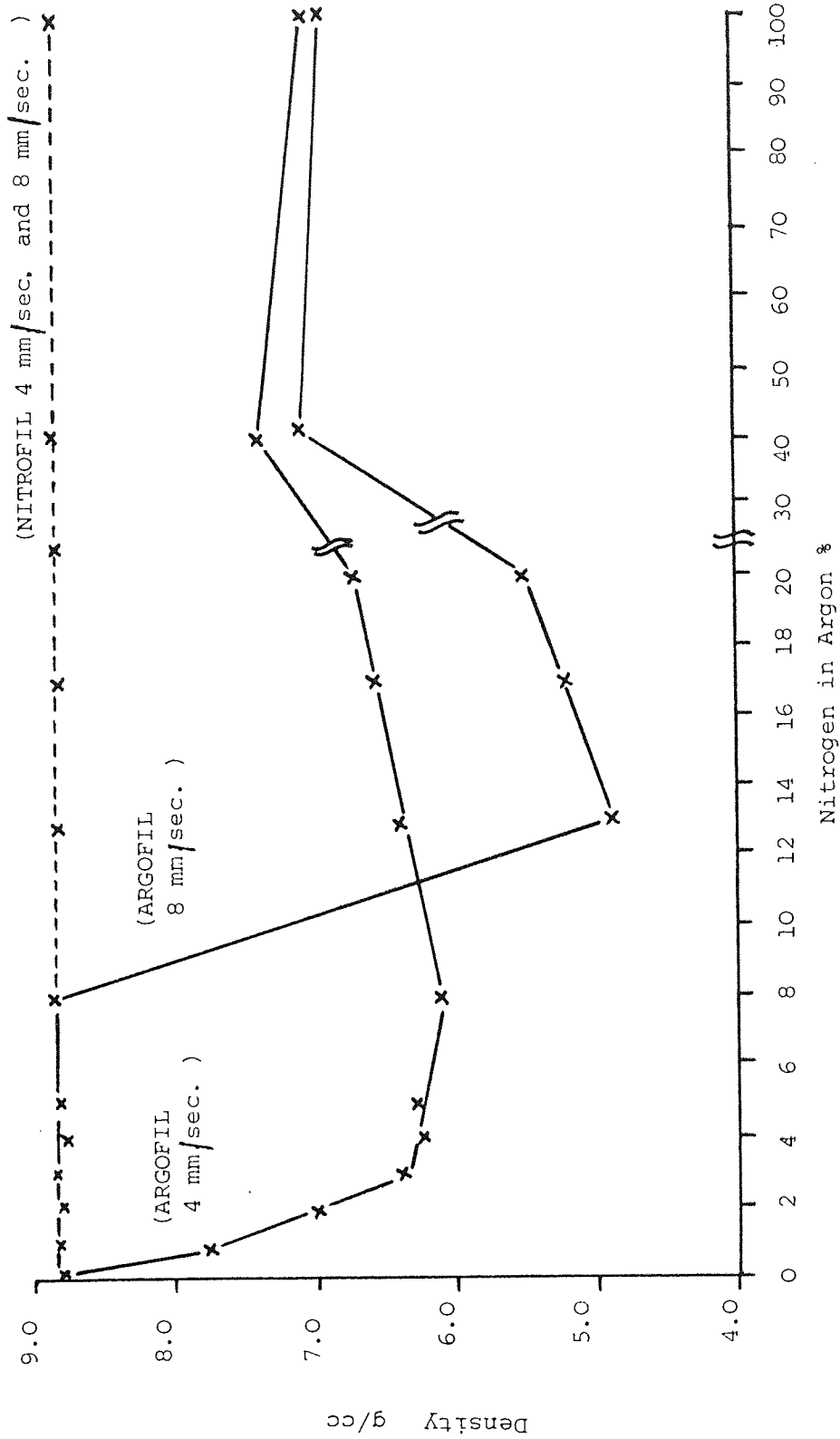


Figure 35
 Effect of Nitrogen and welding speed on the density of M.I.G. Argofil
 and Nitrofil bead on plate runs.